Equilibrium and Stability of Toroidal Pinches(Dissertation_全文)

AUTHOR(S):

Wakatani, Masahiro

EQUILIBRIUM AND STABILITY OF TOROIDAL PINCHES

Masahiro Wakatani

May 1973

Department of Electronics

Kyoto University, Kyoto, Japan

EQUILIBRIUM AND STABILITY OF TOROIDAL PINCHES

Masahiro Wakatani

May 1973

Department of Electronics

Kyoto University, Kyoto, Japan

ACKNOWLEDGMENTS

The author wish to express his appreciation to Professor Ryohei Itatani of Kyoto University for his advice and encouragement during the course of this research, and for his constructive criticism during the preperation of this manuscript as well as to Dr. Hiromu Momota of Kyoto University.

Detailed discussions with Dr. Tuneo Amano of Osaka University and Dr. Hiromu Momota and their many helps in all stages of the work are gratefully acknowledged. They enlightened the author on plasma physics and controlled nuclear fusion research.

Experimental discussions with Dr. Keiichi Hirano of Institute of Plasma physics in Nagoya University are also acknowledged.

It is a pleasure to thank Mr. Tadamoto Tamai of Osaka University, Mr. Masami Watanabe of Kyoto University and Mr. Akihiko Yoshii of Osaka University for their co-operation in the work.

The author also wish to thank all members of Professor Ryohei Itatani's chair, especially to Mr. Hirotada Abe, Mr. Shogo Seki, Mr. Tomonori Takituka and Mr. Kiyoshi Miyake for their valuable discussions on plasma physics and controlled nuclear fusion research.

Use has been made of the electronic computors FACOM 230-60 at Kyoto University and HITAC 8500 at Institute of Plasma Physics in Nagoya University.

ABSTRACT

This work is concerned with theoretical studies of equilibrium and stability of toroidal pinches and Tokamak systems. Of these problems, MHD(magnetohydrodynamic) stability of reverse field diffuse pinch, collisional diffusion in toroidal pinches, Tokamak equilibrium with large poloidal beta β_p and magnetohydrodynamic and tearing instabilities in Tokamaks are investigated.

The stability of reverse field diffuse pinches against kink(or helical) modes is tested by means of Newcomb's criterion for a number of model equilibrium configurations which are obtained by modification of force free fields. Stability diagrams showing the position of the conducting shell for stability are calculated by changing the profile of the axial current density, the average beta and the degree of field reversal. The growth rates of MHD instabilities for some unstable configurations are also calculated. The stability against the resistive tearing modes is examined. It is shown that the reverse field configuration is vulnerable to the tearing instability when the pressure profile is nearly uniform in the central region of the plasma column.

The MHD stability of the toroidal pinch has been carried out in cylindrical geometry neglecting the toroidal effect. When transport phenomena are taken into account, a small toroidicity changes the structure of the equilibrium and leads to results different from those obtained for straight systems. The configuration of toroidal pinches is characterized by a large poloidal magnetic field B_P comparable to a toroidal magnetic field B_T. In the toroidal pinch charged particles can be trapped in the local magnetic mirror formed by both B_T and B_P. Transverse diffusion coefficients including this effect are investigated for three regions of collision frequency i.e., banana regime, plateau regime and MHD regime. Transverse diffusion coefficients are shown to be smaller than D_{GS} which is

given by Galeev and Sagdeev.

The equilibrium of the toroidal plasma in Tokamak type devices has been investigated under the condition $\beta_p = 2\langle p\rangle/Ba^2 \lesssim 1$, where $\langle p\rangle$ is the average pressure and B_a is the poloidal magnetic field at the plasma boundary r=a. The problem of equilibrium of an axisymmetric toroidal plasma column can be solved in the expansion with respect to inverse aspect ratio $\varepsilon=a/R$. It can be shown that if $\beta_p>>1$, then $\beta_p a/R$ is taken as the parameter of the expansion in the equilibrium problem instead of a/R. A general formulation of toroidal plasma column with $\beta_p>>1$ and some examples of Tokamak equilibria obtained by this formulation are given.

The MHD stability of Tokamak equilibrium is also studied in the cylindrical geometry neglecting the toroidal effects. This may be a good approximation for non-localized kink modes. The method to analyze the stability against kink modes is based on solving the linearized MHD equations as an eigen-value problem. The growth rates of MHD instabilities are calculated as eigen-values of the linearized MHD equations. Stability diagrams are obtained by changing the profile of the toroidal current. The influence of the position of the conducting shell on the stability is also investigated. The stability of a current carrying plasma in the strong longitudinal magnetic field against tearing instability is studied for two types of equilibrium configurations. The one is the resistive tearing mode which occurs when the singular point (where $\vec{k}\cdot\vec{B}=0$) falls into the plasma column surrounded by a vacuum. The other is the resistive tearing mode which occurs when the singular point falls into the pressureless plasma surrounding the plasma column.

CONTENTS

INTRODUCTION

A 'toroidal pinch' denotes a toroidal discharge stabilized by a longitudinal magnetic field which is of the same magnitude as the magnetic field due to the discharge current. A reverse field pinch[1] in which the toroidal magnetic field is reversed outside the plasma column, a screw pinch[2),3),4)] which is stabilized with current flowing in the pressureless plasma surrounding the plasma column and a stabilized pinch[1),2)] in which the toroidal magnetic field becomes small outside the plasma column are typical devices of toroidal pinches. The macroscopic stability of these systems has been demonstrated and encouraging evidence of their potentiality has been obtained,e.g., with respect to the high value of β (the ratio of plasma pressure to magnetic pressure). In the toroidal devices of the Tokamak type[5)] a plasma column is confined by the magnetic field generated by a current flowing along the plasma. The current also has the function of plasma heating. In order to render the plasma macroscopically stable, a longitudinal magnetic field is produced in the toroidal chamber with field lines being parallel to the plasma column. With a sufficiently strong magnetic field, stable plasma confinement has been achieved in Tokamak systems. As Tokamaks may be important to controlled thermonuclear reactions, many experimental works are carried out.[6),7),8)] Accordingly it is of great interest to take the theoretical study of equilibrium and stability in toroidal pinches and Tokamak systems.

The equilibrium of the toroidal plasma in Tokamak type devices has been first studied by Shafranov.[9)] The problem of equilibrium of an axisymmetric toroidal plasma column in a magnetic field can be solved generally in the expansion with respect to inverse aspect ratio $\varepsilon = a/R$. Further progress in this problem has been done by many authors.[10),11),12)] These investigations, however, have been limitted to the equilibrium of low pressure plasma with $\beta_p = 2\langle p\rangle/B_a^2 \lesssim 1$, where $\langle p\rangle$ is the average pressure over the cross section of the plasma

column and B_a is the poloidal magnetic field at the plasma boundary $r = a$. An important step in demonstrating feasibility of a Tokamak fusion reactor is maximizing β. At large $\beta(\sim 1)$, however, it has been unclear that pressure balance between plasma and magnetic field could exist. Recently Shafranov and Yurchenko[13] considered the equilibrum of a toroidal plasma with $\beta_p \gg 1$ and $\beta_p a/R \ll 1$. They showed that if $\beta_p \gg 1$, then $\beta_p a/R$ is taken as the parameter of the expansion in the equilibrium problem instead of a/R. Laval, Maschke, Pellat and Rosenbluth[14] studied a plasma with $\beta_p \sim R/a$ contained in a torus of elliptical cross section. Strauss[15] showed, for the plasma being contained in a torus of rectangular cross section, that equilibria with arbitrary β_p are available. Callen and Dory[16] showed equilibria with $\beta_p > R/a$ which have one magnetic axis, but found that as $\beta_p \to R/a$ region of reverse current appears in the plasma column. Recent analyses of MHD stability[17),18] have suggested that the plasma column in a non-circular conducting shell is more stable than in a circular conducting shell. These works draw the attension to the interest of non-circular cross section in toroidal pinches and Tokamaks. Green, Johnson and Weimer[19] have shown that the magnetic surfaces are elliptically distorted as well as non-concentric even if $\beta_p \lesssim 1$. Yoshii, Nakatani and Amano[20] have extented the method of Green, Johnson and Weimer to the plasma $\beta_p \gg 1$ and $\beta_p a/R < 1$ in a non-circular conducting shell. These equilibrium considerations seem to give no limitations for high value of β but requirement for MHD stability does limit β.

The MHD instability is, as is well known, dangerous instability for confinement of current carrying plasmas. Various authors have discussed the theory of MHD instability in a current carrying plasma. Kruskal[21] and Shafranov[22] have shown that the total axial current must be smaller than the so-called 'K.S.limit' in order to assure the stability against the kink(or helical) instability, when the axial magnetic field is nearly uniform. This K.S.limit is an important quantity for MHD stability in Tokamak type devices. As

far as the infinite conductive plasma in the cylindrical geometry is concerned, formulation of the problem has been almost accomplished by Newcomb.[23] The remaining difficulty of the theoretical work is more related to the problem of configuration. For example, many analytical works are based on the particular current profile such as homogeneous or skin current distribution. Thus some ambiguity exists when it is required to compare the experimental results with the theoretical prediction. Rosenbluth[24] studied carefully the structure of the skin current layer in the cylindrical linear pinch and showed that if the axial magnetic field is reversed, the configuration is hydromagnetically stable. Corpley and Whiteman[25] have studied numerically the stability of reverse field diffuse pinches by the use of Newcomb's criterion. Recently Robinson[26] has obtained a semi-quantitative analytic expression for the threshold of MHD stability in the case of reverse field configurations. Amano, Tamai and Wakatani[27] investigated the stability of reverse field diffuse pinches by means of Newcomb's criterion in changing the axial current profile from the skin like current profile to the nearly uniform one. This investigation clarified the threshold of the MHD stability as functions of current profiles, average beta and the degree of field reversal.

Shafranov[28] carried out the analysis of kink(or helical) modes in current carrying toroidal plasmas in Tokamak type devices with cylindrical geometry neglecting toroidal effects. It is investigated that the detailed dependence of the MHD stability conditions on the toroidal current profile by means of the energy principle.[29] Okabayashi[30] assured the results of Shafranov using numerical procedures. Amano, Wakatani and Watanabe[31] investigated the same problems in various current profiles by solving the linealized MHD equations derived by Hain and Lüst.[32] This method has an advantage of knowing the growth rate of MHD instability and its profile of the perturbation.

In a screw pinch Freidberg[33] calculated the growth rate of the

kink mode by solving the linearized MHD equations for incompressible plasmas. On the other hand, Goedbloed and Hagenbeuk,[34] in a screw pinch, calculated the growth rates of MHD instabilities by the linearized MHD equations for compressible plasmas and showed that compressibility turns out to have little influence on the kink modes but for the interchange(or local helical) modes there is a pronounced effect of compressibility which is always destabilizing. Bodin et al.[1] studied the growth rates of MHD instabilities to compare the experimental results in the toroidal pinch with the MHD theory. Amano, Tamai and Wakatani[27] also calculated the growth rates in the reverse field diffuse pinch surrounded by a vacuum by the use of the linearized MHD equations including compressibility.

Furth, Rosenbluth and Killeen[35] showed that if dissipative effects are included in MHD equations, a pinch plasma stable within the ideal MHD equations becomes vulnerable to three types of resistive instabilities such as resistive interchange mode, rippling mode and tearing mode. Johnson, Green and Coppi[36] examined the effect of resistivity on the stability of MHD equilibria mainly in the stellarator type devices.[37] Successively Coppi, Green and Johnson[38] (we shall call them as CGJ) considered the effects of small electrical resistivity, viscosity and thermal conductivity on MHD instabilities in a diffuse linear pinch configuration, including the effect of the β. Coppi[39] found that the ion gyro-radius has the effect of slowing down all resistive modes and in most cases of making them overstable. Coppi and Rosenbluth[40] also found that the resistive interchange mode can be stabilized if viscous diffusion due to ion-ion collision is taken into account. Amano, Tamai and Wakatani[27] investigated the stability against resistive tearing modes in the reverse field diffuse pinch and estimated the growth rate of the tearing instability by the method of CGJ.

Extensive observations have been reported[41),42)] of kink like (or helical like) magnetic perturbations in Tokamaks. These have usually been interpreted as kink like MHD modes of a current

carrying plasma. Such modes are of two types; the MHD kink mode of a plasma with a free boundary which occurs when the singular point (where $\vec{k}\cdot\vec{B} = 0$) falls into the vacuum outside the plasma column, and the resistive tearing mode which occurs with somewhat slower growth rate when the singular point falls into the conducting plasma. The kink and tearing modes are essentially the same, as both are driven by the magnetic field energy of the poloidal field. The only difference is that the growth rate of kink mode is limited only by inertia, whereas the growth rate of tearing mode is to some extent limited by the resistivity of the plasma. Theoretical studies of resistive tearing modes in a Tokamak plasma have been developed by Shafranov,[28] and Amano, Wakatani and Watanabe,[31] and Furth, Rutherford and Selberg.[43] Rutherford, Furth and Rosenbluth[44] considered the non-linear effect on the tearing mode.

As we have noted, extensive studies have been made on the toroidal equilibrium of a plasma for the case of the ideal MHD equations. Several authors[45),46] have taken into account the transport phenomena of the plasma. In these cases a small toroidicity changes the structure of the equilibrium and leads to results entirely different from those obtained for straight systems, in absolute values as well as in the dependence of the transport coefficients on the parameters that characterize the magnetic field and the plasma. The calculation of the diffusion flux made by Pfirsch and Schlüter[45] showed that when the toroidicity is taken into account, the diffusion coefficient gets an additional factor $(1+8\pi^2/\iota^2)$ where ι is the angle of rotational transform. For $\iota \ll 2\pi$ this factor gives an important increase of the diffusion velocity and changes the functional dependence on poloidal and/or toroidal components of the magnetic field. The results of this investigation, which was done in the MHD approximation, are correct only in the case of a sufficiently collisional plasma for which the mean free path is much less than the characteristic dimension of the torus. Recently many experiments concern low density and/or high temperature

plasmas with rare collisions for which the MHD approximation is not valid. In the limit of low collision frequency the same problem was studied with kinetic equations by Galeev and Sagdeev,[46] afterwards Kovrizhnikh[47] and Rutherford.[48] The results of these investigations showed the important role of the particles with small longitudinal velocity, in particular the so-called 'trapped particles', in the diffusion of a rarely collisional plasma. The work of Galeev and Sagdeev stimulated the interest of theoreticians on the problem of collisional diffusion. They concerned a more detailed and more rigorous analysis of transport processes,[49),50] and also the extension to another toroidal systems confining high temperature plasmas. For example, Stringer[51),52] have studied transport processes by taking into account non-coincidence of equipotential surfaces with the magnetic surfaces. Ware[53] and Rutherford, Kovrizhnikh, Rosenbluth and Hinton[54] have considered the effect of electric field driving the toroidal current on transport phenomena. Galeev, Sagdeev, Furth and Rosenbluth[55] and Frieman[56] have investigated collisional diffusion in the system without axial symmetry such as the stellarator [37]. Wakatani and Itatani[57] have studied collisional diffusion in toroidal pinches.

The MHD stability theory applied in this thesis is summarized in Chapter I. Chapter II is devoted to the stability of reverse field diffuse pinches. The current profile of the reverse field diffuse pinch is varied from a nearly skin current distribution to a nearely uniform one. To test the MHD stability by Newcomb's criterion requires numerical integration of the Euler-Lagrange equation. The information gained, however, concerns only the threshold of the stability. In order to obtain the information about the growth rate and the eigen function, the linearized MHD equation is solved as an eigen value problem. The analysis of the stability of the reverse field diffuse pinch against the resistive tearing mode is done with the method of CGJ, because CGJ considered the diffuse linear pinch with a cylindrical configuration and included the effect of β.

The investigation of collisional diffusion in toroidal pinches can be seen in Chapter III. In Chapter IV, by making assumptions with respect to the dependence of the plasma pressure and the toroidal current on magnetic surfaces, the problem of Tokamak equilibrium in a weakly distorted conducting shell including ellipticity and triangularity is solved with $\beta_p >> 1$ and $\beta_p a/R \lesssim 1$. For Tokamaks the procedure adopted to study the MHD stability is to integrate the linearized MHD equations numerically from which are obtained the growth rate and the eigen function of the MHD instability. The investigation of the stability of Tokamak equilibrium against the resistive tearing mode is also carried out. Chapter V is devoted to describe these results.

項欠

CHAPTER I

SUMMARY OF MHD STABILITY THEORY

§ 1 Introduction

Investigation of MHD stability can be done by looking for the growth of small perturbations near an equilibrium configuration. The equilibrium is said to be unstable if any solution increases indefinitely in time; if no such solution exists, the equilibrium is stable. The MHD stability of a linear pinch with the current confined to an indefinitely thin layer has been analytically studied in detail.[24] Although the stability of a diffuse linear pinch may be important to compare the experimental results with the theoretical prediction, its analysis needs numerical techniques as will be shown in later chapters. To consider the features of an equilibrium configuration which are desirable for stability we will use the hydromagnetic energy principle[29] fundamentally. This energy principle is based on the study of the potential energy associated with the small perturbation and makesit possible to evaluate the stability of a system without actually finding a growth rate of the perturbation. From the energy principle, variational principle can be formulated to obtain necessary and sufficient conditions for the stability of the diffuse linear pinch. This work was done by Newcomb[23] and the results are summarized in §2. We consider the non-localized displacements or kink(or helical)modes together with the localized displacements or interchange modes in the investigation to determine the threshold of the MHD stability. This is carried out by means of the Newcomb's criterion derived from the hydromagnetic energy principle.

The information gained by the Newcomb's criterion, however, concerns only the threshold of the MHD instability. It is necessary to solve the linearized MHD equations for obtaining its growth rate and its profile of the displacement. Conveniently, in the cylindrical linear pinch the linearized MHD equations reduce to the one equation of the variable ξ_r[32] which denotes the r component of the displacement. This reduction is shown in §3. From the viewpoint of experiments, it is important to know the growth rate of the MHD instability, when the equilibrium configuration fails to satisfy the Newcomb's criterion. The growth rates of MHD instabilities can be evaluated as eigen values of the equation for ξ_r. This consideration will be applied in Chapters II and V.

Dissipative effects remove certain restrictions on the instability which is available in the ideal MHD equations.[35] In the presence of small dissipation, a non-local kink instability(or a non-local helical instability) can also arise in a current carrying plasma. This is the so-called tearing mode. Here we consider electrical resistivity, η, as a dissipative effect. The analysis of the effect of small electrical resistivity on the MHD stability in a diffuse linear pinch is done with the method given by Coppi, Green and Johnson.[38] This method is summarized in §4.

Finally we will note that MHD equations are written in rationalized Gaussian unit with c=1.

§ 2 Newcomb's Criterion[23)]

In the theory of Newcomb, the plasma can be regarded as an ideal fluid, i.e., we can neglect the dissipative terms in the MHD equations. The basic equations describing an ideal fluid are

$$\rho \frac{d\vec{v}}{dt} = -\text{grad } p + \vec{J} \times \vec{B} \quad , \tag{1.1}$$

$$\frac{\partial \rho}{\partial t} + \text{div}(\rho \vec{v}) = 0 \quad , \tag{1.2}$$

$$\vec{E} + \vec{v} \times \vec{B} = 0 \quad , \tag{1.3}$$

$$\frac{d}{dt}(p\rho^{-\gamma}) = 0 \quad , \tag{1.4}$$

$$\text{rot } \vec{E} = -\frac{\partial \vec{B}}{\partial t} \quad , \tag{1.5}$$

$$\text{rot } \vec{B} = \vec{J} \quad , \tag{1.6}$$

$$\text{div } \vec{B} = 0 \quad . \tag{1.7}$$

Let $\vec{E}$ be the electric field, $\vec{B}$ the magnetic field, $\vec{J}$ the current density, ρ the mass density, p the pressure, γ the ratio of specific heats and $\vec{v}$ the fluid velocity. These equations are written in rationalized Gaussian unit with c=1.

Mathematically the problem of stability reduces to the investigation of small perturbations about an equilibrium state. If the perturbation amplitudes are small, the linealized equations of motion can be used. Let $\tilde{\rho}$, $\tilde{p}$ and $\vec{b}$ represent small deviations from the equilibrium values ρ, p and $\vec{B}$. The equations describing the static equilibrium are derived from eqs.(1.1) ~ (1.7):

$$\vec{J} \times \vec{B} = \text{grad } p \quad , \tag{1.8}$$

$$\text{rot } \vec{B} = \vec{J} \quad , \tag{1.9}$$

$$\text{div } \vec{B} = 0 \quad . \tag{1.10}$$

The linearized equations of eqs. (1.1) ~ (1.7) can be written in the form:

$$\frac{\partial \tilde{\rho}}{\partial t} + \text{div } (\rho \vec{v}) = 0 \quad , \tag{1.11}$$

$$\rho \frac{\partial \vec{v}}{\partial t} + \text{grad } \tilde{p} = \text{rot } \vec{B} \times \vec{b} + \text{rot } \vec{b} \times \vec{B} \quad , \tag{1.12}$$

$$\frac{\partial \tilde{p}}{\partial t} + \vec{v} \text{ grad } p + \gamma p \text{ div } \vec{v} = 0 \quad , \tag{1.13}$$

$$\frac{\partial \vec{b}}{\partial t} = \text{rot } (\vec{v} \times \vec{B}) \quad . \tag{1.14}$$

As it is not convienient to use the velocity $\vec{v}$, we treats the displacement from an equilibrium position $\vec{\xi}$, in which case $\vec{v} = \partial \vec{\xi}/\partial t$. Using this variable, eqs. (1.11), (1.13) and (1.14) can be integrated with respect to time:

$$\tilde{\rho} = - \text{div } (\rho \vec{\xi}) \quad , \tag{1.15}$$

$$\tilde{p} = - \vec{\xi} \text{ grad } p - \gamma \, p \text{ div } \vec{\xi} \quad , \tag{1.16}$$

$$\vec{b} = \text{rot } (\vec{\xi} \times \vec{B}) \quad . \tag{1.17}$$

Substitution of these expressions into eq. (1.12) results in a single second order differential equation for $\vec{\xi}$:

$$\rho \frac{\partial^2 \vec{\xi}}{\partial t^2} = \vec{F}\{\vec{\xi}\} = \text{grad}(\vec{\xi}\ \text{grad}\ p + \gamma\ p\ \text{div}\ \vec{\xi}) + \text{rot}\ \vec{B} \times \text{rot}\ (\vec{\xi} \times \vec{B}) + \text{rot}[\ \text{rot}(\vec{\xi} \times \vec{B})\ ] \times \vec{B} \quad . \tag{1.18}$$

The energy integral is obtained from eq. (1.18) in the form

$$W = \frac{1}{2}\int_{V_i} d\vec{r}\ \{\vec{Q}^2 + \vec{J}\cdot\vec{\xi}\times\vec{Q} + \vec{\xi}\ \text{grad}\cdot\text{div}\ \vec{\xi} + \gamma p(\text{div}\ \vec{\xi})^2\} \tag{1.19}$$

where $\vec{Q} = \text{rot}\ (\vec{\xi} \times \vec{B})$ and V_i denotes the volume occupied by the plasma.

The method of Newcomb is based on the hydromagnetic energy principle which gives an expression for the change in the potential energy of the system, W, when it is subjected to a displacement $\vec{\xi}$. If $W>0$ for every displacement $\vec{\xi}$ satisfying the boundary condition, the equilibrium configuration is stable; if $W<0$ for any allowable $\vec{\xi}$, it is unstable.

To derive the necessary and sufficient condition for MHD stability of a cylindrical symmetric static equilibrium described by eqs. (1.8), (1.9) and (1.10), the usual assumption are made:

(i) the plasma is infinitely conducting,

(ii) the stress tensor is isotropic so that a scalar pressure can be defined,

(iii) the plasma is bounded by a perfectly conducting shell at r=b.

It follows from symmetry considerations that the small amplitude motions of a linear pinch can be analyzed into normal modes for which ξ_r, $i\xi_\theta$ and $i\xi_z$ are real functions of r multiplied by exp (imθ - ikz). We can therefore limit ourselves to displacements of this form without loss of generality. Thus we obtain a stability criterion for each set of values of m and k.

Dropping the exponential factor, we transform ξ_r, ξ_θ and ξ_z to the real variable ξ,η and ζ:

$$\xi = \xi_r,$$

$$\eta = \vec{\nabla}\cdot\vec{\xi} - \frac{1}{r}\frac{d}{dr}(r\xi_r) = \frac{im}{r}\xi_\theta - ik\xi_z ,$$

$$\zeta = i(\vec{\xi} \times \vec{B})_r = i\xi_\theta B_z - i\xi_z B_\theta \quad . \tag{1.20}$$

The components ξ_θ and ξ_z are given in terms of η and ζ by

$$\xi_\theta = i\frac{kr\zeta - rB_\theta\eta}{mB_\theta - krB_z} \quad ; \qquad \xi_z = i\frac{m\zeta - rB_z\eta}{mB_\theta - krB_z} \quad . \tag{1.21}$$

We substitute these expressions for ξ_θ and ξ_z into the energy integral as given by eq. (1.19), using only the real part of the complex $\vec{\xi}$ because W is a quadratic, the result is

$$W(\xi,\eta,\zeta) = \frac{\pi}{2}\int_o^b r dr\{ \Lambda(\xi, \frac{d\xi}{dr}) + \gamma p \left[\eta + \frac{1}{r}\frac{d}{dr}(r\xi)\right]^2$$

$$+ \frac{k^2r^2 + m^2}{r^2}[\zeta - \zeta_0(\xi, \frac{d\xi}{dr})]^2 \} \qquad (1.22)$$

where

$$\Lambda(\xi, \frac{d\xi}{dr}) = \frac{1}{k^2r^2 + m^2}\left[(mB_\theta - krB_z)\frac{d\xi}{dr} - (mB_\theta + krB_z)\frac{\xi}{r}\right]^2$$

$$+ \left[(mB_\theta - krB_z)^2 - 2B_\theta\frac{d}{dr}(rB_\theta)\right]\frac{\xi^2}{r^2}, \qquad (1.23)$$

$$\zeta_0(\xi, \frac{d\xi}{dr}) = \frac{-r}{k^2r^2 + m^2}\left[(krB_\theta + mB_z)\frac{d\xi}{dr} + (mB_z - krB_\theta)\frac{\xi}{r}\right].$$

(1.24)

A pinch is stable if and only if $W(\xi,\eta,\zeta)$ is positive for every set of trial functions (ξ,η,ζ) with ξ satisfying the boundary conditions

$$\begin{cases} \xi(0) = 0 & \text{if } m \neq 1 \\ \xi'(0) = 0 & \text{if } m = 1 \end{cases}$$

and $\xi(b) = 0$. (1.25)

Let us define

$$W(\xi) = \min_{\eta,\zeta} W(\xi,\eta,\zeta). \qquad (1.26)$$

The indicated minimization with respect to η and ζ is trivial. Since the terms involving η and ζ are positive difinite and can be made to vanish by setting

$$\eta = -\frac{1}{r}\frac{d}{dr}(r\xi) \quad , \tag{1.27.a}$$

$$\zeta = \zeta_0 \ (\xi, \frac{d\xi}{dr}) \quad , \tag{1.27.b}$$

we obtain

$$W(\xi) = \frac{\pi}{2}\int_0^b rdr \ \Lambda(\xi, \frac{d\xi}{dr}) \quad . \tag{1.28}$$

Equation(1.27.a) is equivalent to $\nabla\cdot\vec{\xi} = 0$; hence W is minimized by incompressible perturbations. Furthermore, Λ does not contain γ, so that the stability criterion is independent of γ. In particular, by choosing $\gamma = \infty$,we see that the stability criterion is unchanged by replacing the plasma with an incompressible fluid.

A more convenient form of the energy principle is obtained by integrating eq.(1.28) by parts to eleminate the term in $\xi\frac{d\xi}{dr}$:

$$W(\xi) = \frac{\pi}{2}\int_0^b dr \ [\ f(\frac{d\xi}{dr})^2 + g\xi^2\ ] \quad , \tag{1.29}$$

where f and g, which are functions of r with m and k as parameters, are given by

$$f = \frac{r(mB_\theta - krB_z)^2}{k^2r^2 + m^2} \quad , \tag{1.30}$$

$$g = \frac{1}{r}\frac{(mB_\theta + krB_z)^2}{k^2r^2 + m^2} + \frac{1}{r}(mB_\theta - krB_z)^2 - \frac{2F_\theta}{r}\frac{d}{dr}(rB_\theta)$$

$$- \frac{d}{dr}\left(\frac{k^2r^2B_z^2 - m^2B_\theta^2}{k^2r^2 + m^2}\right). \qquad (1.31)$$

The coefficient f is never negative, but g may have either sign. Another useful expression for g is obtained:

$$g = \frac{2k^2r^2}{k^2r^2 + m^2}\cdot\frac{dp}{dr} + \frac{1}{r}(mB_\theta - krB_z)^2\frac{k^2r^2 + m^2 - 1}{k^2r^2 + m^2}$$

$$+ \frac{2k^2r}{(k^2r^2 + m^2)^2}(k^2r^2B_z^2 - m^2B_\theta^2). \qquad (1.32)$$

From eq. (1.29), it can be shown that a linear pinch is stable for all values of m and k if and only if it is stable for m = 1, $-\infty < k < \infty$ and for m = 0, $k \to 0$.

If we now try to minimize W with respect to ξ, we obtain the Euler-Lagrange equation

$$\frac{d}{dr}\left(f\frac{d\xi}{dr}\right) - g\xi = 0 \quad . \qquad (1.33)$$

The solution of this equation satisfying the necessary boundary condition (1.25) gives stationary but not necessary minimal values of W. To proceed any further we have to study the form of the solution of eq. (1.33). The first point to notice is that the equation has a singular point whenever f = 0, i.e., for all r satisfying

$$mB_\theta - krB_z = 0 \quad , \tag{1.34}$$

and these singular points, r_s, devide the plasma into a number of sub-intervals $[0, r_1]$, $[r_1, r_2] \cdots\cdots [r_n, b]$. They are called independent sub-interval by Newcomb as it can be shown that an equilibrium configuration is stable if and only if the energy integral, W, is positive independently in each sub-interval.

Near a singular point, r_s, the expressions for f and g reduce to

$$f = \alpha x^2, \qquad \alpha > o,$$

$$g = \beta \quad , \tag{1.35}$$

where $x = |r - r_s|$. The expressions for α and β are obtained from eqs.(1.30) and (1.32):

$$\alpha = \frac{r_s B_\theta^2 B_z^2}{B^2} \left(\frac{d\ell n\mu}{dr}\right)^2,$$

$$\beta = \frac{2B\theta^2}{B^2} \frac{dp}{dr} \quad , \tag{1.36}$$

where $\mu = B_\theta/rB_z$ and $B^2 = B_\theta^2 + B_z^2$. As α and β are constants, the Euler-Lagrange equation becomes

$$\alpha \frac{d}{dx}\left(x^2 \frac{d\xi}{dx}\right) - \beta\xi = 0, \tag{1.37}$$

which has solutions x^{-n_1} and x^{-n_2} where n_1 and n_2 are the roots of the equation

$$n^2 - n - \beta/\alpha = 0 \quad . \tag{1.38}$$

The roots are real if $\alpha + 4\beta > 0$ and this reduces to Suydam's necessary condition:[58]

$$\frac{r}{8} B_z^2 \left(\frac{d\ell n\mu}{dr}\right)^2 + \frac{dp}{dr} > 0 \ , \tag{1.39}$$

where all quantities are evaluated at r_s. We shall assume that Suydam's necessary condition for stability is satisfied, then n_1 and n_2 are real. We take $n_1 < n_2$ and the solution proportional to x^{-n_2} is called the large solution. The other is called the small solution, although it may tend to infinity at the singular point. The small solution at $r = 0$ is defined with $\xi(0) = 0$ for $m \neq 1$ and $\xi'(0) = 0$ for $m = 1$.

In terms of these definitions, the necessary and sufficient conditions for stability can be stated as follows. The simplest of the criterion is:

(a) for specified m and k, an equilibrium configuration is stable in an independent sub-interval if and only if the solution of the Euler-Lagrange equation that is small at one singular point is not zero at any interier point of the sub-interval.

Other criterion can be derived that are equivalent to the above statement but are more useful for numerical test of stability.

One such set of conditions that is used in later chapters is as follows.

(b) For specified m and k, an equilibrium configuration is stable if and only if:

(i) Suydam's necessary condition is satisfied at the end points of the sub-interval if they are singular;

(ii) if $\xi_1(r)$ and $\xi_2(r)$ are the solutions of the Euler-Lagrange equation satisfying

$$\xi_1(r) \text{ is small at } r_1 \quad , \qquad \xi_1(r_0) = 1$$

$$\xi_2(r) \text{ is small at } r_2 \quad , \qquad \xi_2(r_0) = 1$$

where r_0 is some interior point of a sub-interval $[r_1, r_2]$, and if

$$\xi_0(r) = \begin{cases} \xi_1(r) & , \quad r_1 < r < r_0 \\ \xi_2(r) & , \quad r_0 < r < r_2 \end{cases}$$

then ξ_0 does not vanish anywhere in the sub-interval $[r_1, r_2]$;

(iii) and

$$\xi_1'(r_0) > \xi_2'(r_0) \quad . \tag{1.40}$$

Until now, it is assumed that the plasma is bounded by a conducting shell at r = b. Let us now suppose the case where the pressure vanishes at r = a and the region between r = a and r = b

is replaced with a vacuum. In this region the potential energy is described as

$$W_V = \frac{\pi}{2}\int_a^b (\text{rot } \vec{a})^2 \, d\vec{r} \quad , \tag{1.41}$$

where $\vec{a}$ represents vector potential of the perturbed magnetic field. The r component of the perturbed magnetic field in the vacuum region, b_r, is given by

$$ib_r \equiv \psi(r) = C_1 I_m'(kr) + C_2 K_m'(kr), \tag{1.42}$$

where I_m and K_m are modified Bessel functions and C_1 and C_2 are constants. In the vacuum region, Newcomb's criterion must be applied to ψ instead of ξ. Thus the boundary conditions are that ψ is continuous at the plasma boundary(i.e., the r component of the perturbed magnetic field is continuous,as a diffuse pinch will be treated) and $\psi = 0$ at $r = b$.

Newcomb has shown that a vacuum and a pressureless plasma are equally stable if there is no singular point in the vacuum region, but the pressureless plasma is more stable if there is a singular point.

§ 3 Growth Rate of MHD Instability[32)]

We shall investigate the growth rate of MHD instability in a diffuse linear pinch. For this purpose we introduce cylindrical coordinate r, θ, z about the axis of symmetry. Inhomogeneity of the pressure, the density, and the magnetic field is restricted to the r-direction. The field component, B_r, vanishes and the components B_θ and B_z depend only on r. The current density in the plasma is determined by Maxwell's equation (1.6); the radial component, Jr, therefore vanishes and the other components are given by

$$J_\theta = -\frac{dB_z}{dr} \quad , \tag{1.43}$$

$$J_z = \frac{1}{r}\frac{d}{dr}(rB_\theta) \quad . \tag{1.44}$$

The radial distribution of the plasma pressure p is governed by the MHD equilibrium equation (1.8), which reduces to

$$\frac{dp}{dr} + B_z\frac{dB_z}{dr} + \frac{B_\theta}{r}\frac{d}{dr}(rB_\theta) = 0 \quad . \tag{1.45}$$

In this section, there is no essential difference between the analysis for a compressible plasma and for an incompressible one. Because the equations for the incompressible plasma can be easily derived from those for the compressible one, we shall give the derivation for a compressible plasma.

Starting from eq.(1.18) and taking normal mode solutions

$$\vec{\xi} = (\xi_r(r), \xi_\theta(r), \xi_z(r))e^{\omega t+im\theta-ikz} \quad , \tag{1.46}$$

we obtain three coupled equations:

$$\begin{pmatrix} \omega^2\rho\mu/r \\ i\omega^2\rho(rB_\theta\eta - kr\zeta)/(mB_\theta - krB_z) \\ i\omega^2\rho(m\zeta - rB_z\eta)/(mB_\theta - krB_z) \end{pmatrix} = \begin{pmatrix} (-F^2/r - 2B_\theta(\frac{B_\theta}{r})'/r)\mu + \\ -i\,(2kB_\theta B_z/r^2)\mu + \\ i(2kB_\theta^2/r^2)\mu + \end{pmatrix}$$

$$\begin{pmatrix} + ((\gamma p/r + B^2/r)\mu')' + \gamma(p\eta)' + \{(kB_\theta + mB_z/r)\zeta\}' + 2(kB_\theta/r)\zeta \\ + i(\gamma mp/r^2 + B_z(mB_z/r + kB_\theta)/r)\mu' + i(\gamma mp/r)\eta + i((k^2 + m^2/r^2)B_z)\zeta \\ - i(\gamma kp/r + B_\theta(mB_z/r + kB_\theta)/r)\mu' - i\gamma kp\eta - i((k^2 + m^2/r^2)B_\theta)\zeta \end{pmatrix}$$

(1.47.a)
(1.47.b)
(1.47.c)

where we have used the variables $\mu = r\xi, \eta, \zeta$ (see eq. (1.20)) and accents mark differentiation with respect to r.
From eqs. (1.47.b) and (1.47.c) we can derive

$$\eta = (2kB_\theta\omega^2\rho\,(kB_\theta + mB_z/r)\,/\,Nr^2)\mu + \\ -\{(\gamma pG(\omega^2\rho + F^2) - \omega^2\rho\,(kB_\theta + mB_z/r)^2)/Nr\}\,\mu' \qquad (1.48)$$

and

$$\zeta = (2kB_\theta(\omega^2\rho B^2 + \gamma pF^2)/Nr^2)\mu \\ - \{(kB_\theta + mB_z/r)\,(\gamma pF^2 + \omega^2\rho(\gamma p + B^2))/Nr\}\mu' \,, \qquad (1.49)$$

where $N = \omega^4\rho^2 + \omega^2\rho G(\gamma p + B^2) + G\gamma pF^2$

$F = mB_\theta/r - kB_z$

and $G = k^2 + m^2/r^2$.

Equation (1.47.a) can be rewritten as

$$- \{ (\omega^2\rho + F^2 + 2B_\theta(B_\theta/r)')/r\}\mu + [\{(\gamma p + B^2)/r\}\mu' + \gamma p\eta$$

$$+ (kB_\theta + mB_z/r)\zeta]' + (2kB_\theta/r)\xi = 0 \quad . \tag{1.50}$$

Substitution of eqs.(1.48) and (1.49) into eq.(1.50) reduces

$$[\frac{(\omega^2\rho + F^2)\ \{\omega^2\rho(\gamma p + B^2) + \gamma pF^2\}}{N} \cdot \frac{1}{r}(r\xi)']'$$

$$+ [- \omega^2\rho - F^2 - 2B_\theta(\frac{B_\theta}{r})' + \frac{4k^2B_\theta^2}{r} \frac{\rho\omega^2B^2 + \gamma pF^2}{N}$$

$$+ r \{ \frac{2kB_\theta(mB_z/r + kB_\theta)}{r^2} \frac{\rho\omega^2(\gamma p + B^2) + \gamma pF^2}{N} \}']\xi = 0 \ , \tag{1.51}$$

where we have used the relation $\mu = r\xi$. Here ρ, ω and γ are the density, the growth rate and the ratio of specific heats, respectively.

When we tend γ to infinity, we obtain another second order

differential equation :

$$[\, a(r\xi)' \,]' - b\xi = 0$$

where $$a = \frac{r(\omega^2\rho + F^2)}{k^2r^2 + m^2}$$

and $$b = \omega^2\rho + F^2 - 2B_\theta(\frac{B\theta}{r})' + 2mr\,[\frac{FB\theta}{r(k^2r^2 + m^2)}]'$$

$$- \frac{4k^2F^2B\theta^2}{(k^2r^2 + m^2)\,(\rho\omega^2 + F^2)} \quad . \tag{1.52}$$

Equation (1.52) is equivalent to that derived by Freidberg[33] and describes incompressible motion of a plasma.

Also when we tend ω^2 to zero in eq.(1.51) or eq.(1.52), we obtain a marginal equation equivalent to a Euler-Lagrange equation (1.33). These procedures will make the physical picture of Newcomb's criterion clear.

§ 4 Resistive Tearing Instability[38)]

The following set of equations defines the model we work with.

$$\rho \frac{d\vec{v}}{dt} = - \text{grad } p + \vec{J} \times \vec{B} \quad , \tag{1.1}$$

$$\frac{\partial \rho}{\partial t} + \text{div } (\rho \vec{v}) = 0 \quad , \tag{1.2}$$

$$\vec{E} + \vec{v} \times \vec{B} = \eta \vec{J} \quad , \tag{1.3'}$$

$$\frac{\rho^{\gamma}}{\gamma - 1} \frac{d}{dt} (p \rho^{-\gamma}) = \eta J^2 \quad , \tag{1.4'}$$

$$\text{rot } \vec{E} = - \frac{\partial \vec{B}}{\partial t} \quad , \tag{1.5}$$

$$\text{rot } \vec{B} = \vec{J} \quad , \tag{1.6}$$

$$\text{div } \vec{B} = 0 \quad . \tag{1.7}$$

In eqs. (1.3') and (1.4') we include resistivity η which is a constant scalar as a dissipative effect.

We examine the behavior of this system by looking for the growth of small perturbations near an equilibrium state. As the resistivity allows almost all configurations diffuse away, it is difficult to find a steady state solution of the above equations. The way we choose is to devise a limiting procedure in which the resistivity is small. Then it is reasonable that the growth rates of the instability are very much larger than the rate of resistive diffusion. This allows us to ignore the effect of resistivity on

the equilibria which we consider. The particular class of equilibria which we choose is the diffuse linear pinch.

Newcomb[23] throughly studied the stability of the diffuse linear pinch in the absence of resistivity, which has been shown in § 2. We will lean on Newcomb's work. Newcomb considered an infinitely long linear pinch. We differ slightly from Newcomb in making it periodic over a set length $2\pi/k$ and thus approximating a torus.

Now the basic equations are linearized around the equilibrium. For the dependent variables in these equations we choose the fluid displacement $\vec{\xi}$ and the magnetic field perturbation $\vec{b}$. We can take advantage of the symmetry of the problem to consider one Fourier mode

$$\vec{\xi} = \vec{\xi}(r)e^{(\omega t + im\theta - inkz)} \quad . \tag{1.53}$$

In terms of these quantities eq.(1.1) becomes:

$$-\rho\omega^2\vec{\xi} + (\vec{\nabla} \times \vec{B}) \times \vec{b} + (\vec{\nabla} \times \vec{b}) \times \vec{B}$$

$$+ \vec{\nabla} [\gamma p \operatorname{div} \vec{\xi} + \vec{\xi} \operatorname{grad} p - \frac{2\eta(\gamma-1)}{\omega} (\vec{\nabla} \times \vec{B}) \cdot (\vec{\nabla} \times \vec{b})] = 0. \tag{1.54}$$

The first is the inertia, the next two are the perturbed magnetic force, and the last contains the solution of the equation of state for the perturbed pressure. To obtain an equation for the magnetic field perturbation we combine Ohm's law (1.3') and Maxwell's equations (1.5) ~ (1.7) :

$$\vec{b} + \frac{\eta}{\omega} \vec{\nabla} \times \vec{\nabla} \times \vec{b} = \vec{\nabla} \times (\vec{\xi} \times \vec{B}) \quad . \tag{1.55}$$

We want to examine the behavior of eqs.(1.54) and (1.55) in the limit as the resistivity vanishes. We will assume that the growth rate is proportional to a fractional power of the resistivity. Thus it is much larger than diffusion which vanishes linearly with the resistivity, and much smaller than the growth rates of MHD instabilities which are independent of the resistivity. From eqs. (1.54) and (1.55) this limit ($\eta \to 0$) leads straight to the Euler-Lagrange equation (1.33) which Newcomb studied. This equation is well behaved everywhere except near the radius which is called as a singular point in § 2. Such a radius, where the displacement becomes infinite, must satisfy

$$q(r) \equiv \frac{B_\theta(r)}{krB_z(r)} = \frac{n}{m} \quad . \tag{1.56}$$

Here q is called as a safty factor in the MHD stability analysis of Tokamak type devices.

In this case we need to re-do the calculation only in a small region near the singular point in order to obtain displacement which is finite everywhere. Clearly if the displacement is large inertia will be important. It is also true that the current diverges at the singular point. Thus even a small resistivity may be as important as inertia in limiting the displacement. No matter how small the resistivity the term proportional to η in eq.(1.55) may be large near the singular point.

Equation (1.33) is an excellent approximation to eqs.(1.54) and (1.55) everywhere except near the singular point. It could have rewritten with the radial component of the perturbed magnetic field:

$$\psi = (nkrB_z - mB_\theta)\, \xi_r/r \quad , \tag{1.57}$$

$$\frac{d}{dr} f^* \frac{d\psi}{dr} - f^* g^* \psi = 0 \quad , \tag{1.58}$$

where

$$f^* = \frac{r^3}{n^2k^2r^2 + m^2}$$

$$g^* = \frac{n^2k^2r^2 + m^2}{r^2} + \frac{(n^2k^2r^2 - m^2)}{r^2(n^2k^2r^2 + m^2)} + \frac{2n^2k^2r^2}{(nkrB_z - mB_\theta)} \left(\frac{1}{rar}\frac{dp}{}\right)$$

$$- \frac{(nkrB_z + mB_\theta)}{(nkrB_z - mB_\theta)} \left(\frac{2}{rB^2}\frac{dp}{dr}\right) + \frac{(nkrB_\theta + mB_z)}{(nkrB_z - mB_\theta)} \left(\frac{2\sigma}{B^2}\frac{dp}{dr} - \frac{d\sigma}{dr}\right)$$

$$- \frac{1}{r}\frac{d}{dr}\left(\frac{r}{B^2}\frac{dp}{dr}\right) + \frac{2n^2k^2r^2}{n^2k^2r^2 + m^2}\left(\frac{1}{rB^2}\frac{dp}{dr}\right) + \left(\frac{1}{B}\frac{dp}{dr}\right)^2 + \frac{2mnk\sigma}{n^2k^2r^2+m^2} - \sigma^2$$

and $$\sigma = \frac{\vec{J}\cdot\vec{B}}{B^2} \quad .$$

In the outer regions there is dissipationless, slow, inertia-free motion. We call these the 'hydromagnetic regions'. In a thin layer near the singular point, which we will call the 'resistive layer', we must search for a different set of equations in which resistivity and inertia both play a role. Within a resistive layer some terms of eqs.(1.54) will be more important than others. This evaluation depends upon the relative size of the resistive layer and on the growth rate of the instability. If the pressure gradients near the singular point are too small to drive an interchange instability, a slower instability driven by forces in the hydromagnetic region may be present. We usually use the name tearing modes to denote this type of modes. Thus we consider tearing ordering $\omega \propto \eta^{3/5}$ treated in CGJ.[38]

We can obtain the boundary condition for the inner equations by

matching to the solution of Euler-Lagrange equation in the hydromagnetic region. We must use the solution which satisfies the proper boundary condition at the outer boundary or at the axis of the system. If the solution vanishes at any point outside the resistive layer the system is hydromagnetically unstable by the Newcomb's criterion and the small resistivity has no important effect. We therefore restrict consideration to cases in which Newcomb's criterion is satisfied. To obtain the boundary condition for the inner region by a procedure of matching we only need the logarithmic derivative of the outer solution at the outer edge of the resistive layer. In the treatment of the tearing ordering it is convinient to match the logarithmic derivative of ψ.

Near the singular point $r = r_s$, the asympototic form of ψ near r_s is obtained from eq.(1.58)

$$\psi = [\ C_1 + C_2 \frac{2\pi B^2 \sigma'}{k\iota' B_z{}^2} \ell n\ |\frac{r - r_s}{r_s}|\ ][\frac{r - r_s}{r_s} + \cdots\cdots\ ]$$

$$+ C_2[\ 1 + \cdots\cdots] \quad , \tag{1.59}$$

where $\iota \equiv 2\pi B_\theta / krB_z$ and accent denotes the derivatice with respect to r. In eq.(1.59) the term with coefficient C_1 corresponds to a small solution and the term with C_2 corresponds to a large solution in the terminology of § 2. The ratio C_1/C_2 is the significant quantity which determines the matching.

In the inner region the solution for ψ is obtained in CGJ:[38]

$$\psi = \psi_0[\ 1 + D\ell n|X| + \cdots\cdot] + [\ E + \psi_0 \frac{2\pi B^2 \sigma'}{k\iota' B_z{}^2} \ell n|\frac{r - r_s}{r_s}|\ ]$$

$$\times [\frac{r - r_s}{r_s} + \cdots\cdots] \ , \tag{1.60}$$

for large negative X, where $X = (r - r_s)/(\ell L_R)$, $\ell = (L_R/r_s)^{1/5}$

$$D = -\frac{2p'l^2}{r_s B_z{}^2 l'^2}\bigg|_{r=r_s} , \qquad L_R = \left(\frac{B^2 r_s{}^2 a^2}{m^2 B_z{}^2 l'^2}\right)^{1/6} S^{-1/3}$$

$$Q_R = \left(\frac{m^2 l'^2 B_z{}^2 r_s^4}{B^2 a^2}\right)^{1/3} S^{-1/3} \tau_H^{-1} , \text{ and } E, \psi_0 \text{ are constants.}$$

Here S is the ratio of resistive time $\tau_R = a^2/\eta$ to hydromagnetic time $\tau_H = a\sqrt{\rho}/B$. We must choose E and ψ_0 so that eq.(1.60) matches the solution in the outer region. The term proportional to D is small in the outer region. Thus if we set

$$E = \psi_0 \left(C_1^{(-)}/C_2^{(-)}\right) , \tag{1.61}$$

the two solutions match, where $C_1^{(-)}$, $C_2^{(-)}$ are coefficients of eq. (1.59) in $r < r_s$. If this solution is continued to large positive value of X, we obtain

$$\psi = \psi_0[\, 1 + D\ell n|X| + \cdots\cdot] + \psi_0 \left[\frac{C_1^{(-)}}{C_2^{(-)}} + \Delta(Q) + \frac{2\pi B^2 \sigma'}{k l' B_z{}^2} \ell n \left|\frac{r - r_s}{r_s}\right|\right]$$

$$\times \left[\frac{r - r_s}{r_s} + \cdots\cdot\right] , \tag{1.62}$$

here $$\Delta(Q) = \lim_{X\to\infty} [\psi'(X) - \psi'(-X)]/\psi_0 . \tag{1.63}$$

This matches the solution in the outside region (see eq.(1.59)),

if

$$\Delta(Q) = \Delta \equiv ({C_1}^{(+)}/{C_2}^{(+)}) - ({C_1}^{(-)}/{C_2}^{(-)}), \qquad (1.64)$$

where ${C_1}^{(+)}$ and ${C_2}^{(+)}$ are coefficients of eq.(1.59) in $r > r_s$. This condition (1.64) determines the growth rate of tearing modes $Q = \omega/Q_R \ell^4$. From the equation in the inner region, an explicit expression for $\Delta(Q)$ can be obtained. Following CGJ,[38] we find

$$\Delta(Q) = (\pi/4\ell^6 Q^{1/4}) F(a,b,c) \qquad (1.65)$$

with

$$F(a,b,c) = [a-D + \frac{D+a^2b-Dab+ac}{d}] \frac{\Gamma\{\frac{1}{4}(3+ab-d)\}}{\Gamma\{\frac{1}{4}(5+ab-d)\}}$$

$$+ [a - D - \frac{D+a^2b-Dab+ac}{d}] \frac{\Gamma\{\frac{1}{4}(3+ab+d)\}}{\Gamma\{\frac{1}{4}(5+ab+d)\}}$$

where $a = \ell^6 Q^{3/2}$, $b = 1/\gamma\beta$, $C = (\frac{k_1 r}{\pi l})^2$, $d^2 = a^2b^2 + 2Db - C$, $\beta = 2p(r_s)/B^2$ and Γ denotes the Gamma function.

The resistive skin depth L_η is defined in CGJ as

$$L_\eta = L_R(\frac{\omega}{Q_R})^{1/4} . \qquad (1.66)$$

A sufficient condition for stability

$$\Delta < 0 \quad ; \quad D \leqslant 0 \qquad (1.67)$$

is obtained by noticing that $\Delta(Q)$ of eq.(1.65) is positive if D vanishes or is negative.

When D vanishes, $\Delta(Q)$ vanishes as ab becomes small and d tends to zero. Thus in this case

$$\Delta < 0 \tag{1.68}$$

is the necessary and sufficient condition for stability against tearing modes.

Furthermore when β is very small, F becomes

$$F(a,b,c) = (2a - 3D)\frac{\Gamma\{\frac{1}{4}(3-\frac{D}{a})\}}{\Gamma\{\frac{1}{4}(5-\frac{D}{a})\}} + D \tag{1.69}$$

Equation (1.65) will be used for reverse field pinches in Chapter II and eq.(1.69) will be used for Tokamak systems in Chapter V.

CHAPTER II

STABILITY OF REVERSE FIELD DIFFUSE PINCHES[27)]

§ 1 Introduction

The MHD stability of axially symmetric linear pinches has been investigated for more than a decade. Kruskal [21)] and Shafranov[22)] have derived the so called K.S.limit for stability with respect to the kink (or helical) instability, when the axial magnetic field B_z is nearly uniform. Taylor[59)] considered the MHD stability of the stabilized pinch with skin currents, in which B_z field drops nearly to zero in the outside of the plasma column. Rosenbluth[24)] has carefully studied the structure of the skin current layer and has shown that the stabilized pinch configuration is actually unstable unless the B_z field is reversed in the outside of the main plasma.

In actual plasmas, skin current distribution can not be realized and we always have diffused current configurations or diffuse pinches. The investigation of the MHD stability of diffuse pinches has been facilitated by the powerful method due to Newcomb,[23)] which has been shown in § 2 of Chapter I. Corpley and Whiteman[25)] have studied numerically the stability of some examples of reverse field diffuse pinches, which are characterized by skin like current profiles, by use of Newcomb's criterion. Robinson[26)] also has obtained a semi-quantitative analytic expression of the position of the conducting shell for the threshold of stability and other useful relations in the case of reverse field configuration.

Furth, Rosenbluth and Killeen[35)] have demonstrated that if we include resistivity in the MHD equations, a pinch plasma stable within the ideal MHD analysis can become vulnerable to the resistive

instabilities. Thus, we need to study the stability against the resistive modes, in particular, non-local tearing modes. The stability against resistive tearing instabilities in diffuse pinches is not sufficiently investigated until now.

It is the purpose of this Chapter to study the stability of reverse field diffuse pinches against MHD instabilities and tearing modes. We first give a variety of equilibria by modifying force free configurations. Our basic parameters to characterize equilibrium are the profile of the J_z current distribution, which is an essential feature of our model equilibrium, the ratio between the values of B_z at the axis and at the conducting shell and the averaged beta. This method makes it possible to examine the stability in various equilibrium configurations and to find plasma parameters suitable for controlled thermonuclear fusion research as well as to confirm results obtained by above mentioned authors. The region outside the plasma column is assumed to be a vacuum in contrast with the screw pinch case.[3),4)] The position of conducting shell for threshold of the stability, R_W, is calculated numerically for several classes of the above parameters. The stability diagrams thus obtained include the followings; (i) R_W versus the J_z current profile, (ii) R_W versus average β and (iii) R_W versus the degree of field reversal.

The stability of the stabilized pinch is also briefly discussed and it is shown to be unstable against the MHD instability.

It is important to know the growth rate of the MHD instability, when the equilibrium configuration fails to satisfy Newcomb's criterion and becomes unstable. Hence the growth rates of the MHD instability for typical unstable configurations are calculated. The information of the profile of the displacement is also obtained.

The analysis of the stability against the resistive tearing instability is done with the method of CGJ.[38)] It is shown that the reverse field configuration is vulnerable to the tearing instability when the pressure profile is nearly flat in the central region of the plasma column.

In § 2, the method to solve the equilibrium equation is described. In § 3, we test the MHD stability of several reverse field diffuse pinches by means of Newcomb's criterion. In § 4, the growth rate of the MHD instability is calculated for some typical unstable configurations. Section 5 is devoted to the analysis of the stability against the resistive tearing modes. The results are discussed in § 6.

§ 2 MHD Equilibrium

In this section, we describe the method to obtain the MHD equilibria defined by eqs. (1.8) ~ (1.10). We consider axisymmetric linear pinch configurations given by

$$J_\theta = -\frac{dB_z}{dr}, \qquad J_z = \frac{1}{r}\frac{d}{dr}(rB_\theta)$$

$$\frac{dp}{dr} = J_\theta B_z - J_z B_\theta, \tag{2.1}$$

in the cylindrical coordinates (r,θ,z).

It should be noted that there are five unknown quantities $P(r)$, $B_\theta(r)$, $B_z(r)$, $J_\theta(r)$ and $J_z(r)$, while there are three relations between them. Therefore we must give any two functions to specify an equilibrium configuration. As we are interested in the J_z current profile, let us first give $J_z(r)$. From the second equation of (2.1), $B_\theta(r)$ is obtained. Now we construct a force free field $J_\theta^{(0)}$, $B_z^{(0)}$ from these J_z and B_θ,

$$J_\theta^{(0)} B_z^{(0)} - J_z B_\theta = 0, \quad J_\theta^{(0)} = -\frac{dB_z^{(0)}}{dr}. \tag{2.2}$$

Integrating eqs. (2.2), we get

$$B_z^{(0)}(r) = \pm\sqrt{(B_z^{(0)}(0))^2 - 2\int_0^r J_z B_\theta dr}. \tag{2.3}$$

Next we modify $B_z^{(0)}$ by $B_z^{(1)}$ to support a plasma pressure,

$$B_z(r) = B_z^{(0)}(r) + B_z^{(1)}(r). \qquad (2.4)$$

Then the pressure becomes

$$p(r) = p_0 - \frac{1}{2} B_z^{(1)}(r)(2B_z^{(0)}(r) + B_z^{(1)}(r)), \qquad (2.5)$$

where p_0 is a constant. This method of constructing equilibria has the advantage that we can obtain any desired pressure profile easily by appropriately choosing $B_z^{(1)}$.

As parameters to specify a J_z current distribution we use α and δ shown in Fig.II-1. The expression for a J_z current profile is given in the form

$$\left.\begin{aligned} J_z &= \alpha && (0<r/a\leqslant 1-\delta) \\ &= 1 + 4(\alpha-1)\left(\frac{r}{a} + \frac{\delta}{2} - 1\right)^2/\delta^2 && (1-\delta<r/a\leqslant 1-\frac{\delta}{2}) \\ &= 1 - 4\left(\frac{r}{a} + \frac{\delta}{2} - 1\right)^2/\delta^2 && (1-\frac{\delta}{2}<r/a\leqslant 1.0) \end{aligned}\right\} \qquad (2.6)$$

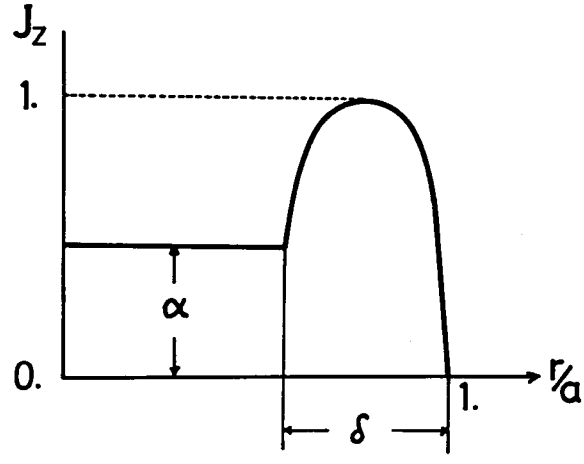

Fig.II-1. J_z current distribution; α and δ characterize the distribution.

Two more parameters characterize our equilibrium configurations. The one parameter denotes the ratio R_B defined by

$$R_B = \frac{B_z(b)}{B_z(0)} , \tag{2.7}$$

where $B_z(b)$ and $B_z(0)$ denote the value of B_z at the conducting shell r = b and at the axis, respectively. The other parameter to characterize a configuration is the average β,

$$\beta = \int_0^a \frac{2\int_0^a prdr}{(B_z^2 + B\theta^2)rdr} \times 100 . \tag{2.8}$$

In the case of reverse field pinches it is convenient to take $B_z^{(0)} = 0$ in a<r<b and to choose $B_z^{(1)}$ in the form shown in Fig.II-2. From eq.(2.3), we determine $B_z^{(0)}(0)$, then calculate $B_z^{(0)}(r)$ in 0<r<a. $B_z^{(1)}(0)$ and $B_z^{(1)}(a)$ are given numerically according to the value of $B_z^{(0)}(0)$, then $B_z^{(1)}(r)$ is determined by means of interpolation. Hence, we get

$$\left.\begin{aligned} p_0 &= \frac{1}{2}\{B_z^{(1)}(b)\}^2 , \\ R_B &\simeq B_z^{(1)}(b) \,/\, B_z^{(0)}(0), \\ \beta &\simeq \frac{B_z^{(1)}(0)}{B_z^{(0)}(0)} + \frac{\{B^{(1)}(b)\}^2}{2\{B_z^{(0)}(0)\}^2} , \end{aligned}\right\} \tag{2.9}$$

where p_0 has been determined from the condition $p(a) = 0$ and the relation $B_z^{(1)} \ll B_z^{(0)}$ has been used. Figure II-3 illustrates a reverse field configuration thus obtained and Fig.II-4 shows its pitch variation (here, the pitch of the magnetic field line is defined by rB_z/B_θ).

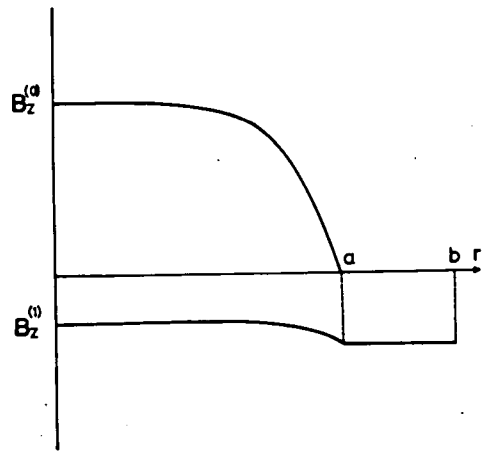

Fig.II-2. $B_z^{(0)}$ and $B_z^{(1)}$ which give a reverse field pinch.

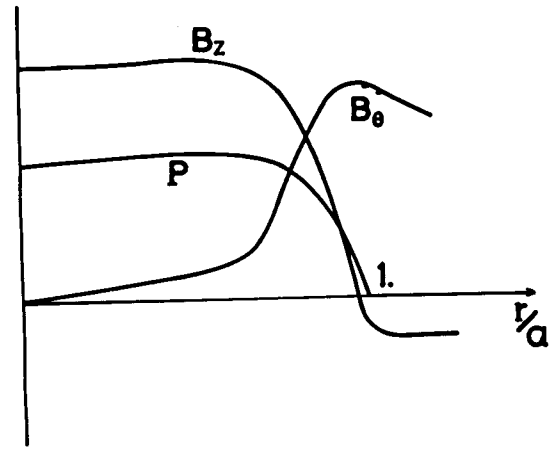

Fig.II-3. A reverse field configuration; β=20%, P_B=-0.18, α=0.1, δ=0.4.

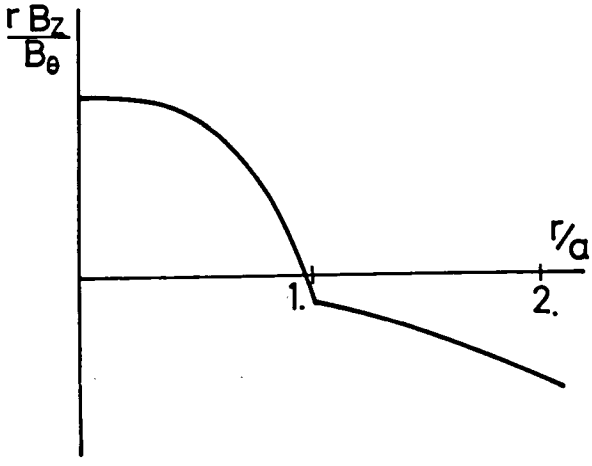

Fig.II-4. Pitch of magnetic field line in a reverse field pinch.

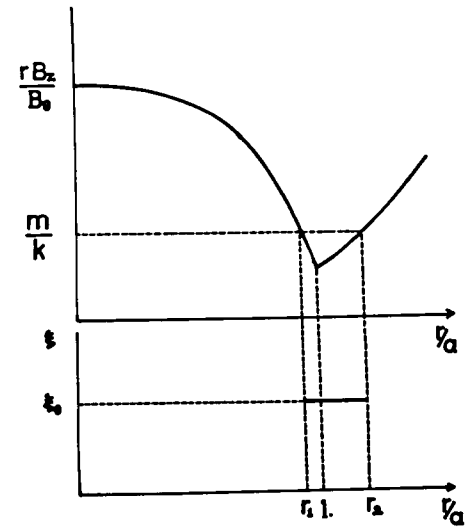

Fig.II-5. Pitch of magnetic field line in a stabilized pinch and displacement ξ which makes W negative.

For the case of stabilized pinches $B_z^{(0)}$ and $B_z^{(1)}$ are taken in the form shown in Fig.II-6. $B_z^{(0)}(r)$ and $B_z^{(1)}(r)$ are given by the same method as above mentioned. Thus in this case, we obtain

$$\left.\begin{aligned} p_0 &= 0 \ , \\ R_B &\simeq B_z^{(0)}(b) \,/\, B_z^{(0)}(0) \ , \\ \beta &\simeq B_z^{(1)}(0) \,/\, B_z^{(0)}(0) \ . \end{aligned}\right\} \qquad (2.10)$$

Figure II-7 illustrates a stabilized pinch configuration and Fig. II-5 shows its pitch variation.

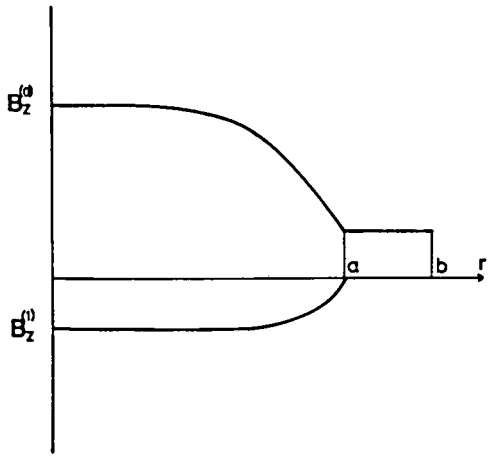

Fig.II-6. $B_z^{(0)}$ and $B_z^{(1)}$ which give a stabilized pinch.

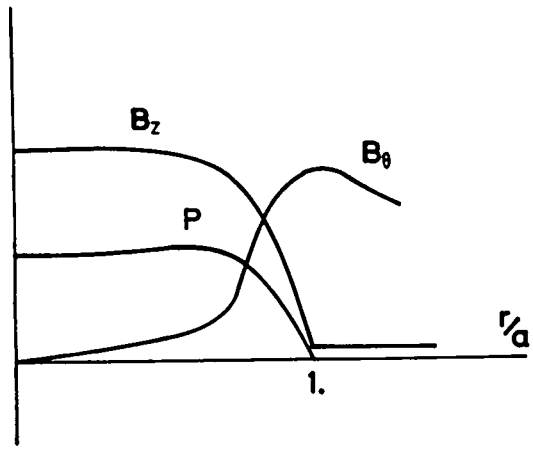

Fig.II-7. A stabilized pinch configuration; β=15%, R_B=0.05, α=0.1, δ=0.4.

§ 3 Test of MHD Stability by Means of Newcomb's Criterion

In this section, we test the stability of reverse field diffuse pinches obtained in § 2 by means of Newcomb's criterion. We assume that the region outside the main plasma column is surrounded by a vacuum, since this configuration gives more stringent condition for the stability than the case where a pressureless plasma surrounds the plasma as we have noted in § 2 of Chapter I.

Let us first consider reverse field configurations with negative R_B. Under these circumstances we have at most one singular point for specified m and k, considering eq. (1.34) or eq. (1.56) and the pitch variation shown in Fig.II-4. When no singular point is present, our procedure to analyze the stability is as follows. Starting from the small solution of eq. (1.33) at r = 0, we solve the Euler-Lagrange equation numerically with Hamming's modified predictor corrector method until the plasma boundary r = a. If the solution vanishes before the boundary, the configuration is unstable. If it does not, the zero point of the vacuum solution ψ obtained from the matching condition at r = a (see eq.(1.57)) determines the position of the conducting shell R_W for the threshold of the stability, since the plasma column becomes stable when the shell is located inside R_W. When one singular point exists and lies in the vacuum region, the procedure is the same as above according to the remark in the last paragraph in § 2 of Chapter I. When a singular point lies at r_s in the main plasma, we have to consider the two intervals $0<r<r_s$ and $r_s<r<a$, seperately. In the sub-interval $0<r<r_s$, we use Newcomb's criterion for the form of (1.40). All the configurations we have tested have proved stable in this interval only if Suydam's condition (1.39) is fulfilled at r_s. In the interval $r_s<r<a$, we solve the Euler-Lagrange equation starting from the small solution at r_s. Again the configuration is unstable if ξ vanishes before r = a. If it does not, the position of the conducting shell is obtained in the same way stated above.

In this way the position of the conducting shell for stability R_W (m,k) is determined for specified m and k. To assure the stability against every m and k modes, we must find the smallest value of R_W (m,k). According to § 2 of Chapter I, however, we only need to test the stability against the modes m = 0 as k → 0 and m = 1 for all values of k.

Figure II-8 shows the stability diagram of the configuration shown in Fig.II-3. We note that Suydam's condition can be satisfied everywhere in this configuration, because the pressure gradient is slightly positive near the axis and the pressure gradient is negative in the region where the shear is large. In Fig.II-8 the abscissa is the wave number k and the ordinate is R_W, normalized by the plasma radius a. The stable region lies below the curve. It is recognized that R_W must be less than 2.2 to assure the stability against all the modes.

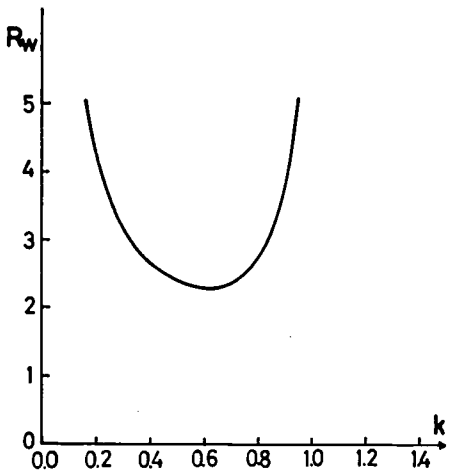

Fig.II-8. Stability diagram of the configuration shown in Fig. II-3. The abscissa is the wave number k and the ordinate is R_W, the position of the conducting shell for stability normalized by the plasma radius.

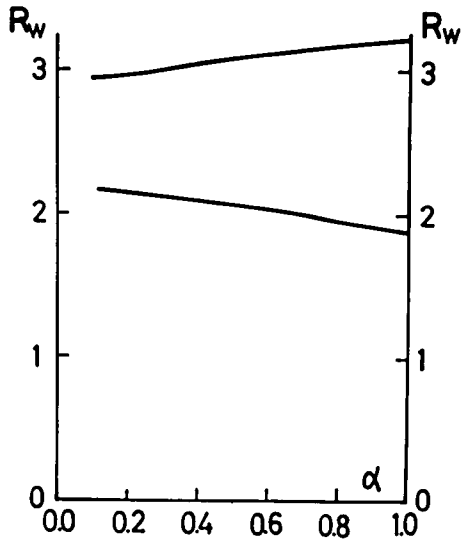

Fig.II-9. The position of the conducting shell to stabilize all modes as a function of α, in the case of β=15%, R_B=-0.2, δ=0.4. The upper line shows m=0 mode and the lower line shows m=1 mode.

Figures II-9 and II-10 show the position of the shell to stabilize all modes as a function of α and δ which characterize the current distribution (see Fig.II-1). The $\alpha = 0$ means a skin like current and $\alpha = 1$ gives a nearly uniform diffuse current.
For α = const, the stability improves as the width δ becomes small. For δ = const, the stability improves as α becomes small. Accordingly the stability condition becomes more stringent as the current distribution changes from a skin current to a uniform diffuse current. In Fig.II-9, we have not calculated for small α because $\delta = 0.4$ and $\alpha \to 0$ make an realistic current distribution.

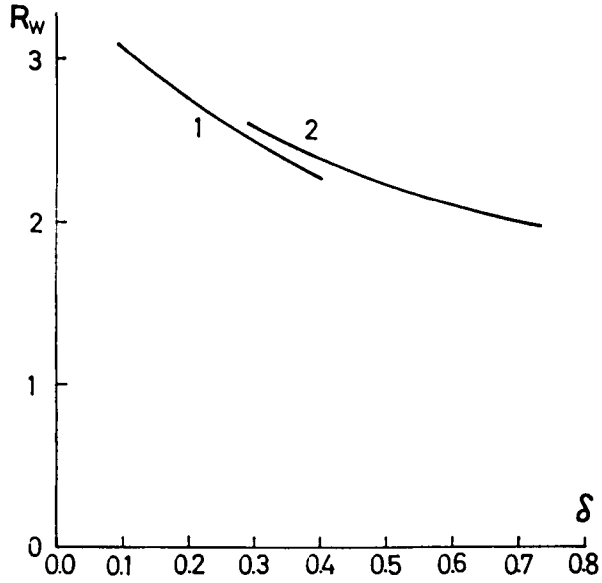

Fig.II-10. The position of the conducting shell to stabilize all modes as a function of δ. 1) $\beta = 19\%$, $R_B = 0$, $\alpha = 0.1$. 2) $\beta = 14\%$, $R_B = 0$, $\alpha = 0.1$.

Figure II-11 shows the position of the conducting shell as a function of the degree of field reversal. The stability against the m = 0 mode steadily improves as $|R_B|$ becomes large, while the stability against the m = 1 mode becomes worse. We note R_W has a minimum near R_B = -0.1 for the m = 0 mode.

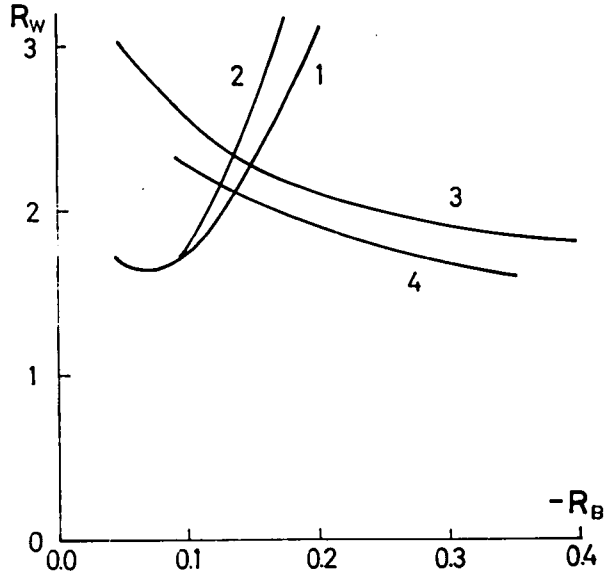

Fig. II-11. The position of the conducting shell as a function of the degree of field reversal for β = 15%. 1) m = 0 mode, α = 0.1, δ = 0.4. 2) m = 0 mode, α = 1.0. 3) m = 1 mode, α = 0.1, δ = 0.4. 4) m = 1 mode, α = 1.0.

Figure II-12 shows R_W versus plasma pressure β. The stability becomes worse as β becomes large. Beta can be as large as 50% if R_W is sufficiently close to one. We can also see that the stability condition becomes worse for the case of a diffuse current distribution than for the case of a skin like current.

Let us now briefly consider the case where $R_B>0$, i.e., the case of stabilized pinch. The pitch of the magnetic field line in the stabilized pinch shown in Fig.II-5 has a minimum at the surface of the plasma column. The pinch can be stabilized by a positive pressure

gradient near the pitch minimum point; however, as the pressure gradient is usually negative near the edge of the plasma column, the stabilized pinch is unstable.

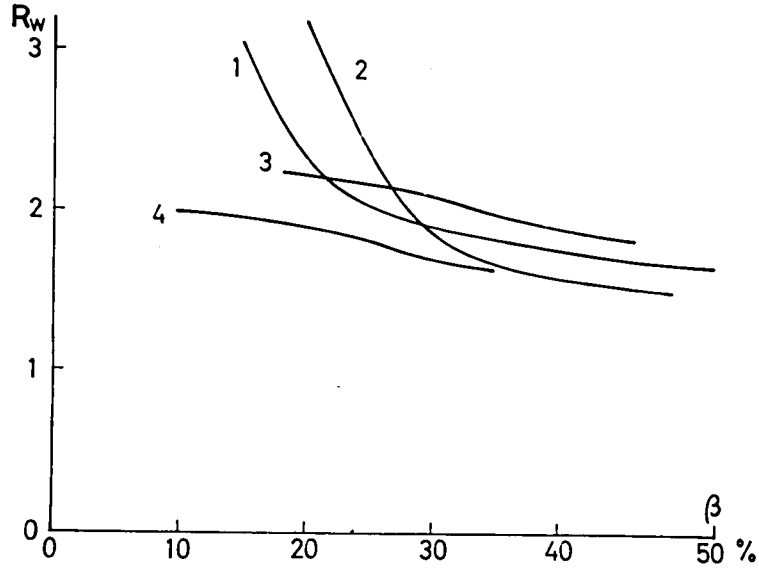

Fig.II-12. The position of the conducting shell as a function of plasma pressure β for R_B = -0.2. 1) m = 0 mode, α = 0.1, δ = 0.4. 2) m = 0 mode, α = 1.0. 3) m = 1 mode, α = 0.1, δ = 0.4. 4) m = 1 mode, α = 1.0.

We can understand the above fact by use of the energy integral (see eq.(1.29)).[29] Two singular points, r_1, r_2, or the Euler-Lagrange equation can appear near the pitch minimum point, r_{min}, for some (m,k). Then, as $(m/k - rB_z/B_\theta)\big|_{r = r_{min}}$ can be made as small as desired by a proper choice of (m,k), the function g(r) becomes approximately $2k^2r^2dp/dr/(k^2r^2+ m^2)$ in $r_1<r<r_2$. If dp/dr<0, then g(r)<0 and the energy integral

$$W(\xi) = \frac{\pi}{2}\int_{r_1}^{r_2} g\xi^2 dr \simeq \frac{\pi}{2}\xi_0^2\int_{r_1}^{r_2} g dr<0, \qquad (2.11)$$

for the displacement $\xi = \xi_0 = \text{const}$ in $r_1<r<r_2$ and $\xi = 0$ otherwise (see Fig.II-5).

We have tasted numerically the possibility to stabilize the stabilized pinch by a small positive pressure gradient in the edge of the plasma. It has been recognized that a very small positive gradient, $1/p\ dp/dr \simeq 0.01$ is sufficient to stabilize the pinch; however, R_B should be less than 0.05 in order to make $P_W>2$.

§ 4 Growth Rate of MHD Instability

When the equilibrium configuration does not satisfy Newcomb's criterion, magnetohydrodynamic kink instability can occur. From the viewpoint of the experiment it seems important to estimate the growth rate of the kink instability. Such a calculation has been done by Freidberg[33] for the case of the screw pinch by means of eq. (1.52) for an incompressible plasma.

In order to calculate the growth rate, we use the equation of motion in the r direction (1.51). The boundary conditions belonging to eq.(1.51) are :

$$r\xi = 0 \quad \text{at } r = 0,$$

ξ connects with ψ given by eq. (1.57) at $r = a$,

and $\psi = 0$ at $r = b$,

where a and b denote the radius of the plasma column and of the conducting shell respectively. The eq.(1.51) includes compressibility of the plasma. The motivation for choosing this equation is that the growth rates obtained from incompressible displacements in general do not give the fastest ones.

When the equilibrium configuration does not satisfy Newcomb's criterion, we obtain the growth rate $\omega>0$ for ξ which satisfies the boundary conditions. Figure II-13 illustrates the form of the displacement $r\xi$ and the magnetic penturbation ψ in the reverse field pinch configuration. The magnetic perturbation ψ in the plasma region is derived from ξ by use of eq.(1.57). From this figure the displacement of m = 1 mode is nearly constant over the plasma column. The configuration used to obtain the displacement is the reverse field diffuse pinch with $\alpha=1.0$.

We calculated the growth rates for two cases: the one is b = 2.5 and the other is b = 3.0. The wave number k was chosen so as to give

the smollest Rw in the test of Newcomb's criterion.

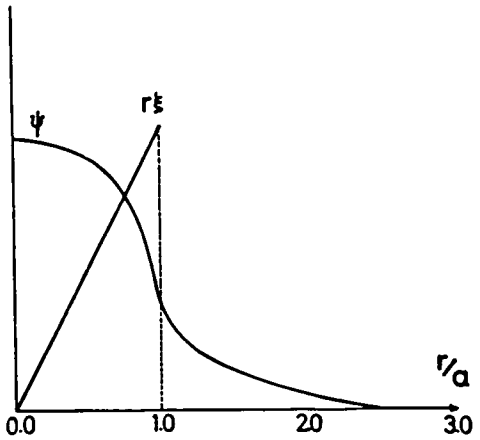

Fig.II-13. The form of displacement $r\xi$ and the magnetic field perturbation ψ for the case of ω_N=0.707, b=2.5, β=41%, R_B=-0.2, α=1.0, calculated for the mode m=1 and k=0.9.

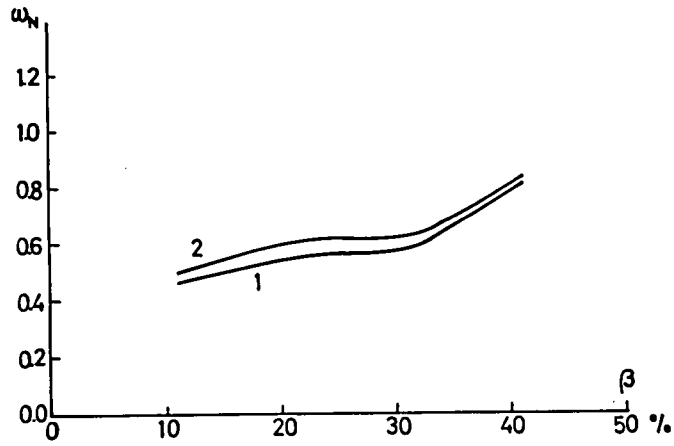

Fig.II-14. The growth rate ω_N as a function of plasma pressure β for R_B=-0.2, α=1.0. 1) b=2.5, 2) b=3.0.

In Fig.II-14, ω_N denotes the growth rate normalized by the transit time of Alfvén wave defined by $a\rho(0)/\sqrt{B_\theta(a)}$. Figure II-14 shows that the growth rate becomes smaller as β becomes smaller. It also shows that the growth rate gets larger when the position of conducting shell is placed more far from the plasma column.

Up to here, we calculated the growth rates of kink modes. If the pressure gradient near the center of the plasma column becomes negative, Suydam's necessary condition (1.39) cannot be satisfied. Hence the so-called 'Suydam' mode or interchange mode can appear. For example, we show the growth rates of Suydam mode and kink mode in the equilibrium characterized by β = 24%, R_B = -0.2, α = 1.0 and b = 2.0. The growth rate of Suydam mode is ω_N = 0.019 which is much smaller than the growth rate of kink mode ω_N = 0.417.

§ 5 Resistive Tearing Instability

Up to this section we have investigated the stability of the diffuse pinch by use of the ideal MHD equations with infinite conductivity. As we have shown in § 4 of Chapter I, if we include resistivity in MHD equations, a pinch plasma stable within the ideal MHD analysis becomes vulnerable to resistive instabilities. CGJ have considered the resistive instabilities in a diffuse linear pinch with a cylindrical configuration and have also included the effect of finite beta. We shall follow the method of CGJ to analyze the stability of reverse field configurations given in § 2 against the resistive tearing instability.

We had some difficulty when we applied the CGJ theory of the tearing mode to the reverse field configuration given in § 2. The numerically calculated ψ does not easily coincide the theoretical form of eq.(1.59), owing to the finite pressure gradient. Therefore we have decided to take the following procedure in order to match the asymtotic form to the CGJ theory. We deliberately make a constant pressure region in the center of the plasma column by adjusting $B_z^{(1)}(r)$ of eq.(2.5). $B_z^{(1)}(0)$ and $B_z^{(1)}(a)$ are given to make a profile shown in Fig.II-2, by use of the value of $B_z^{(0)}(0)$. For $r \lesssim 0.8$, we make the pressure equal to $\bar{p}$ by determining $B_z^{(1)}(r)$ from eq.(2.5),

$$B_z^{(1)}(r) = -B_z^{(0)}(r) + \sqrt{\{B_z^{(0)}(r)\}^2 - 2(\bar{p} - p_0)} \ , \qquad (2.12)$$

where $p_0 = \frac{1}{2}\{B_z^{(1)}(a)\}^2$

and $\bar{p} = p_0 - \frac{1}{2} B_z^{(1)}(0)(2B_z^{(0)}(0) + B_z^{(1)}(0))$.

For otherwise $B_z^{(1)}(r)$ is extrapolated to the value of $B_z^{(1)}(a)$.

As this assumption makes the parameter D (see eq.(1.60)) equal to zero, the relation for the growth rate of the tearing mode, eq.(1.65), becomes:

$$\Delta(Q) = \frac{\pi}{4\ell^2 Q^{1/4}} F(a, b, c) \tag{2.13}$$

and

$$F(a, b, c) = [a + \frac{a^2 b + ac}{d}] \frac{\Gamma\{\frac{1}{4}(3 + ab - d)\}}{\Gamma\{\frac{1}{4}(5 + ab - d)\}}$$

$$+ [a - \frac{a^2 b + ac}{d}] \frac{\Gamma\{\frac{1}{4}(3 + ab + d)\}}{\Gamma\{\frac{1}{4}(5 + ab + d)\}} , \tag{2.14}$$

where $a = \ell^6 Q^{3/2}$, $b = 1/\gamma\beta$, $c = (\frac{k_1}{\pi_1'})^2$, $d^2 = a^2 b^2 - c$ and $Q = \omega/Q_R \ell^4$.

The numerical analysis of the stability against tearing modes was performed by changing parameters β and R_B. Numerically calculated values of Δ, ω and L_η defined by eq.(1.66) are shown in Fig.II-15 ~ Fig.II-18. The conducting shell was placed at r = 1.5a to assure Newcomb's criterion for stability.

From these figures we observe that:

i) In the region $0.2<r/a<0.7$, resistive tearing instability can appear, since for m = 1 modes Δ's are always positive. The reverse field configurations, however, are stable against m = 2 mode when $r/a<0.65$ for parameter ranges $15\%<\beta<31\%$ and $-0.25<R_B<-0.05$.

ii) The growth rate of m = 1 mode decreases when β becomes small. For example, when $S = 10^4$, the growth rate of the resistive tearing instability is about $0.01\tau_\mu^{-1}$. The dependence of S on plasma parameters is shown in Fig.II-19.

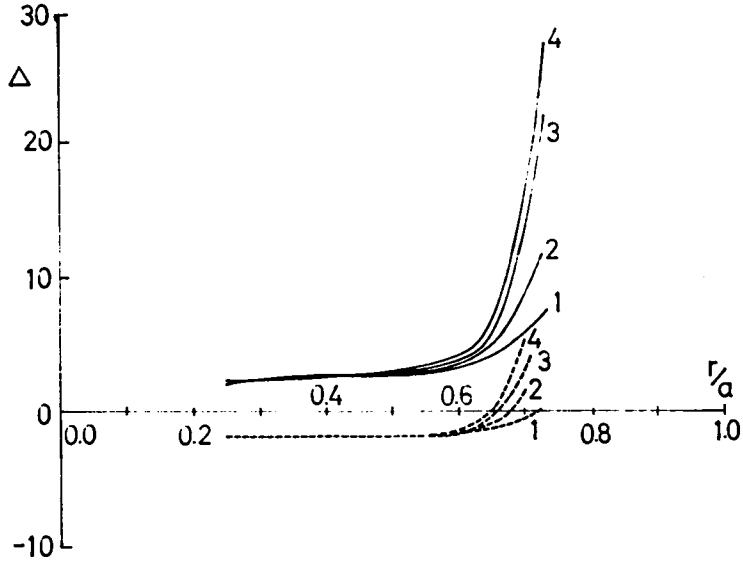

Fig.II-15. Δ as a function of r/a when plasma pressure β changes for P_B = -0.15, α = 1.0. Solid lines show m = 1 mode and dotted lines show m = 2 mode. 1) β = 15%, 2) β = 20%, 3) β = 26%, 4) β = 31%.

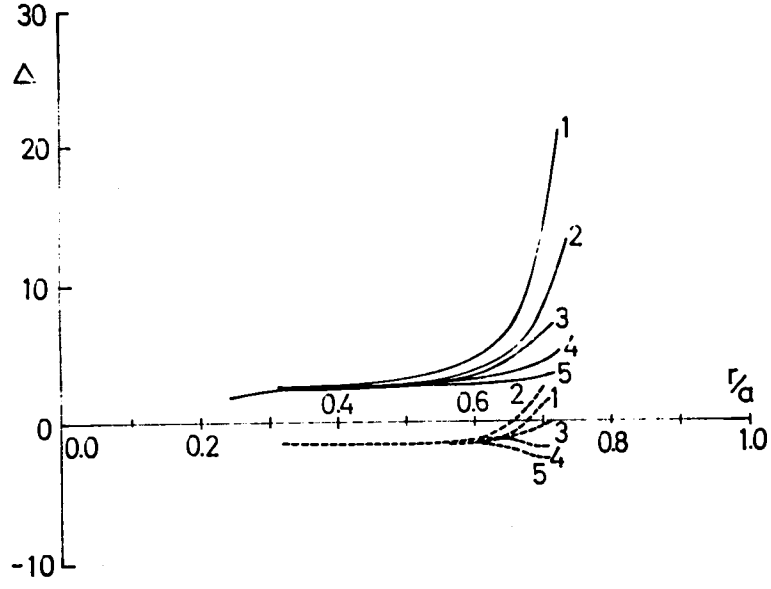

Fig.II-16. Δ as a function of r/a when the degree of field reversal P_B changes for β = 15%, α = 1.0. Solid lines show m=1 mode and dotted lines show m=2 mode. 1) R_B=-0.05, 2)R_B=-0.1, 3) R_B=-0.15, 4) R_B=-0.20, 5) R_B= -0.25.

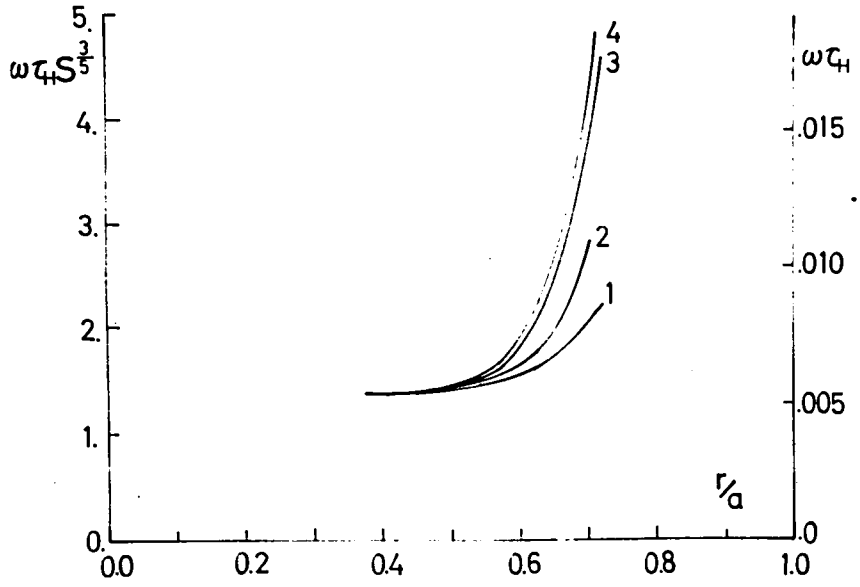

Fig.II-17. Growth rate of tearing instability (m=1 mode) as a function of r/a when plasma pressure β changes for R_B=-0.15. The left ordinate shows the normalized growth rate defined by $\omega\tau_H S^{3/5}$ and the right ordinate shows the growth rate $\omega\tau_H$ when $S=10^4$. 1) β=15%, 2) β=20%, 3) β=26%, 4) β=31%.

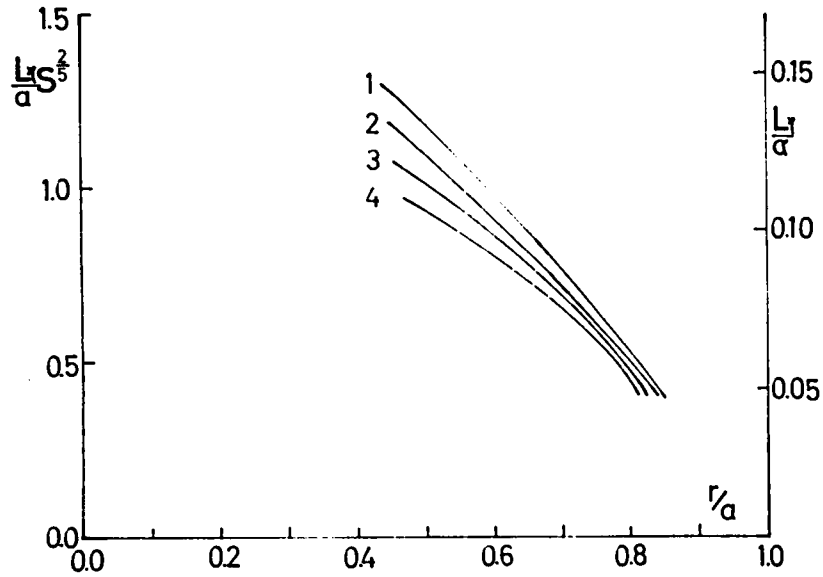

Fig.II-18. Resistive skin depth Lη/a of tearing instability(m=1 mode) as a function of r/a when plasma pressure β changes for R_B=-0.15. The left ordinate shows $L\eta/a\ S^{2/5}$ and the right ordinate shows Lη/a when $S=10^4$. 1) β=15%, 2) β=20%, 3) β =26%, 4) β=31%.

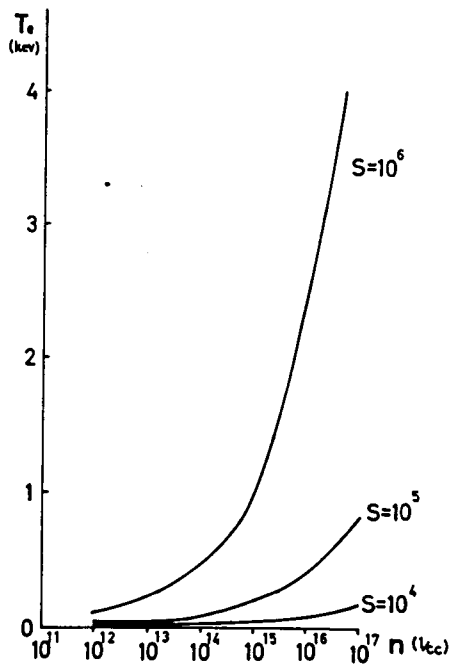

Fig.II-19. Constant S lines as functions of electron temperature T_e and plasma density n for magnetic field $B=3\times10^4$G and plasma radius a=3 cm.

These results suggest that the reverse field configurations are vulnerable to the resistive tearing instability, although the above treatment of the resistive tearing instability is restricted to the special type of the equilibrium. It should be noted, however, that there still remains the possibility that the positive pressure gradient in the central region of the plasma column can stabilize the resistive tearing instability. This is understood from that as the positive pressure gradients make the parameter D negative, the stability criterion for tearing modes (1.67) may be assured.

§ 6 Conclusion and Discussion

The stability of reverse field diffuse pinches against the hydromagnetic and resistive instabilities has been investigated. We have chosen the cylindrical linear pinch as the approximation to the toroidal pinch, in order to apply the Newcomb's criterion for MHD stability. This may be a good approximation as long as kink like modes are treated. By means of Newcomb's criterion, the MHD stability has been tested for a number of equilibrium configurations which are obtained by modification of force free fields. The equilibrium is characterized by the profile of the J_z current distribution. This method is convenient to obtain various equilibria of diffuse pinches and it is confirmed that a small deviation from the J_z current profile given in eq.(2.6) does not change stability diagrams essentially. Stability diagrams showing the position of the conducting shell for the threshold of the stability have been calculated by changing the shape of the axial current distribution, the average beta and the degree of field reversal. The following results are obtained: i) the reverse field diffuse pinch is stable against MHD instabilities if $k \to 0$ or $k \to \infty$; (ii) the stability against the $m = 0$ mode improves as α or $|R_B|$ becomes large, while the stability against the $m = 1$ mode improves as α or $|R_B|$ becomes small; (iii) stability condition becomes more stringent as the current distribution changes from a skin like current profile to a uniform one; (iv) as β becomes large, the strict condition that a conducting shell is sufficiently close to the plasma is imposed on the stability. Thus stability diagrams shows the reverse field diffuse pinch is stable against MHD modes for sufficiently high values of β and available compression ratio $R_W \gtrsim 2$.

The growth rates of MHD instabilities have been calculated for unstable reverse field configurations. It is shown that the growth rates of kink modes are $\omega \sim (0.4 \sim 0.6)\, a(\rho(0))^{1/2}/B_\theta(a)$. This expression gives large growth rate for typical plasma parameters of toroidal

pinches.[1),2)] Therefore kink modes are dangerous for confinement of high β plasmas in toroidal pinches. The shape of the displacement $\xi(r)$ is also obtained and it shows that the plasma column moves as a whole due to the m = 1 kink mode.

The stability against the resistive tearing instability has been examined with the method given in CGJ.[38)] It is shown that the reverse field configuration is vulnerable to the resistive tearing instability with m = 1 when the pressure profile is nearly uniform in the central region of the plasma column. The growth rates of m = 1 tearing modes are estimated for typical parameters of toroidal pinches and it is shown that tearing modes have slower growth rates than those of kink modes. The growth rate of tearing mode, however, depends on electron temperature as $T_e^{-2/5}$. From this fact, it is important to obtain a high temperature plasma by means of compression or Joule heating in reverse field diffuse pinches. It is noted that the positive pressure gradient in the central region of plasma has a stabilizing effect on the resistive tearing modes and the negative pressure gradient drives another instability such as interchange modes with larger growth rates.[38)]

CHAPTER III

COLLISIONAL DIFFUSION IN TOROIDAL PINCHES[57)]

§ 1 Introduction

Galeev and Sagdeev[46)] firstly indicated that taking account of the presence of so-called trapped particles leads to a sharp increase in the diffusion coefficients at rare collision frequency, in comparison with that given by Pfirsch and Shlüter.[45)] Galeev and Sagdeev (hereafter we shall call ref.46 of Galeev and Sagdeev as GS) investigated a low β toroidal plasma such as plasmas in Tokamaks, where the assumption that a toroidal magnetic field is much larger than a poloidal magnetic field is usually available. On the other hand, toroidal pinches such as reverse field pinches,[1),2)] stabilized pinches[1),2)] and scerw pinches[3)] have realized $B_p \simeq B_T$ by driving a toroidal current comparable to K-S limit,[21),22)] or by a compression. In Tokamaks, experimental efforts are recently devoted to realize $q \to 1$[60)], i.e. to strengthen the poloidal field, where q is a safty factor.

Transport phenomena in toroidal pinches, however, have not been discussed in detail so far. In this Chapter we investigate collisional diffusion in diffused toroidal pinches following the scheme of GS above mentioned. This is an extension of the scheme of GS. GS treated transport phenomena in rarely collisional plasmas by use of the kinetic equation with the collision terms in the Landan form. Particles confined in an axisymmetric toroidal magnetic system are subdivided into two groups, trapped particles and untrapped particles, according to trajectories of their guiding center motion. When a collision frequency decreases, the mean free path becomes larger than

the connection length of a torus and trapped particles begin to play a dominant role in transport phenomena. It is shown that the pitch angle scattering in the velocity space for barely trapped particles is essential in this regime. Then the displacements of trapped particles as a consequence of the 'banana' motion can lead to an appreciable increase in the transport coefficient. The physical meaning of this enhanced collisional diffusion is understood through the random walk theory. GS also considered transport phenomena in the intermediate collision frequencies (in which collisions are not very rare so that a Maxwellian particle distribution can be established). GS assumed that, as the banana motion is masked by Coulomb collisions, Landau collision term in the kinetic equation may be replaced with the simple collision term $\nu^j_{eff}\, f_j^{(1)}$, where $f_j^{(1)}$ is the first order distribution function and ν^j_{eff} is an effective collision frequency. It is shown that the diffusion coefficient in this regime is independent of the collision frequency.

Transverse diffusion coefficients given in GS must be modified in some respects in toroidal pinches. Since equilibrium configurations of toroidal pinches can be determined by the pressure balance equation, a prameter including the plasma pressure such as 'Shafranov's Λ'[61] appears to describe the magnetic fields of toroidal pinches. Thus the local magnetic mirror in the toroidal pinches is formed by the inhomogeneity of a poloidal magnetic field as well as that of a toroidal magnetic field. And the connection length of a torus is shortened by the poloidal magnetic field comparable to the toroidal one. This shortening of the connection length reduces the period with which a trapped particle forms a closed trajectory projected on the meridional plane. From this fact, we find that the width of the banana, which is proportional to the displacement from a magnetic surface as a consequence of the drift motion, is also reduced.

The collisional diffusion in collision dominated plasmas is investigated in the framework of MHD equations. Both J_z and J_θ currents are driven by electric fields in toroidal pinches, while

the J_z current is only driven in Tokamaks. This fact modifies the well known 'Pfirsch-Schlüter factor'.[45)]

In § 2 the guiding center equations in a toroidal pinch are given. Section 3 is devoted to obtain the diffusion coefficient at rare collision frequencies and in § 4 is obtained the diffusion coefficient at intermediate collision frequencies. In § 5 we use MHD equations to investigate the diffusion in toroidal pinches. In § 6, the last section, the diffusion coefficients obtained in § 3 ~ § 5 are discussed and compared with those given in GS.

§ 2 Equilibrium and Guiding Center Equations

In order to simplify the analysis, we assume that the minor radius of the toroidal pinch is much smaller than the major radius. Following Kadomtsev and Pogutse,[62] we introduce curvilinear coordinates (r, θ, ζ) which tend to the usual cylindrical coordinates system when the major radius R_0 tends to infinity. It can be assumed that magnetic surfaces in the cross section ζ = const are a system of nested circles and the equation r = const defines a magnetic surface. Then the axially symmetric toroidal magnetic field is expressed by $\vec{B} = (0, B_\theta, B_\zeta)$. For small values of $\varepsilon = r/R_0$, the toroidal magnetic field to an accuracy of order ε is given by

$$B_\zeta = B_\zeta{}^0(r)(1 - \varepsilon\cos\theta). \tag{3.1}$$

In this approximation, the poloidal magnetic field can be written in the form

$$B_\theta = B_\theta{}^0(r)(1 - \Lambda(r)\cos\theta), \tag{3.2}$$

when Λ is a small asymmetric parameter given by Shafranov[61] that depends on the distribution of the plasma pressure p and the poloidal magnetic field B_θ,

$$\Lambda(r) = \frac{r}{R_0}\{1 + \frac{8\pi p}{B_\theta{}^{02}} - \frac{1}{r^2 B_\theta{}^{02}}\int_0^r (16\pi p + B_\theta{}^{02})rdr\}. \tag{3.3}$$

Furthermore, the absolute magnitude of the magnetic field $\vec{B}$ can be written in the form

$$B = B_0(r)(1 - \delta\cos\theta), \tag{3.4}$$

where

$$\delta = (\Lambda B^0{}_\theta{}^2 + \varepsilon B^0{}_\zeta{}^2)/B_0{}^2 \text{ and } B_0{}^2 = B^0{}_\theta{}^2 + B^0{}_\zeta{}^2.$$

The equations for the guiding center in the radial electric field specified by the potential $\Phi(r)$ and also in the magnetic field given by eqs.(3.1)(3.2) and (3.4) are:

$$\frac{dr}{dt} = -\frac{v_{11}{}^2 + \mu B_0/m}{\Omega_c{}^0 B_0} B_\zeta \frac{\delta}{r} \sin\theta \quad . \tag{3.5}$$

and

$$r\frac{d\theta}{dt} = -\frac{v_{11}{}^2 + \mu B_0/m}{\Omega_c{}^0 B_0{}^2} B_\zeta (B_0\delta)' \cos\theta - \frac{v_{11}{}^2 + \mu B_0/m}{\Omega_c{}^0 B_0{}^2} B_\zeta B_0'$$

$$+ \frac{cB_\zeta{}^0}{B_0{}^2} \Phi' - v_{11}\frac{B_\theta{}^0}{B_0} \quad , \tag{3.6}$$

where v_{11} and $v_\perp$ denote the components of the velocity parallel and perpendicular to the magnetic field respectively, $\Omega_c{}^0 = eB_0/mc$ is the gyrofrequency and $\mu = mv_\perp{}^2/2B$ is the magnetic moment. Because of the toroidal symmetry in the toroidal pinch, it is sufficient to consider only the projection of the particle trajectory on the (r,θ) plane. In order to describe the motion of the particle in the forms of eqs.(3.5) and (3.6), the relations

$$r_{ci}\frac{1}{n}\frac{dn}{dr} << 1 \quad ; \quad r_{ci}\frac{1}{B_0}\frac{dB_0}{dr} << 1, \tag{3.7}$$

are assumed. Therefore we have neglected the term arising from the current flowing in the plasma as compared to the remaining terms in

eq.(3.6). In addition, we assume that temperature of the plasma confined in the toroidal pinch is so high (i.e., large conductivity is available) that the effect of a driving electric field can be ignored. Using the conservation of a particle energy E and the conservation of the adiabatic invariant μ, we can find the longitudinal velocity of a particle

$$v_{11} = \pm \{\frac{2}{m}[E - \mu B - e\Phi]\}^{1/2}. \tag{3.8}$$

As $\varepsilon << 1$ is assumed and a charged particle moves almost along a magnetic field line, we allow to neglect the toroidal drift. Then we can write eq.(3.6) in the following form

$$r\frac{d\theta}{dt} = -\sigma\frac{B_0}{B_\theta^0}[\{v^2 + \frac{B^0\theta^2}{B_0^2}(v_E - v_M)^2\}\delta]^{1/2}[2\kappa^2 - 1 + \cos\theta]^{1/2} \tag{3.9}$$

where

$$v^2 = 2(E - e\Phi)/m,\ \sigma = \mathrm{sign}[v_{11}(r_0,0) - \frac{B_\theta^0}{B_0}\{v_E(r_0) - v_M(r_0)\}],$$

$$2\kappa^2 = [v_{11}(r_0, 0) - \frac{B\theta^0}{B_0}\{v_E(r_0) - v_M(r_0)\}]^2 / [\{v^2 + \frac{B^0\theta^2}{B_0^2}(v_E - v_M)^2\}\delta],$$

$$v_E = \frac{cB_\zeta^0}{B_0}\Phi',\quad v_M = \frac{v_T^2}{\Omega_c^0 B_0^2 B_\zeta^0 B_0'} \text{ and } v_T^2 = 2T/m.$$

It is then obvious that particle with the value $\kappa^2<1$ will be trapped in the magnetic field of the toroidal pinch. This trapping

effect arises because the magnitude of the magnetic field along the line of force varies from an inner portion of the toroidal tube to an outer portion and vice versa.

§ 3 Collisional Diffusion in the Panana Regime

We shall now consider the case of very rare collisions. In this case the relaxation time for the trapped particle distribution due to collisions is much larger than the period associated with their motion

$$\frac{\delta}{\nu_j} >> \tau_j = \frac{qR_0}{v_{Tj}\sqrt{\delta}} \quad , \tag{3.10}$$

where

$$\nu_j = \frac{16\sqrt{\pi}\lambda e^4 n}{3m_j v_{Tj}^2} \quad \text{and} \quad q = \frac{rB_\zeta}{RB_\theta}$$

is the safety factor. The L.H.S of (3.10) denotes effective collision time. Since the Landam form is used to describe the Coulomb term of collisions, the effective collision frequency is $\nu_j(v^2_{Tj}/(\Delta v)^2)$, where Δv denotes the velocity interval in which the distribution function is substantially changed. As for trapped particles in the toroidal pinch Δv is nearly equal to $\sqrt{\delta}v_{Tj}$, which is derived from eq.(3.8). Under these conditions, as a first approximation we can neglect all the effects of collisions and the general solution of the kinetic equation can be written only in terms of the constants of motion

$$f_t = f_t^{(0)}(\mu,\ E,\ J)\ ;\quad f_u = f_u^{(0)}(\mu,\ E,\ J,\sigma\ ), \tag{3.11}$$

where f_t and f_u are the distribution functions for the trapped and untrapped particles respectively and J is the generalized angular momentum. Writing the particle distribution function in the form

$$f_j = f_j^{(0)}(E,\mu,J;\sigma) + f_j^{(1)}(E,\mu,J\ ;\sigma,\theta) + \cdots, \tag{3.12}$$

we solve the kinetic equation by the method of successive approximation. In addition, we linearize the Landau collision term since deviations from the Maxwellian distribution are important only in a narrow region of velocity space for trapped particles. Then the kinetic equation is assumed to have the form:

$$\left(-v_{11}\frac{B_\theta{}^0}{B_0} - \frac{\mu B_0/m}{\Omega_c{}^0 B_0{}^2} B_\zeta{}^0 B_0' + \frac{cB_\zeta{}^0}{B_0{}^2}\Phi'\right)\frac{1}{r}\frac{\partial f_j^{(1)}}{\partial\theta}$$

$$= \Sigma_j' \frac{2\pi\lambda e_j{}^2 e_j'^2}{m_j}\left(\eta_j' + \eta'_j{}' - \frac{\eta_j'}{2x_j'}\right)\frac{\sqrt{2}}{v_{Tj}\sqrt{x_j}}\frac{\partial}{\partial v_{11}}\left(\frac{1}{m_j}\frac{\partial f_j^{(0)}}{\partial v_{11}}\right.$$

$$\left. + \frac{2v_{11}}{m_j' v^2_{Tj'}} f_j^{(0)}\right) \qquad (3.13)$$

where

$$\eta_j' = \eta(x_j') = \frac{2}{\sqrt{\pi}}\int_0^{x_j'} e^{-t}\sqrt{t}\,dt, \quad \eta'(x_j) = \frac{\partial\eta(x_j)}{\partial x_j}$$

and

$$x_j = \frac{2\mu B_0}{m_j v_{Tj}{}^2} .$$

Here, we have neglected the derivative of the first order distribution function with respect to the r coordinate, and have assumed that the order of magnitude of δ is comparable to that of ε. Furthermore, in the first approximation the distribution function is most sensitive to changes in the longitudinal velocity and we can neglect all the other derivative in eq.(3.13). And we have assumed that the curvature drift does not play any important role in the particle diffusion across the magnetic surface.

It is convenient to transform the variables $v_\perp$, v_{11} and θ into

the new variables μ, κ^2 and θ by making use of the following relation

$$v_{11} = \frac{c}{B_0}\frac{B_\zeta{}^0}{B_\theta{}^0}\Phi' - \frac{(\mu B_0/m)B_0'}{\Omega_c{}^0 B_\theta{}^0} + 2\sigma\left[\frac{\mu B_0}{m}\delta\left(\kappa^2 - \sin^2\frac{\theta}{2}\right)\right]^{1/2} . \qquad (3.14)$$

The transformation of the variables, then, leads eq.(3.13) to a simple form:

$$-\frac{B_\theta{}^0}{B_0}\sqrt{2x_j\delta}\,v_{Tj}\frac{1}{r}\frac{\partial f_j^{(1)}}{\partial\theta} = \delta^{-1}\nu_j A(x_j)\frac{\partial}{\partial\kappa^2}\left\{\sigma\left(\kappa^2 - \sin^2\frac{\theta}{2}\right)^{1/2}\left(\frac{\partial f_j{}^0}{\partial\kappa^2} + 2x_j\delta f_j^{(0)}\right) + \sqrt{2x_j\delta}\,C(x_j)f_j^{(0)}\right\} , \qquad (3.15)$$

where

$$A(x_j) = \frac{3\sqrt{\pi}}{4}\Sigma_j'\left(\eta_j' + \eta'_j - \frac{\eta_j'}{2x_j'}\right)x_j^{-3/2} \quad \text{and}$$

$$C(x_j) = \frac{1}{v_{Tj}}\frac{cB_\zeta{}^0}{B_0 B_\theta{}^0}\Phi' - \frac{B_\zeta{}^0 B_0'}{\Omega_c{}^0 B_\theta{}^0 B_0}\frac{v_{Ti}x_j}{2} .$$

Using the same procedure given in GS, we can find both the distribution function for untrapped particles $f_{uj}^{(0)}$ and that for trapped particles $f_{tj}^{(0)}$ from eq.(3.15). Substituting the expression for $f_{uj}^{(0)}$ or $f_{tj}^{(0)}$ into the R.H.S. of eq.(3.15), we can find the first order distribution function.

Multiplying the particle distribution function $f_j^{(0)} + f_j^{(1)}$ by the particle velocity across the magnetic surface $(\mu B_0/m\Omega_c{}^0)(B_\zeta{}^0/B_0)$ $\times(\delta/r)\sin\theta$ and integrating over (μ, κ^2, θ), we can obtain the particle flux across the magnetic surface. Here, we consider separately the contributions to the flux from untrapped particles and from trapped

particles as well as from particles in the transion layer.
The resultant contribution to the particle flux is calculated to give

$$\langle nv\rangle_{untrap} = -\frac{\sqrt{2\delta}}{\pi^{3/2}}\frac{\nu_j r_{cj} B_\zeta{}^0}{B_\theta{}^0}\int_0^\infty A(x_j)e^{-x_j-C(x_j)^2}x_j^{3/2}\{4 - \frac{\pi^2}{2} + 2\int_1^\infty \frac{d\alpha}{\alpha^{1/2}}$$

$$\times [K(\alpha^{-1/2}) - \frac{\pi^2}{4E(\alpha^{-1/2})}]\}n(C(x_j) + \frac{r_{cj}B_\zeta{}^0}{2B_\theta{}^0}\frac{1}{n}\frac{dn}{dr})dx_j, \qquad (3.16)$$

from untrapped particles ($\kappa^2>1$) and

$$\langle nv\rangle_{trap} = -\frac{2\sqrt{2\delta^3}\nu_j r_{cj}}{B_\theta{}^0\pi^{3/2}}\int_0^\infty A(x_j)e^{-x_j-C(x_j)^2}x_j^{5/2}n(C(x_j) +$$

$$\frac{r_{cj}B_\zeta{}^0}{2B_\theta{}^0}\frac{1}{n}\frac{dn}{dr})dx_j, \qquad (3.17)$$

from trapped particles ($\kappa^2<1$). As $\langle nv\rangle_{untrap} \propto \delta^{1/2}$ and $\langle nv\rangle_{trap} \propto \delta^{3/2}$, the latter can be neglected as compared with the former. For the contribution from the transition layer we can obtain the following expression

$$\langle nv\rangle_{transition} = -\frac{\nu_j v_{Tj}{}^4}{2B_\Theta{}^0\Omega_{cj}{}^0}\int_0^\infty dx_j A(x_j)x_j\int_0^{2\pi} d\theta \sum_\sigma \sigma(\kappa^2 - \sin^2\frac{\theta}{2})$$

$$\times\{\frac{\partial f_{uj}^{(0)}}{\partial\kappa^2} - \frac{\partial f_{tj}^{(0)}}{\partial\kappa^2}\}\Big|_{\kappa^2=1} = -\nu_j\sqrt{\frac{\pi\delta}{2}}\ \frac{B_\zeta{}^0}{B_\theta{}^0 r_{cj}}\int_0^\infty e^{-x_j-C(x_j)^2}A(x_j)x_j^{3/2}n$$

$$\times (c(x_j) + \frac{r_{cj}B_\zeta{}^0}{2B_\theta{}^0}\frac{1}{n}\frac{dn}{dr})dx_j. \qquad (3.18)$$

After the numerical estimation of the integral on the R.H.S of eqs. (3.16) and (3.17), we obtain finally the total flux $\langle nv \rangle \simeq \langle nv \rangle_{untrap} + \langle nv \rangle_{transition}$ as

$$\langle nv \rangle = -\nu_j r_{cj}^2 \sqrt{\delta} \left(\frac{B_\zeta^0}{B_\theta^0}\right)^2 \{1.3\left(\frac{dn}{dr} + \frac{e_j n}{T_j}\Phi'\right) - 1.5\frac{B_0'}{B_0} n\}. \qquad (3.19)$$

Because the plasma is neutral, an electric field must arise in such a way as to reduce the ion diffusion to a level of electron diffusion. Under the circumstances the diffusion becomes ambipolar and the ambipolar electric field is $-ne_i\Phi' = p_i'$.

We obtain the electron flux from eq.(3.19), substituting $j = e$,

$$\langle nv \rangle = -\nu_e r_{ce}^2 \sqrt{\delta} \left(\frac{B_\zeta^0}{B_\theta^0}\right)^2 \{1.3\left(1 + \frac{T_i}{T_e}\right)\frac{dn}{dr} - 1.5\frac{B_0'}{B_0} n\}. \qquad (3.20)$$

Accordingly the transverse diffusion coefficient is obtained

$$D_\perp \simeq \{1.3\left(1 + \frac{T_i}{T_e}\right) + \frac{6\pi n(T_e + T_i)}{B_0^2}\}\varepsilon^{-3/2}\sqrt{\frac{\delta}{\varepsilon}}\nu_e r_{ce}^2 q^2 \qquad (3.21)$$

for

$$\nu_e << \frac{v_{Te}}{r}\frac{B_\theta^0}{B_\zeta^0}\delta^{3/2} .$$

Here, the relation $-B_0B_0' \simeq 4\pi p'$ is used and the second term in the curly bracket is the order of the magnitude of β. We note here that a parameter δ appears in this expression of the diffusion coefficient, which will be discussed in § 6.

§ 4 Collisional Diffusion in the Plateau Regime

Here we consider the case in which a Maxwellian distribution can be established by virtue of collisions in a narrow region of velocity space, $\Delta v \sim \sqrt{\delta}\, v_T$, within the period of gyration of the trapped particle in the closed trajectory. We assume that collisions can be neglected for the untrapped particles. Then, our limitations on the collision frequency can be expressed by the inequality

$$\frac{B_\theta{}^0}{B_0}\frac{v_{Tj}}{r} > \nu_j > \delta^{3/2}\frac{B_\theta{}^0}{B_\zeta{}^0}\frac{v_{Tj}}{r} . \qquad (3.22)$$

The solution of the kinetic equation can now be sought in the form of an expansion in ε,

$$f_j(v_\perp, v_{11}, r, \theta) = f_j^{(0)}(v_\perp, v_{11}, r) + f_j^{(1)}(v_\perp, v_{11}, r, \theta) + \cdots\cdots \qquad (3.23)$$

where

$$f_j^{(0)} = \frac{n_j(r)}{\pi^{3/2} v_{Tj}{}^3} \exp\left[-\frac{v_\perp{}^2 + v_{11}{}^2 + 2e\Phi/m_j}{v_{Tj}{}^2}\right]$$

is a local Maxwellian distribution. Now the linearization of the kinetic equation takes the form:

$$\left(\theta\frac{B_\theta{}^0}{B_0}v_{11} - \frac{2v_{11}{}^2 + v_\perp{}^2}{2\Omega_c{}^0 B_0{}^2} B_\zeta{}^0 B_0{}' + \frac{cB_\zeta{}^0}{B_0{}^2}\Phi'\right)\frac{1}{r}\frac{\partial f_j^{(1)}}{\partial\theta} = -\nu_{eff}^j f_j^{(1)}$$

$$+\frac{2v_{11}^2+v_\perp^2}{2\Omega_c{}^0 B_0}B_\zeta^0\frac{\delta}{r}\sin\theta\frac{\partial f_j^{(0)}}{\partial r}-\frac{v_\perp^2}{B_0}B_\theta{}^0\frac{\delta}{r}\sin\theta\frac{\partial f_j^{(0)}}{\partial v_{11}}\,, \tag{3.24}$$

where the collision term is simply replaced by an approximate term of the form $-\nu_{eff}{}^j f_j^{(1)}$, and $\nu_{eff}{}^j$ denotes an effective collision frequency. Assuming the dependence of $f_j^{(1)}$ on the angle θ as an exponential form $e^{\pm i\theta}$, we can write the solution of the eq.(3.24),

$$f_j^{(1)}=\sum_{\pm}\{[\frac{2v_{11}^2+v_\perp^2}{4\Omega_c{}^0 B_0}B_\zeta{}^0\delta\frac{\partial}{\partial r}-\frac{v_\perp^2}{2B_0}B_\theta{}^0\,\delta\frac{\partial}{\partial v_{11}}]f_j^{(0)}$$

$$\times\,(-\frac{B_\theta{}^0}{B_0}v_{11}-\frac{2v_{11}^2+v_\perp^2}{2\Omega_c{}^0 B_0{}^2}B_\zeta{}^0 B_0{}'+\frac{cB_\zeta^0}{B_0{}^2}\Phi'\mp iv_{eff}{}^j)^{-1}\}e^{\pm i\theta}\,. \tag{3.25}$$

Multiplying this expression by the radial drift velocity of the particle (eq.(3.5)) and integrating over the velocity space, we obtain the particle flux across the magnetic surface:

$$\langle nv\rangle=-\int_0^{2\pi}d\theta\int_0^\infty v_\perp dv_\perp\int_{-\infty}^\infty dv_{11}f_j^{(1)}\frac{2v_{11}^2+v_\perp^2}{2\Omega_c{}^0}\frac{\delta}{r}\frac{B_\zeta{}^0}{B_0}\sin\theta$$

$$\simeq-\frac{\sqrt{\pi}}{4}\left|\frac{B_0}{B_\theta{}^0}\right|\frac{B^0{}_\zeta{}^2 r_{cj}{}^2}{B_0{}^2}\frac{}{r}v_{Tj}\delta^2\,\exp(-\frac{\bar{v}_{11}{}^2}{v_{Tj}{}^2})\frac{dn}{dr}\,. \tag{3.26}$$

Here the curvature drift has also been neglected and $\overline{v_{1l}}$ denotes the pole of the delta function, which appears as a consequence of $\nu_{eff}{}^{j} \to 0$,

$$\overline{v_{1l}} = \frac{cB_\zeta{}^0}{B_\theta{}^0 B_0}\,\Phi' - \frac{v_{Tj}{}^2\, B_\zeta{}^0}{2\Omega_c{}^0\, B_\theta{}^0 B_0}\,B_0' \,. \tag{3.27}$$

As we discussed before, the transverse diffusion becomes ambipolar. Then the diffusion coefficient is obtained from eq.(3.27) calculated for electrons

$$D_\perp \simeq \frac{\sqrt{\pi}}{4}\left|\frac{B_0}{B_\theta^0}\right| \frac{B^0{}_\zeta{}^2}{B_0{}^2}\,\frac{r_{ce}}{r}\,\frac{cT_e}{eB_0}\,\delta^2, \tag{3.28}$$

for

$$\delta^{3/2}\,\frac{v_{Te}}{r}\,\frac{B_\theta{}^0}{B_\zeta{}^0} < \nu_e < \frac{v_{Te}}{r}\,\frac{B_\theta{}^0}{B_0}\,.$$

Here we note that, although this expression is again similar to that given in GS, the quantity δ appears in this formula.

§5 Collisional Diffusion in the MHD Regime

In the case of relatively short mean free paths (which is smaller than the connection length of the toroidal pinch), the influence of particle trapping in local magnetic mirrors can be completely neglected, i.e.,

$$\nu_j \gg \frac{v_{Tj}}{r} \frac{B_\theta{}^0}{B_0} \,. \tag{3.29}$$

The toroidal contribution to the diffusion coefficient is due to a quite regular motion of particle which, at the outer contour of the torus, is directed outward across the magnetic surface, while at the inner contour it is directed inward across the magnetic surface.

For the sake of simplicity, we consider only the particle flux, assuming the uniform temperature distribution. To describe the convection it is sufficient to use the MHD equilibrium equation

$$\vec{\nabla} p = \vec{J} \times \vec{B} \quad , \tag{3.30}$$

Ohum's law

$$\vec{E} + \vec{v} \times \vec{B} = \frac{\vec{J}_\parallel}{\sigma_\parallel} + \frac{\vec{J}_\perp}{\sigma_\perp} \tag{3.31}$$

and the condition of quasi-neutrality

$$\operatorname{div} \vec{J} = 0, \tag{3.32}$$

where $\sigma_\parallel$ and $\sigma_\perp$ denote parallel and perpendicular conductivity

respectively. Under the eq.(3.31) and taking account of the eq.(3.30), we find

$$\vec{v}_{\perp} = \frac{\vec{E} \times \vec{B}}{B^2} - \frac{1}{\sigma_{\perp}} \frac{\vec{\nabla} p}{B^2} \qquad (3.33)$$

where the second term describes the transverse collisional diffusion. Multiplying eq.(3.31) by $\vec{B}$, we obtain

$$\vec{J} \cdot \vec{B} = \sigma_{\parallel} \vec{E} \cdot \vec{B} \quad . \qquad (3.34)$$

Denoting $\vec{J}_{\parallel} = \alpha \vec{B}$, we find from eq.(3.34)

$$\alpha(r,\theta) = \frac{\sigma_{\parallel}}{B^2} \{ B_{\zeta} E_{\zeta}{}^{0}(r)(1 - \varepsilon \cos\theta) + B_{\theta} E_{\theta} \}, \qquad (3.35)$$

where E_{ζ} is determined under the conditions where the equilibrium configuration is stationary and

$$\oint E_{\zeta} \, d_{\zeta} = \text{const.} \qquad (3.36)$$

Using eq.(3.32) and div $\vec{B} = 0$, we obtain

$$\vec{B} \cdot \vec{\nabla} \alpha = -\text{div } \vec{J}_{\perp} = -(\vec{B} \times \vec{\nabla} p) \cdot \vec{\nabla} \left(\frac{1}{B^2} \right) - \frac{1}{B^2} \vec{\nabla} \cdot (\vec{B} \times \vec{\nabla} p). \qquad (3.37)$$

The second term is equal to zero through eq.(3.30) and the both sides of eq.(3.37) are rewritten as

$$B_\theta \frac{\partial \alpha}{\partial \theta} \simeq B \frac{dp}{\zeta dr} \frac{2}{B^3} \frac{dB}{d\theta} = \frac{2}{B_0^2} B_\zeta^0 \frac{dp}{dr} \delta \sin\theta \quad . \tag{3.38}$$

Integrating eq.(3.38), we can find

$$\alpha = \alpha_0(r) - \frac{2B_\zeta^0}{B_\theta^0 B_0^2} \delta \frac{dp}{dr} \cos\theta \quad , \tag{3.39}$$

where $\alpha_0(r)$ is the independent part of α from θ. The poloidal electric field is divided into two parts,

$$E_\theta = E_\theta^0(r) + E_\theta^{(1)}(r,\theta), \tag{3.40}$$

where $E_\theta^{(1)}$ denotes the electric field for maintaining an equilibrium in the toroidal system. Equating the zeroth order and the first order of ε respectively in eq.(3.35) and eq.(3.39), we can find

$$\alpha_0(r) = \sigma_{\parallel} (E_\zeta^0 B_\zeta^0 + E_\theta^0 B_\theta^0)/B_0^2, \tag{3.41}$$

and

$$E_\theta^{(1)} = -\frac{2B_\zeta^0}{\sigma_{\parallel} B_\theta^{0\,2}} \frac{dp}{dr} \delta\cos\theta + \{2(\varepsilon-\delta)\frac{B_\zeta^0 E_\zeta^0}{B_\theta^0} + (\Lambda-2\delta)E_\theta^0\}\cos\theta. \tag{3.42}$$

The toroidal correction for $\vec{v}_\perp$ is defined as

$$v_r^{(1)} = \frac{E_\theta^{(1)} B_\zeta^0 - E_\zeta^{(1)} B_\theta^0}{B_0^2} + \frac{E_\theta^0 B_\zeta^{(1)} - E_\zeta^0 B_\theta^{(1)}}{B_0^2} + 2\frac{E_\theta^0 B_\zeta^0 - E_\zeta^0 B_\theta^0}{B_0^2} \delta\cos\theta, \tag{3.43}$$

where $E_\zeta^{(1)}$, $B_\zeta^{(1)}$ and $B_\theta^{(1)}$ denotes $-\varepsilon E_\zeta{}^0\cos\theta$, $-\varepsilon B_\zeta{}^0\cos\theta$ and $-\Lambda B_\theta{}^0\cos\theta$ respectively. Using eq.(3.42) and the definition of δ, we can rewrite eq.(3.43) as

$$v_r^{(1)} = -\frac{2B^0{}_\zeta{}^2}{\sigma_{\parallel} B_0{}^2 B^0{}_\theta{}^2}\frac{dp}{dr}\delta\cos\theta - (\varepsilon-\delta)\frac{B_0{}^2}{B^0{}_\theta{}^2}\frac{(\vec{E}\times\vec{B})_0}{B_0{}^2}\cos\theta , \qquad (3.44)$$

where $(\vec{E}\times\vec{B})_0$ denotes $(E_\theta{}^0 B_\zeta{}^0 - E_\zeta{}^0 B_\theta{}^0)$. Furthermore we define $v_r^{(0)}$ as

$$v_r^{(0)} = \frac{(\vec{E}\times\vec{B})_0}{B_0{}^2} - \frac{1}{\sigma_\perp}\frac{1}{B_0{}^2}\frac{dp}{dr}. \qquad (3.45)$$

Combining eq.(3.43) with eq.(3.45), we obtain

$$v_r^{(1)} = -\left\{\frac{2B^0{}_\zeta{}^2}{\sigma_{\parallel} B^0{}_\theta{}^2 B_0{}^2}\delta + \frac{1}{\sigma_\perp B^0{}_\theta{}^2}(\varepsilon-\delta)\right\}\frac{dp}{dr}\cos\theta$$

$$-(\varepsilon-\delta)\frac{B_0{}^2}{B^0{}_\theta{}^2} v_r^{(0)}\cos\theta \qquad (3.46)$$

Since we have treated the equilibrium where eq.(3.30) is available and time independent electric field $E_\zeta{}^0$ and $E_\theta{}^0$ maintain the same configuration during the time scale of collisional diffusion, the magnitude of $v_r^{(0)}$ may be small and the second term of eq.(3.46) can be negligible.

The mean particle flux across the magnetic surface is obtained when $v_r^{(1)}$ is multiplied by $(1+\varepsilon\cos\theta)$ in order to take account the variation of the surface element in the toroidal pinch and then

averaged over θ:

$$\langle v_r^{(1)} \rangle = -\frac{B^0{}_\zeta{}^2}{B_0{}^2} \{ \frac{2\varepsilon\delta}{\sigma_\parallel B^0{}_\theta{}^2} + \frac{B_0{}^2}{\sigma_\perp B^0{}_\theta{}^2 B^0{}_\zeta{}^2} \varepsilon(\varepsilon-\delta) \} \frac{dp}{dr} . \qquad (3.47)$$

Accordingly the toroidal particle flux due to binary collisions is

$$\langle n v_r^{(1)} \rangle = -\frac{1}{\sigma_\perp B_0{}^2} \{ 1 + \frac{\sigma_\perp}{\sigma_\parallel} \frac{B^0{}_\zeta{}^2}{B^0{}_\theta{}^2} \varepsilon\delta + \frac{B_0{}^2}{B^0{}_\theta{}^2} \varepsilon(\varepsilon-\delta) \} \frac{dp}{dr} . \qquad (3.48)$$

From this equation we obtain the transverse diffusion coefficient across the magnetic surface:

$$D_\perp = \nu_e r_{ce}{}^2 \{ 1 + \frac{2\sigma_\perp}{\sigma_\parallel} q^2 \frac{\delta}{\varepsilon} + \frac{B_0{}^2}{B^0{}_\zeta{}^2} q^2 (1-\frac{\delta}{\varepsilon}) \} , \qquad (3.49)$$

for

$$\nu_e >> \frac{v_{Te}}{r} \frac{B^0{}_\zeta}{B^0} .$$

In the case where the condition $\varepsilon=\delta$ is available, the usual form of Pfirsch-Schlüter factor is obtained.

§ 6 Conclusion and Discussion

Transverse diffusion coefficients in a toroidal pinch have been investigated for three regions of collision frequencies. The configuration of the toroidal pinch is characterized by the large poloidal magnetic field B_P comparable to the toroidal magnetic field B_T.

In toroidal pinches particles can be trapped in a local magnetic mirror formed by both a toroidal magnetic field and a poloidal magnetic field. The condition $B_P \simeq B_T$ also reduces the connection length of a toroidal pinch. Transverse diffusion coefficients including these effects are shown to be smaller than D_{GS} which is given by Galeev and Sagdeev. In the banana region $D_\perp \simeq D_{GS}\sqrt{\delta/\varepsilon}$ is obtained and in the plateau region $D_\perp \simeq D_{GS}(\delta^2/\varepsilon^2)$, where ε denotes r/R_0 and a small parameter δ denotes the inhomogeneity of the magnetic field in toroidal pinches. The appearance of the factor δ/ε means that the inhomogeneity of the poloidal magnetic field in the toroidal geometry can not be neglected in toroidal pinches. Here it is noted that a safety factor included in D_{GS} may be smaller than or comparable to unity. In the MHD region $D_\perp$ also includes the factor δ/ε. Figure III-1 shows the diffusion coefficient in the toroidal pinch as a function of electron-ion collision frequency ν_{ei}. The dotted line shows diffusion coefficients given in GS. The poloidal magnetic field comparable to the toroidal magnetic field diminishes the diffusion coefficient, so the slope of the line denoted by 1 as well as the slope of the line denoted by 3 are decreased. In addition, the relation $B_P \simeq B_T$ increases the collision frequency at which trapped particles contribute mainly to the transport phenomena. This is seen, in Fig.III-1, from that the point of intersection of lines 2 and 3 shifts to the right side as compared with that shown by GS.

A typical value of Λ is approximately equal to $\varepsilon(3/4 - \beta_p)$, (i.e. in the case of uniform toroidal current), where $\beta_p = 8\pi\bar{p}/B_p^2$

and $\bar{p}$ denotes a plasma pressure averaged over the cross section of the torus. Thus, if β_p increases from the small value, Λ becomes small and δ decreases (see eq.(3.4)).

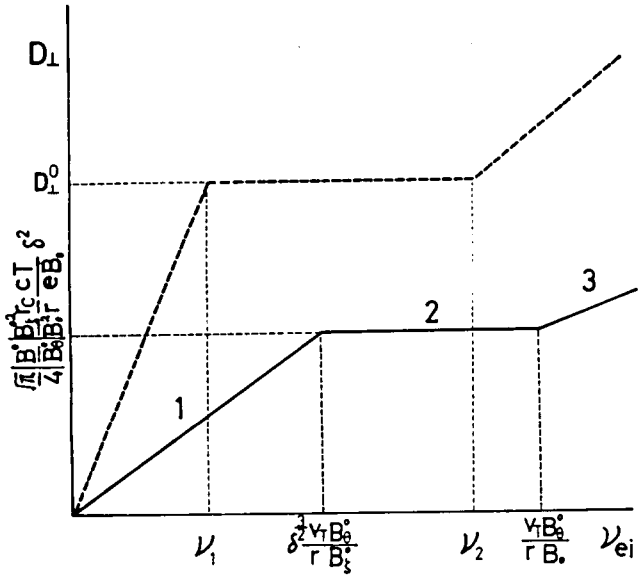

Fig.III-1. The transverse diffusion coefficient as a function of electron-ion collision frequency ν_{ei}. The solid line shows the transverse diffusion coefficient in a toroidal pinch and the dotted line shows that given in GS. Here,

$$D_\perp^0 = \frac{\sqrt{\pi}}{4}|B^0|B^{0\,2}/|B_\theta^0|B_0^2 \cdot r_c/r \cdot cT/eB_0 \cdot \varepsilon^2,$$

$$\nu_1 = B_\theta^0/B_\zeta^0\ v_T/r \cdot \varepsilon^{3/2} \text{ and } \nu_2 = B_\theta^0/B_\zeta^0 \cdot v_T/r,$$

and it is noted that $B_\theta^0 \ll B_\zeta^0$ in these expressions.

Conclusively, the toroidal pinch characterized by the relation $B_P \simeq B_T$ has a great advantage to the confinement of high temperature plasmas in view of the collisional diffusion in the equilibrium state.

CHAPTER IV

HIGH β_p EQUILIBRIUM OF TOKAMAKS[20]

§ 1 Introduction

As a result of recent experimental studies[5),6),41),42)] made on Tokamaks it is of great interest to take the theoretical study of MHD equilibria and stability in Tokamaks as far toward the reactor regime as possible. The problem of MHD equilibrium of an axisymmetric toroidal plasma column have usually been solved in the first approximation of an expansion with respect to $\varepsilon = a/R$, where a and R are the minor and major radius of the toroidal plasma respectively. Most studies have been concerned with low plasma pressure i.e., $\beta_p \lesssim 1$. Here poloidal beta is defined by $\beta_p = 2\langle p\rangle/B_a^2$, where $\langle p\rangle$ is the average pressure and B_a is the magnitude of the poloidal magnetic field at the plasma boundary r = a. Shafranov[9),10)] showed that to $O(\varepsilon^2)$ the magnetic surfaces are nested circles. Recently, using the ordering $\beta_p \sim 1$ and studying a toroidal plasma seperated from vacuum by a sharp boundary, Green, Johnson and Weimer[19)] have carried their calculation to $O(\varepsilon^3)$ and shown that the magnetic surfaces are elliptically distorted as well as non-concentric.

For large value of β, it has been unclear that pressure balance between plasma and magnetic field could exist and it has been popularly supported that there is an equilibrium limit of $\beta_p < \varepsilon^{-1}$.[11)] Considering special distributions of pressure and current, a number of workers have studied equilibrium configuration in which $\beta_p \sim \varepsilon^{-1}$. Some features of these results are as follows. Laval et al.[14)] have studied a diffuse plasma contained in a torus with elliptical cross section. Strauss[15)] has shown, for the plasma being contained

in a torus of rectangular cross section, that equilibria with arbitrary β_p are possible. In both cases, the pressure vanishes at the surrounding conducting shell. Callen and Dory[16] showed equilibria of the toroidal plasma with vacuum contained in a conducting shell and found in the case of $\beta_p > \varepsilon^{-1}$ they have only one magnetic axis and as $\beta_p \to \varepsilon^{-1}$ regions of reverse current appear in the plasma. This is in contrast with the Mercier's[11] suggestion that as $\beta_p \to \varepsilon^{-1}$ a second magnetic axis appears at the inner side of the torus. Also Shafranov and Yurchenko [13] studied equilibria of toroidal plasma column with vacuum contained in an elliptically distorted conducting shell under the conditions $\beta_p \gg 1$, $\beta_p a/R \ll 1$.

It is important to notice that if $\beta_p \gg 1$, then $\beta_p a/R$ should be taken as the parameter of the expansion in the equilibrium equation instead of a/R. Otherwise the validity of the expansion is not assured.

In this Chapter, we shall investigate high β_p equilibria of the toroidal plasma with vacuum contained in the elliptically or triangularly distorted conducting shell. As recent analyses of MHD stability suggest[17),18)] that the plasma in a non-circular conducting shell is more stable than the plasma in a circular shell, it is necessary to study equilibrium of a plasma contained in a non-circular shell theoretically.

In § 2 we shall solve the equilibrium equation using the expansion with respect to $\varepsilon^k (0<k\leq 1)$. This fractional expansion makes it possible to satisfy $\beta_p \gg 1$ and $\beta_p \varepsilon < 1$. The problem is to find the curvilinear coordinates (r,θ,ϕ) in which the surfaces r = const coinside with the magnetic surfaces. This point of view in solving equilibrium equations has been developed by Green, Johnson and Weimer.[19] We take the ordering $\beta_p \sim \varepsilon^{k-1}$ and show that the equilibrium equation can be solved to any order of ε by appropriately choosing the coordinates. For example, we treat the case k = 1/3(i.e. $\beta_p \sim \varepsilon^{-2/3}$) and make the calculation up to the order ε^{3k}(or ε) including the contribution to ellipticity and triangularity of the magnetic surfaces.

In § 3, some examples obtained by the formulation developed here will be shown. We can solve the equilibrium analytically for a uniform current distribution. For a non-uniform current distribution, however, we must use numerical techniques such as Runge-Kutta method with automatic intervals. Section 4 is devoted to discussions.

§ 2 Solution of the MHD Equilibrium Equation

Following to Green, Johnson and Weimer[19] we shall describe a general formulation to solve the equilibrium equation for a toroidal plasma. This is convenient for application to Tokamak systems.

We take an axially symmetiric curvilinear coordinate system in which the magnetic surfaces coincide with the coordinate r = const. The transformation between the (r,θ,ϕ) and the cylindrical coordinates system (X,ϕ,Z) can be written formally as (see Fig.IV-1)

$$X = X(r,\theta)$$
$$Z = Z(r,\theta) \qquad (4.1)$$

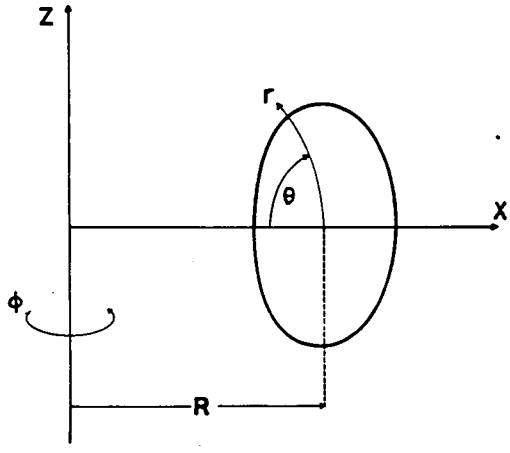

Fig.IV-1. Coordinates.

In the (r,θ,ϕ) coordinates, the magnetic axis is at r = 0, or X = R and Z = 0. In this coordinate system, the contravariant components of the magnetic field are given by the formulas,

$$B^r = 0, \quad B^\theta = \frac{RB_0}{XJ} f(r), \quad B^\phi = \frac{RB_0}{X^2} h(r), \qquad (4.2)$$

where $J = \frac{\partial X}{\partial \theta}\frac{\partial Z}{\partial r} - \frac{\partial X}{\partial r}\frac{\partial Z}{\partial \theta}$ is the Jacobian. From eqs.(4.2) the magnetic field is given by

$$\vec{B} = B^{\theta}\hat{e}_{\theta} + B^{\phi}\hat{e}_{\phi} \ , \tag{4.3}$$

where $\hat{e}_{\theta}$ and $\hat{e}_{\phi}$ denote unit vectors. RB_0 is introduced to make $f(r)$ and $h(r)$ dimensionless and the factor $1/XJ$ makes eq.(4.3) divergence free magnetic field. From eq.(4.3), $\vec{j}$ can be written as

$$\begin{aligned} \vec{j} &= j^{\theta}\hat{e}_{\theta} + j^{\phi}\hat{e}_{\phi} \ , \\ j^{\theta} &= -\frac{RB_0}{XJ}\, h'(r) \ , \\ j^{\phi} &= \frac{RB_0}{XJ}\left[\frac{\partial}{\partial r}\frac{f}{XJ}\left\{\left(\frac{\partial X}{\partial \theta}\right)^2 + \left(\frac{\partial Z}{\partial \theta}\right)^2\right\} - \frac{\partial}{\partial \theta}\frac{f}{XJ}\left(\frac{\partial X}{\partial \theta}\frac{\partial X}{\partial r} + \frac{\partial Z}{\partial \theta}\frac{\partial Z}{\partial r}\right)\right] \end{aligned} \tag{4.4}$$

where the accent denotes the derivative with respect to r.

Substituting eqs.(4.3) and (4.4) into eq.(1.8), we have

$$\frac{p'}{R^2 B_0{}^2} + \frac{hh'}{X^2} + \frac{f}{XJ}\left[\frac{\partial}{\partial r}\frac{f}{XJ}\left\{\left(\frac{\partial X}{\partial \theta}\right)^2 + \left(\frac{\partial Z}{\partial \theta}\right)^2\right\} - \frac{\partial}{\partial \theta}\frac{f}{XJ}\left(\frac{\partial X}{\partial r}\frac{\partial X}{\partial \theta} + \frac{\partial Z}{\partial r}\frac{\partial Z}{\partial \theta}\right)\right] = 0 \ . \tag{4.5}$$

To proceed further we expand in powers of the inverse aspect ratio $\varepsilon = a/R$. Green, Johnson and Weimer took the ordering,

$$\left.\begin{aligned} h &= 1 + \varepsilon^2 h^{(2)}(r) \\ f &\sim \varepsilon \\ p &\sim \varepsilon^2 \end{aligned}\right\} \tag{4.6}$$

which corresponds to $q = rB_{\phi}/RB_{\theta} \sim 1$ and $\beta_p \sim 1$. To carry the calculation to third order of ε, $O(\varepsilon^3)$, they put

$$X = R - \varepsilon r\cos\theta - \varepsilon^2\Delta(r) + \varepsilon^3 E(r)\cos\theta$$

$$Z = \varepsilon r\sin\theta + \varepsilon^3 E(r)\sin\theta \qquad (4.7)$$

Here $\Delta(r)$ shows the shift of the centers of the magnetic surfaces from the magnetic axis ($X = R$, $Z = 0$); $E(r)$ determines the ellipticity of the magnetic surfaces. They have obtained that magnetic surfaces are elliptically distorted as well as non-concentric, even if $\beta_p \lesssim 1$.

Let us now treat an equilibrium of high β_p plasma column. In the first place, we adopt the ordering,

$$h(r) = 1 + \varepsilon^{l+k} h^{(l+k)}(r)$$

$$f \sim \varepsilon$$

$$p \sim \varepsilon^{l+k} \qquad (4.8)$$

and $\beta_p \sim \varepsilon^{k-1}$ $\qquad (l \geqslant k > 0)$

We have retained the ordering $f \sim \varepsilon$, since $q>1$ must be satisfied to assure the stability against the MHD instability. Secondly we take the coordinates,

$$X = R - \varepsilon r\cos\hat{\theta} - \varepsilon^{l+2k} T_2\cos\hat{\theta} - \sum_{m=1} \varepsilon^{l+mk} S_m \cos(m-1)\theta$$

$$Z = \varepsilon r\sin\theta + \varepsilon^{l+2k} T_2\sin\theta - \sum_{m=1} \varepsilon^{l+mk} S_m \sin(m-1)\theta \qquad (4.9)$$

Here S_1 denotes the shift of the centers of the magnetic surfaces from the magnetic axis, S_2 and S_3 determine the ellipticity of the magnetic surfaces and the triangularity of them respectively and so on. The parameter T_2 means the labeling of magnetic surfaces and its role in this formulation becomes clear in the following. Then, the metric tensors $g_{\theta\theta}$, $g_{r\theta}$ and Jacobian J are written in the form,

$$g_{\theta\theta} \equiv \left(\frac{\partial X}{\partial \theta}\right)^2 + \left(\frac{\partial Z}{\partial \theta}\right)^2$$

$$= \varepsilon^2 r^2 \{1 + 2\varepsilon^{2k} \frac{T_2}{r} + \varepsilon^{4k} \frac{T_2^2}{r^2}\}$$

$$- \varepsilon^2 r^2 \sum_{m=1} \{2\varepsilon^{mk}(m-1)\frac{S_m}{r} - \sum_{j=1} \varepsilon^{(m+2j)k}(m+j-1)(j-1)\frac{S_{m+j}S_j}{r^2}$$

$$+ 2\varepsilon^{(2+m)k}(m-1)\frac{T_2 S_m}{r^2}\} \cos m\theta \ , \qquad (4.10)$$

$$g_{r\theta} \equiv \frac{\partial X}{\partial \theta}\frac{\partial X}{\partial r} + \frac{\partial Z}{\partial \theta}\frac{\partial Z}{\partial r}$$

$$= -\varepsilon r \sum_{m=1} \{\varepsilon^{mk}(S_m' + (m-1)\frac{S_m}{r}) + \sum_{j=1} \varepsilon^{(m+2j)k}(m+j-1)\frac{S_{m+j}S_j'}{r}$$

$$+ \varepsilon^{(2+m)k}(\frac{T_2 S_m'}{r} + (m-1)\frac{T_2 S_m}{r})\} \sin m\theta \ , \qquad (4.11)$$

and

$$J \equiv \frac{\partial X}{\partial \theta}\frac{\partial Z}{\partial r} - \frac{\partial X}{\partial r}\frac{\partial Z}{\partial \theta}$$

$$= \varepsilon r\{1 + \varepsilon^{2k}(T_2' + \frac{T_2}{r}) + \varepsilon^{4k}\frac{T_2 T_2'}{r}\}$$

$$+ \varepsilon r \sum_{m=1} \{\varepsilon^{mk}(S_m' - (m-1)\frac{S_m}{r}) - \sum_{j=1} \varepsilon^{(m+2j)k}(m+j-1)\frac{S_{m+j}S_j'}{r}$$

$$+ \varepsilon^{(2+m)k}(\frac{T_2 S_m'}{r} - (m-1)\frac{S_m T_2'}{r})\}\cos m\theta, \qquad (4.12)$$

where the accent denotes the derivative with respect to r. Taking notice of the coefficient of cos mθ(or sin mθ) in eqs.(4.10) and (4.11), we find that S_m itself contributes to the order ε^{mk}, while the other terms due to the coupling, e.g. $S_{m+j}S_j/r^2$ or $S_{m+j}S_j'/r$, give ε^{2k} times higher order contributions. Then, if we desire to calculate up to the order ε^{mk}, we need not consider S_{m+j} $(j \geq 1)$.

In this section we specifically consider the case, k = 1/3 (i.e. $\beta_p \sim \varepsilon^{-2/3}$), and the calculation can be carried out to the order ε^{3k}. We can calculate to any higher order systematically,

if desired.

Substituting eqs.(4.10), (4.11) and (4.12) into eq.(4.5) and setting each Fourier coefficient equal to zero, we obtain the following equations:

$$\frac{p'}{f^2B_0^2}+\frac{hh'}{f^2}+\frac{(rf)'}{rf}$$

$$=\varepsilon^{2k}\left[T_2''+\left(2\frac{(rf)'}{rf}-\frac{1}{r}\right)T_2'+\frac{T_2}{r^2}+\left(\frac{3}{2}\frac{(rf)'}{rf}-\frac{1}{r}\right)S_1'^2+\frac{p'r}{B_0^2f^2R}\right.$$

$$\left.\times\left(3S_1'+2\frac{S_1}{r}\right)\right], \tag{4.13}$$

$$S_1''+\left(2\frac{(rf)'}{rf}-\frac{1}{r}\right)S_1'+2\frac{p'r}{B_0^2f^2R}$$

$$=\varepsilon^{2k}\left[\frac{1}{R}-2\frac{p'r}{B_0^2f^2R}\left(\frac{3}{2}S_2'+\frac{3S_2}{2r}+\frac{9}{4}S_1'^2+3\frac{S_1'S_1}{r}+3T_2'+\frac{T_2}{r}\right)\right.$$

$$\left.-S^1{}'\left\{3\left(\frac{(rf)'}{rf}-\frac{1}{r}\right)S_2'-3\frac{S_2}{r^2}+6\frac{(rf)'}{rf}T_2'-2\left(\frac{T_2'}{r}-\frac{T_2}{r^2}\right)+\frac{3(rf)'}{4rf}S_1'^2\right\}\right], \tag{4.14}$$

$$S_2''+\left(2\frac{(rf)'}{rf}-\frac{1}{r}\right)S_2'-\frac{3S_2}{r^2}=-\left(\frac{3p'r}{B_0^2f^2R^2}+\frac{3(rf)'}{2\,rf}S_1'\right)S_1', \tag{4.15}$$

and

$$S_3''+\left(2\frac{(rf)'}{rf}-\frac{1}{r}\right)S_3'-\frac{8S_3}{r^2}=\frac{3S_1'S_2}{r^2}-\frac{S_1'S_2'}{r}-\frac{(rf)'}{rf}\left(3S_1'S_2'+\frac{1}{4}S_1'^3\right)$$

$$-\frac{2p'r}{B_0^2f^2R}\left(\frac{3}{4}S_1'^2-\frac{S_2}{2r}+\frac{3}{2}S_2'\right). \tag{4.16}$$

Equation (4.13) arises from the terms independent of θ. There may be several alternative methods to solve these equations. If the purpose of the calculation is to obtain an equilibrium solution, it is convenient to adjust the labeling parameter T_2 so as to statisfy the following equation,

$$T_2' + (2\frac{(rf)'}{rf} - \frac{1}{r})T_2' + \frac{T_2}{r^2} + (\frac{3}{2}\frac{(rf)'}{rf} - \frac{1}{r})S_1'^2 + \frac{p'r}{B_0^2 f^2 E}(3S_1' + 2\frac{S_1}{r}) = 0 .$$

(4.17)

Therefore we have

$$\frac{p'}{B_0^2} + hh' + \frac{f(rf)'}{r} = 0 \quad . \tag{4.18}$$

We solve eq.(4.14) by the successive approximation. Let $S_1^{(0)}(r)$ be the solution of the equation,

$$S_1^{(0)'} + (2\frac{(rf)'}{rf} - \frac{1}{r})S_1^{(0)'} + 2\frac{p'r}{B_0^2 f^2 E} = 0 \quad , \tag{4.19}$$

then we take the solution in the form

$$S_1(r) = S_1^{(0)}(r) + \varepsilon^{2k} S_1^{(2)}(r) \quad . \tag{4.20}$$

Since $p'(r) = 0$, $h'(r) = 0$ and $f(r) = f_a\, a/r$ are valid in the vacuum region outside the plasma column, $S_1^{(0)}(r)$ is obtained from eq.(4.19)

$$S_1^{(0)}(r) = S_{1a}^{(0)} + \frac{S_{1a}^{(0)'}}{2a}(r^2 - a^2) \quad , \tag{4.21}$$

where $f_a = f(a)$, $S_{1a}^{(0)} = S_1^{(0)}(a)$, $S_{1a}^{(0)'} = S_1^{(0)'}(a)$.
Considering S_1 of the R.H.S. of eq.(4.15) as $S_1^{(0)}$, we have

$$S_2(r) = \frac{S_{2a}}{4}(\frac{r^3}{a^3} + \frac{3a}{r}) + \frac{aS_{2a}'}{4}(\frac{r^3}{a^3} - \frac{a}{r}) \quad , \tag{4.22}$$

where $S_{2a} = S_2(a)$ and $S_{2a}' = S_2'(a)$.
Substituting eqs.(4.21) and (4.22) into eq.(4.16), we find

$$S_3(r) = \frac{S_{3a}}{6}\left(\frac{2r^4}{a^3} + \frac{4a^2}{r^2}\right) + \frac{aS_{3a}'}{6}\left(\frac{r^4}{a^4} - \frac{a^2}{r^2}\right)$$

$$+ \left\{\frac{1}{24}\left(\frac{r^4}{a^4} - 1\right) + \frac{1}{12}\left(\frac{a^2}{r^2} - 1\right)\right\} S_{1a}^{(0)'}(3S_{2a} - aS_{2a}'), \quad (4.23)$$

where $S_{3a} = S_3(a)$ and $S_{3a}' = S_3'(a)$.
In the same way, eq.(4.17) leads to

$$T_2(r) = \frac{r}{a}\left(1 - \ell n\frac{r}{a}\right)T_a + r\ell n\frac{r}{a}T_a' + rS_{1a}^{(0)'}\left\{\frac{1}{4}\left(\frac{r^2}{a^2} - 1\right) - \frac{1}{2}\ell n\frac{r}{a}\right\}, \quad (4.24)$$

where $T_a = T_2(a)$ and $T_a' = T_2'(a)$.
Substituting eqs.(4.21), (4.22), (4.23) and (4.24) into eq.(4.14) we obtain

$$S_1^{(2)}(r) = S_{1a}^{(2)} + \frac{S_{1a}^{(2)'}}{2a}(r^2 - a^2) + \left\{\frac{1}{2R} + \frac{S_{1a}^{(0)'}}{a}\left(T_a' - \frac{T_a}{a} - \frac{S_{1a}^{(0)'2}}{2}\right)\right\} r^2 \ell n\frac{r}{a}$$

$$- \left\{\frac{1}{4R} + \frac{S_{1a}^{(0)'}}{a}\left(T_a' - \frac{T_a}{a} - \frac{S_{1a}^{(0)'2}}{2}\right)\right\}(r^2 - a^2)$$

$$+ \frac{S_{1a}^{(0)'}}{8a}\left\{\frac{3}{a^3}(S_{2a} + aS_{2a}') + \frac{1}{a^2}S_{1a}^{(0)'2}\right\}(r^2 - a^2)^2 . \quad (4.25)$$

To obtain explicit values for the quantities T_a, T_a', S_{ma} and S_{ma}' it is necessary to specify the model of the equilibrium configuration. We take the special model to calculate analytically; constant current density and a parabolic pressure distribution, i.e.,

$$\left.\begin{aligned} f(r) &= \frac{r}{a}f_a \\ p(r) &= B_0^2 f_a^2 \beta_p\left(1 - \frac{r^2}{a^2}\right) \end{aligned}\right\} \quad (4.26)$$

where

$$\beta_p \equiv \frac{4}{B_0^2 f_a^2 a^2}\int_0^a rp(r)dr \quad (4.27)$$

With this model we obtain the following expressions:

$$S_1^{(0)}(r) = \frac{r^2}{2R}\beta_p \quad ,$$

$$S_{1a}^{(0)} = \frac{a^2}{2R}\beta_p \quad ,$$

$$S_{1a}^{(0)'} = \frac{a}{R}\beta_p \quad , \qquad (4.28)$$

$$S_2(r) = \frac{r}{a}S_{2a} + \frac{\beta_p^2}{4}\frac{a^3}{R^2}\left(\frac{r^3}{a^3} - \frac{r}{a}\right) \quad ,$$

$$S_{2a}' = \frac{S_{2a}}{a} + \frac{a^2}{2R^2}\beta_p^2 \quad , \qquad (4.29)$$

$$T_2(r) = \frac{3}{8}\frac{\beta_p^2}{R^2}r^3 \quad ,$$

$$T_a = \frac{3}{8}\frac{\beta_p^2}{R^2}a^3 \quad ,$$

$$T_a' = \frac{9}{8}\frac{\beta_p^2}{R^2}a^2 \quad , \qquad (4.30)$$

$$S_{1a}^{(2)} = \frac{a^2}{8R}\left(1 + 12\frac{S_{2a}}{a}\beta_p + 4\frac{a^2}{R^2}\beta_p^3\right) \quad ,$$

$$S_{1a}^{(2)'} = \frac{a}{4R}\left(1 + 12\frac{S_{2a}}{a}\beta_p + 11\frac{a^2}{R^2}\beta_p^3\right) \quad , \qquad (4.31)$$

and

$$S_3(r) = \frac{r^2}{a^2}S_{3a} - \frac{1}{8}\frac{\beta_p^3}{R^3}a^2r^2\left(1 - \frac{r^2}{a^2}\right) \quad ,$$

$$S_{3a}' = 2\frac{S_{3a}}{a} + \frac{1}{4}\frac{a^3}{R^3}\beta_p^3 \quad . \qquad (4.32)$$

These show that $\beta_p\, a/R$ should be the expansion parameter to solve eq.(4.5).

The remaining parameters S_{2a} and S_{3a} are determined from the shape of the conducting shell. Let the shape of the shell be

$$\left.\begin{aligned} X &= R - S_{1b} - b\cos\theta - T_{2b}\cos\theta - S_{2b}\cos\theta - S_{3b}\cos 2\theta \\ Z &= b\sin\theta + T_{2b}\sin\theta - S_{2b}\sin\theta - S_{3b}\sin 2\theta . \end{aligned}\right\} \quad (4.33)$$

Thus from eqs.(4.22) and (4.23), we obtain

$$S_{2b} = \frac{S_{2a}}{4}\left(\frac{b^3}{a^3} + \frac{3a}{b}\right) + \frac{aS_{2a}'}{4}\left(\frac{b^3}{a^3} - \frac{a}{b}\right) , \quad (4.34)$$

and

$$S_{3b} = \frac{S_{3a}}{6}\left(\frac{2b^4}{a^4} + \frac{4a^2}{b^2}\right) + \frac{aS_{3a}'}{6}\left(\frac{b^4}{a^4} - \frac{a^2}{b^2}\right)$$

$$+ \left\{\frac{1}{24}\left(\frac{b^4}{a^4} - 1\right) + \frac{1}{12}\left(\frac{a^2}{b^2} - 1\right)\right\} S_{1a}^{(0)'}(3S_{2a} - aS_{2a}'). \quad (4.35)$$

The displacement of the center of the plasma cross section from the center of the conducting shell is given in the form;

$$\delta \equiv S_{1a} - S_{1b} + S_{3a} - S_{3b}$$

$$= \frac{S_{1a}'}{2a}(b^2 - a^2) + \left\{\frac{1}{2R} + \frac{S_{1a}^{(0)'}}{a}\left(T_a' - \frac{T_a}{a} - \frac{S_{1a}^{(0)'2}}{2}\right)\right\} b^2 \ell n\frac{b}{a}$$

$$- \left\{\frac{1}{4R} + \frac{S_{1a}^{(0)'}}{a}\left(T_a' - \frac{T_a}{a} - \frac{S_{1a}^{(0)2}}{2}\right)\right\}(b^2 - a^2)$$

$$+ \frac{S_{1a}^{(0)'}}{8a}\left\{\frac{3}{a^3}(S_{2a} + aS_{2a}') + \frac{1}{a^2}S_{1a}^{(0)'2}\right\}(b^2 - a^2)^2$$

$$+ S_{3a} - \frac{S_{3a}}{6}\left(\frac{2b^4}{a^4} + \frac{4a^2}{b^2}\right) - \frac{aS_{3a}'}{6}\left(\frac{b^4}{a^4} - \frac{a^2}{b^2}\right)$$

$$- \left\{\frac{1}{24}\left(\frac{b^4}{a^4} - 1\right) + \frac{1}{12}\left(\frac{a^2}{b^2} - 1\right)\right\} S_{1a}^{(0)'}(3S_{2a} - aS_{2a}') . \quad (4.36)$$

Substituting eqs.(4.28) ~ (4.32) into eqs.(4.34), (4.35) and (4.36) and neglecting a^4/b^4, we obtain

$$S_{2b} = \frac{2a^3}{b^3} S_{2b} - \frac{a^3}{4R^2} \beta_p \tag{4.37}$$

$$S_{3a} = \frac{3}{2} \frac{a^4}{b^4} S_{3b} - \frac{1}{4} \frac{a^4}{Rb^4} \beta_p S_{2b} \tag{4.38}$$

and

$$\delta = \frac{b^2}{2R} \{(\beta_p - \frac{1}{4} + 6\frac{a^2}{b^3} S_{2b}) (1 - \frac{a^2}{b^2}) + \ell n \frac{b}{a}\}$$

$$+ (\frac{3}{2} \frac{b}{R} S_{2b} + \frac{b^4}{8R^3} \beta_p{}^3) (1 - \frac{a^2}{b^2})^2 + \frac{5}{8} \frac{a^2b^2}{R^3} \beta_p{}^3 (1 - \frac{a^2}{b^2})$$

$$+ \frac{a^2b^2}{4R^3} \beta_p{}^3 \ell n \frac{b}{a} . \tag{4.40}$$

Equation (4.40) has been derived on the assumption of a uniform current profile and of a parabolic pressure distribution (see eq. (4.26)). And eq.(4.40) shows that, as βp becomes large, a toroidal plasma column becomes close to the outer conducting shell. As δ depends on S_{2b}, δ can be adjusted by the choice of the conducting shell distorted elliptically.

§ 3 Some Examples of High β_p Equilibria

We calculated some examples of magnetic surfaces by means of the formulation derived in the previous section. Figures IV-2 ~ IV-7 show equilibria with β_p = 2.0 or 3.0 for the case of a uniform current profile and a parabolic pressure distribution given in eq.(4.26). In this calculation, we took R = 5.0, a = 1.0, b = 1.5 and chose some values of S_{2b} and S_{3b}. The figures show the lines r = const i.e., magnetic surfaces. The most outer magnetic surface coincides with the conducting shell. The shaded region denotes a plasma column. The magnetic surfaces are chosen so as to make a difference Δr constant. This does not correspond to the case that the magnetic flux between the adjoining magnetic surfaces is constant. From the magnetic surfaces calculated here, it is possible to pick up the magnetic surfaces so as to make a difference of the magnetic flux contained in the magnetic surface constant. Figures IV-2 and IV-3 show the equilibrium contained in a circular conducting shell. From these two figures, it is shown that the shift of the center of the magnetic surfaces from the magnetic axis depends on β_p.

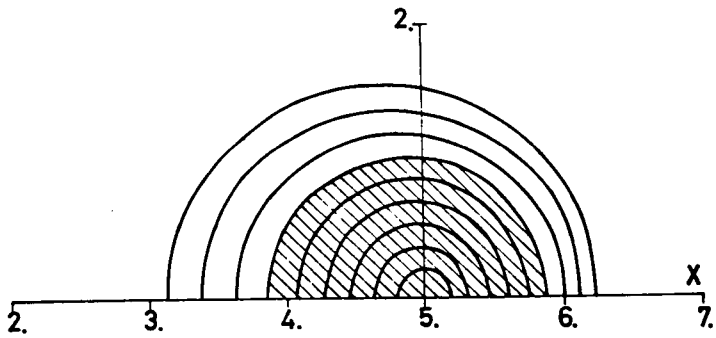

Fig.IV-2. Magnetic surfaces of Tokamak equilibrium with β_p = 2.0, S_{2b} = 0.0, S_{3b} = 0.0 and with the uniform toroidal current.

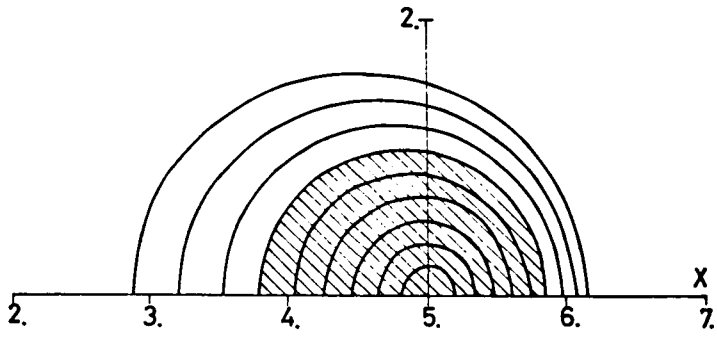

Fig.IV-3. Magnetic surfaces of Tokamak equilibrium with $\beta_p = 3.0$, $S_{2b} = 0.0$, $S_{3b} = 0.0$ and with the uniform toroidal current.

Figures IV-4 and IV-5 show the equilibria contained in an elliptically distorted conducting shell.

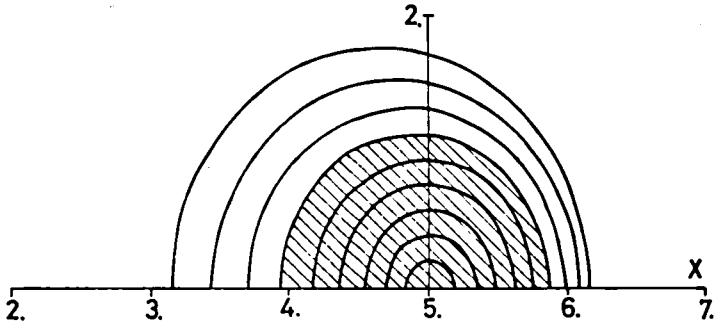

Fig.IV-4. Magnetic surfaces of Tokamak equilibrium with $\beta_p = 3.0$, $S_{2b} = -0.4$, $S_{3b} = 0.0$ and with the uniform toroidal current.

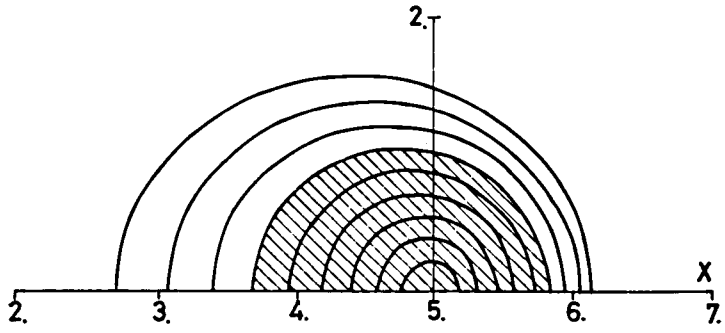

Fig.IV-5. Magnetic surfaces of Tokamak equilibrium with $\beta_p = 3.0$, $S_{2b} = 0.2$, $S_{3b} = 0.0$ and with the uniform toroidal current.

Figures IV-6 and IV-7 show the equilibria contained in a triangularly distorted conducting shell.

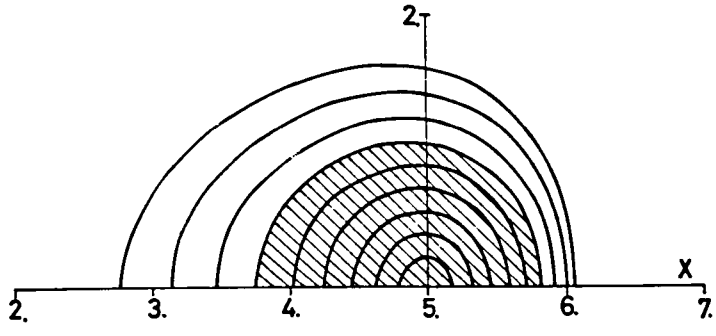

Fig.IV-6. Magnetic surfaces of Tokamak equilibrium with $\beta p = 3.0$, $S_{2b} = 0.0$, $S_{3b} = 0.4$ and with the uniform toroidal current.

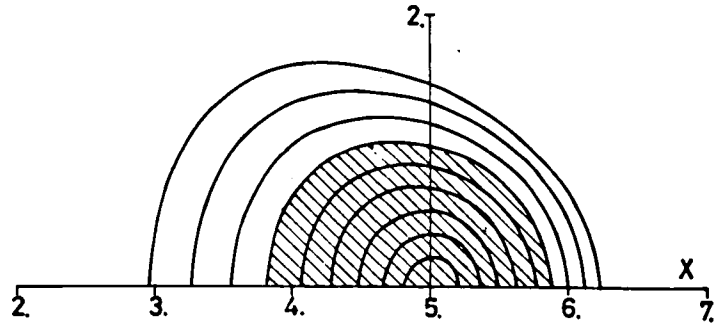

Fig.IV-7. Magnetic surfaces of Tokamak equilibrium with $\beta_p = 3.0$, $S_{2b} = 0.0$, $S_{3b} = -0.4$ and with the uniform toroidal current.

We have given the following model for a non-uniform current profile:

$$f = \frac{r f_a}{a} \frac{5}{3} \left[1 - \frac{2}{5} \left(\frac{r}{a}\right)^3 \right] ,$$

$$p = \frac{\tilde{\beta} B_0^2}{2} \left[1 - \left(\frac{r}{a}\right)^3 \right]^{3/4} \qquad (4.41)$$

and

$$\beta_p = \frac{2}{3} \frac{\Gamma(\frac{7}{3})\Gamma(\frac{2}{3})\tilde{\beta}}{\Gamma(3) \quad f_a^2} , \qquad (4.42)$$

where Γ denotes the Gamma function. The Tokamak T - 3 data can be fitted reasonably by eq.(4.41).[19] Figures IV-8 and IV-9 show the equilibrium with a non-unoform current contained in a circular conducting shell. The corresponding toroidal current profile and the safety factor are shown in Fig.IV-10 and Fig.IV-11. The safety factor q(r) is defined by $h(r)/f(r)\ (J/X)_0$,[63] where $(J/X)_0$ denotes the component independent of θ. These figures show that the high β_p equilibria are confirmed in variously shaped conducting shell.

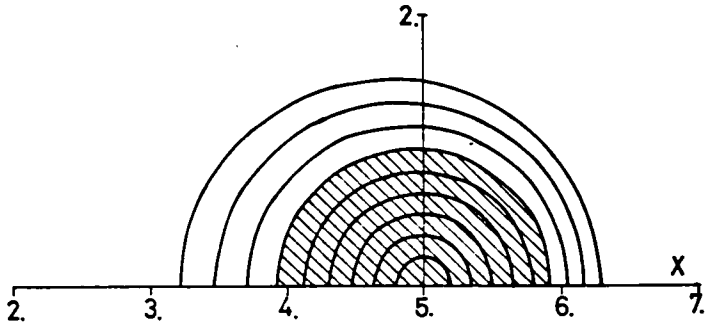

Fig.IV-8. Magnetic surfaces of Tokamak equilibrium with $\beta_p = 2.0$, $S_{2b} = 0.0$, $S_{3b} = 0.0$ and with the non-uniform toroidal current.

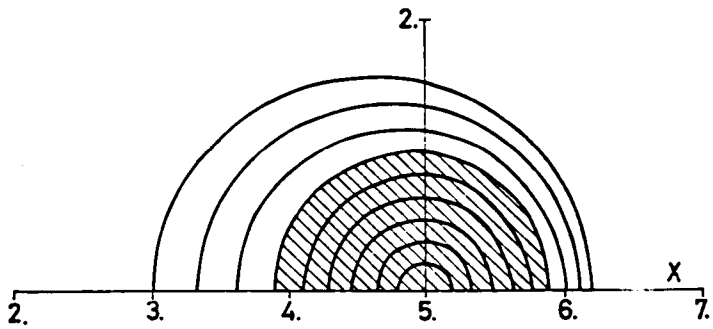

Fig.IV-9. Magnetic surfaces of Tokamak equilibrium with $\beta_p = 3.0$, $S_{2b} = 0.0$, $S_{3b} = 0.0$ and with the non-uniform toroidal current.

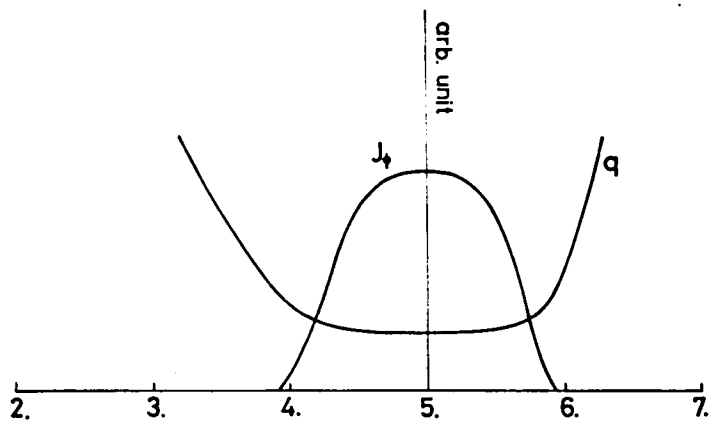

Fig.IV-10. The toroidal current profile and the safety factor corresponding to Fig.IV-8. q(0)=1.

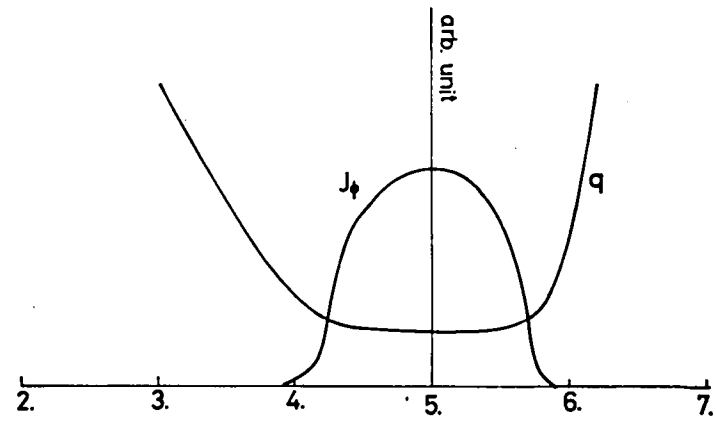

Fig.IV-11. The toroidal current profile and the safety factor corresponding to Fig.IV-9. q(0)=1.

§ 4 Conclusion and Dsicussion

The formulation to obtain equilibrium of a toroidal plasma with vacuum contained in a conducting shell with $\beta_p \sim \varepsilon^{k-1}$ has been developed and some equilibria in a circular or non-circular conducting shell with $\beta_p \sim \varepsilon^{-2/3}$ have been calculated. It is noted, in this ordering $\beta_p \sim \varepsilon^{-2/3}$, that $\beta_p\varepsilon$ is a small quantity enough to satisfy $\beta_p a/R \ll 1$. This formulation is an extension of that given by Green Johnson and Weimer to equilibrium with $\beta_p \gg 1$. Though this is essentially the same method as that given by Shafranov and Yurchenko, this formulation has two merits: (i) the quantities $S_j(r)(j \geq 2)$ corresponding to the deformation of magnetic surfaces have clear physical meanings; (ii) this makes it possible to calculate equilibrium to any order of ε. From this formulation we surmise that equilibrium with one magnetic axis is possible up to $\beta_p \sim \varepsilon^{-1}$. This limitation, however, may be due to the expansion in $\beta_p\varepsilon$ used in solving the equilibrium equation.

The equilibrium with $\beta_p = 3.0$, $R = 5.0$ does not yet show the reversal of the toroidal current.

The ratio of the plasma pressure to the magnetic pressure, β, is related to β_p in the following form

$$\beta = \beta_p \frac{\varepsilon^2}{q_2} , \tag{4.43}$$

where q is a safty factor. Hence β is limitted by both β_p and q. The equilibrium requirement limits β_p and the stability requirement for MHD modes does q. The examples in the case of $\beta_p = 3.0$, $\varepsilon = 0.2$ shown in § 3 correspond to $\beta \sim 0.12/q^2$.

CHAPTER V

MAGNETOHYDRODYNAMIC AND TEARING INSTABILITIES IN TOKAMAKS[31)]

§ 1 Introduction

The MHD stability of a current-carrying plasma in a strong longitudinal magnetic field, such as in Tokamak type devices, has been investigated by many authors.[21),22),59)] In these investigations, skin current or other special current distributions have been treated. Recently Shafranov[28)] has considered the stability for more general current distributions. Here we summarize his results pertinent to our investigation. We consider an axisymmetric cylindrical plasma column with a magnetic field,

$$\vec{B} = (0,\ B_\theta(r),\ B_S)\ , \tag{5.1}$$

where B_S is a constant and $B_S >> B_\theta$. We assume the plasma is in the region $0 \le r \le a$, vacuum in the region $a < r \le b$ and a perfectly conducting shell is located at $r = b$. Let the plasma be subjected to a perturbation $\vec{\xi}(r)\exp(im\theta - ikz)$ as usual. By use of the energy integral eq.(1.29), Shafranov has obtained the following expression for the change of the potential energy W:

$$W = \frac{\pi}{2}\xi_a{}^2 B_a{}^2 \{(1 - \frac{nq_a}{m})^2(1 + m\lambda) - 2(1 - \frac{nq_a}{m})\} + W_f, \tag{5.2}$$

where $B_a = B_\theta(a)$, $\xi_a = \xi_r(a)$, $q_a = kaB_S/mB_\theta$ and $\lambda = (1 + a^{2m}/b^{2m})/(1 - a^{2m}/b^{2m})$. The last term W_f represents the plasma fluid energy,

$$W_f = \frac{\pi}{2}\int_0^a \{f(\frac{d\xi}{dr})^2 + g\xi^2\}dr, \qquad (5.3)$$

where f and g are derived from eqs.(1.30) and (1.32) by substitution of $B_z = B_S$. Due to the hydromagnetic energy principle [29] the instability corresponds $W<0$. If W_f is positive or small negative, the instability can occur due to the second term in the curly bracket of W. An instability caused by this term is called a helical instability by Shafranov, which is equivalent to a so-called kink mode. The two terms in the curly bracket of eq.(5.2) make a negative contribution if

$$1 - \frac{2}{1 + m\lambda} < \frac{nq_a}{m} < 1 \qquad . \qquad (5.4)$$

From this, the following conclusion can be drawn: a helical instability is possible only when magnetic surfaces resonant with the perturbation are located outside the plasma column. For the case of the m = 1 mode, investigating the contribution from W_f carefully, we find that the perturbation $\xi \simeq$ const $(0 \leq r \leq a)$ reduces the term $f\xi'^2$ to a small quantity and that g is proportional to k^2r^2 which is also a small quantity. Therefore, the contribution from W_f can be neglected and the stability criterion of the m = 1 mode is almost independent of the current profile, being given by

$$a^2/b^2 < nq_a < 1 \ . \qquad (5.5)$$

Shafranov has shown that for $m \geq 2$ modes, $g<0$ is possible only in a narrow interval of nq(r) including the resonance value $nq(r_s) = m$, where $0<r_s<a$. For a monotonically decreasing current profile, q(r) is a monotonically increasing function of r as is illustrated in Fig.V-1. Then, if the singular point r_s lies outside the plasma column, W_f is necessarily positive and has a stabilizing effect. Indeed, Shafranov has shown that, for sufficiently rapidly decreasing

current distributions, helical modes with $m \geq 2$ can be stabilized because of this effect.

When nq_a is larger than m and the singular point exists in the plasma column, the instability is possible only for a perturbation satisfying $\xi_a \sim 0$, since otherwise positive contribution of the first term in eq.(5.2) exceeds W_f. Therefore, the stability does not depend on the position of the conducting shell in this case. For these localized helical modes, W_f is small either for $m = 1$ or $m \geq 2$ as discussed above, Shafranov has surmised that this modes can be stabilized if we take into account the toroidal effect.

It is the pourpose of this Chapter to calculate a growth rate of the instability as an eigen value of the equation of motion for ξ. In § 2, we use the equation of motion derived in § 3 of Chapter I and numerically compute the growth rate ω of the helical instability for given plasma equilibria. We consider two kinds of current distribution, the one is that used in Chapter II and the other is a so-called Gaussian distribution. The results are shown in § 3.

In § 4, the stability of the plasma column against the resistive tearing instability is also studied and the growth rate of tearing mode is calculated. In this section we consider two types of tearing modes. The one is excited in a main plasma with large but finite conductivity and the other is excited in a tenuous plasma with finite conductivity which surrounds a main plasma with infinite conductivity. The stability of the latter type of tearing mode is similar to that of nonlocal helical instability. The growth rate of this tearing mode, however, may be smaller than that of nonlocal helical instability. Section 5 is devoted to discussions.

§ 2 Numerical Procedures

In this section we describe the scheme for the numerical calculation of the growth rate.

The equilibrium values $\vec{B}$ and p are given by the method shown in § 2 of Chapter II. The $J_z(r)$, toroidal current profile, is first given and from this $B_\theta(r)$ is obtained. Now we construct force free field $J_\theta^{(0)}$ and $B_z^{(0)}$ from these values of $J_z(r)$ and $B_\theta(r)$ by the equations

$$J_\theta^{(0)} B_z^{(0)} - J_z B_\theta = 0,$$

$$J_\theta^{(0)} = -\frac{dB_z^{(0)}}{dr} \quad . \tag{5.6}$$

Integrating eqs.(5.6), we obtain

$$B_z^{(0)}(r) = \pm\sqrt{(B_z^{(0)}(0))^2 - 2\int_0^r J_z B_\theta dr}. \tag{5.7}$$

Next, we modify $B_z^{(0)}$ by $B_z^{(1)}$ to support the plasma pressure,

$$B_z(r) = B_z^{(0)}(r) + B_z^{(1)}(r). \tag{5.8}$$

Then the pressure becomes

$$p(r) = p_0 - \frac{1}{2} B_z^{(1)}(r)\ (2B_z^{(0)}(r) + B_z^{(1)}(r)), \tag{5.9}$$

where p_0 is a constant. This method of constructing the equilibrium has an advantage that any desired pressure profile is easily obtained by appropriately choosing $B_z^{(1)}(r)$. (see § 2 of Chapter II).

For a given value of $q_a(=q(a))$, equilibria for the following toroidal current profiles have been studied:

$$
\left.
\begin{aligned}
&\text{(i)} \quad J_z = \alpha J_0 \qquad\qquad (0 \le r/a < 0.6) \\
&\qquad = J_0 \{1 + (\alpha - 1)(r/a - 0.8)^2/0.04\} \quad (0.6 < r/a \le 0.8) \\
&\qquad = J_0 \{1 - (r/a - 0.8)^2/0.04\} \qquad (0.8 < r/a \le 1.0)
\end{aligned}
\right\}
$$

$$
\text{(ii)} \quad J_z = J_0 \exp(-\kappa^2 r^2/a^2) \qquad (5.10)
$$

Hereafter, (i) is called by the name of 'α - profile' and (ii) by the name of ' κ-profile'. For the case of κ-profile, the current was modified to be the form of a parabola in the range $0.9 < r/a < 1.0$,

$$
J_z = J_0 \exp(-0.81\kappa^2/a^2)\{1 - (r/a - 0.9)^2/0.01\}\ , \qquad (5.11)
$$

so as to make the current density fall to zero at the plasma boundary.

The equilibrium are constructed for each q_a value so as to make the value of β or β_p remain fixed.

The equation of motion for ξ (1.51) derived in § 3 of Chapter I is numerically solved by use of Hamming's modified predictor-corrector method. We have used eq.(1.51), because generally a compressible fluid plasma gives greater value of ω than incompressible one. From eqs.(1.42) and (1.57), the solution outside the main plasma column is given by

$$
\begin{aligned}
ib_r &\equiv \psi \\
&= (krB_z - mB_\theta)\xi/r \\
&= C_1 I_m'(kr) + C_2 K_m'(kr),
\end{aligned}
\qquad (5.12)
$$

where the accent denotes the derivative with respect to r and the displacement current in vacuum is neglected on the condition that $\omega/k \sim v_A \ll c$, where v_A and c are the Alfvèn and light velocities

respectively.

The boundary conditions are $\xi \sim r^{m-1}$ $(r \to 0)$, ψ and ψ' are continuous across $r = a$, and $\psi(b) = 0$, which determine the growth rate as the eigenvalue of eq.(1.51).

In order to find the eigenvalue ω, the initial guess ω_0 is given to eq.(1.51), which is solved from $r = 0$ to $r = a$. The values of ξ and $d\xi/dr$ at $r = a$ determine the values of C_1 and C_2 for eq. (5.12). The smallest zeropoint r_0 of ψ (if $\xi>0$ for $r<a$, then r_0 is larger than a) is obtained. If $r_0<b$, a larger value of ω, e.g. $2\omega_0$, is given to eq.(1.51), and if $r_0>b$, a smaller value of ω, e.g. $\omega_0/2$, is chosen. After a few iterations, an appropriate value for ω is obtained.

When the singular point is close to the edge of the plasma column ($p \to 0$, $F \to 0$ at $r = a$), double precision arithmetic must be applied in the numerical calculation since $\rho\omega^2 + F^2 \to 0$ there.

The growth rate ω obtained as the eigenvalue of eq.(1.51) is normalized as

$$\lambda_N = \omega \cdot a\sqrt{<\rho>} \,/(B_a \cdot m), \tag{5.13}$$

where $<\rho>$ denotes average density.

§ 3 Growth Rate of MHD Instability

The results obtained by the method described in § 2 are shown as follows.

In Fig.V-1 are illustrated the q profiles corresponding to different toroidal current profiles, where $q(r) = rB_S/RB_\theta$.

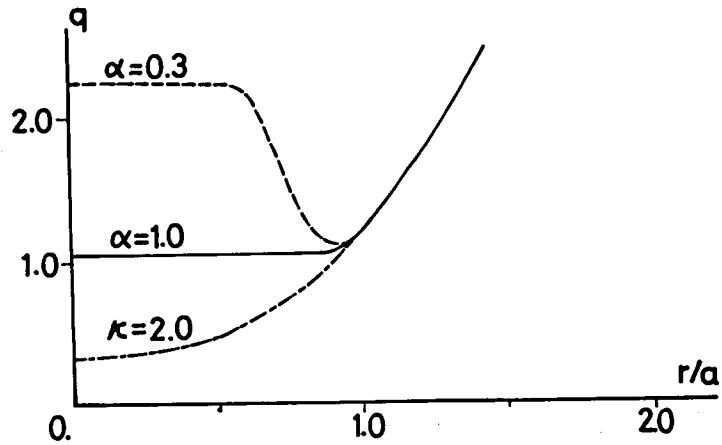

Fig.V-1. $q = rB_S/RB_\theta$ profiles. For radially decreasing current density, q increases monotonously with r, while for radially increasing one, q decreses in the main plasma and then increases outside.

For the radially decreasing current density, e.g. κ-profile, the q value increases monotonously with r, while for the radially increasing one, e.g. α-profile, it decreases in the main plasma and increases outside. The singular point, r_s, corresponds to a magnetic surface where $q(r_s) = m/n$. The former profile (κ, or $\alpha = 1.0$) may have only one singular point, while the latter profile ($\alpha<1.0$) have two. It is noticed that concentration of the current density (large κ value) leads to smaller value of q(r) inside the plasma.

In Fig.V-2 ~ Fig.V-7 are illustrated the normalized growth rates vs q_a value for various toroidal current profiles. Although the range $0<q<(a/b)^2$ is stable for all profiles, this is due to the

fixed value of k = 0.2. This range is unstable for higher k values as shown in Fig.V-7. It should be noted that in accordance with Shafranov, the growth rate for m = 1 helical mode in the range $0 \leq q_a \leq 1$ is independent of the toroidal current profile, while for higher m modes, the stability is increased with more concentration of the toroidal current in the center of the plasma column.

Figure V-2 shows the growth rate for α = 0.1-toroidal current profile: the current density is concentrated in the outer region of the main plasma. If the radius of the conducting shell is twice that of the main plasma (b/a = 2.0), the helical instability occurs in a wide range of q_a value. On the other hand when the shell is moved closer to the main plasma (b/a = 1.2), stability is considerably enhanced.

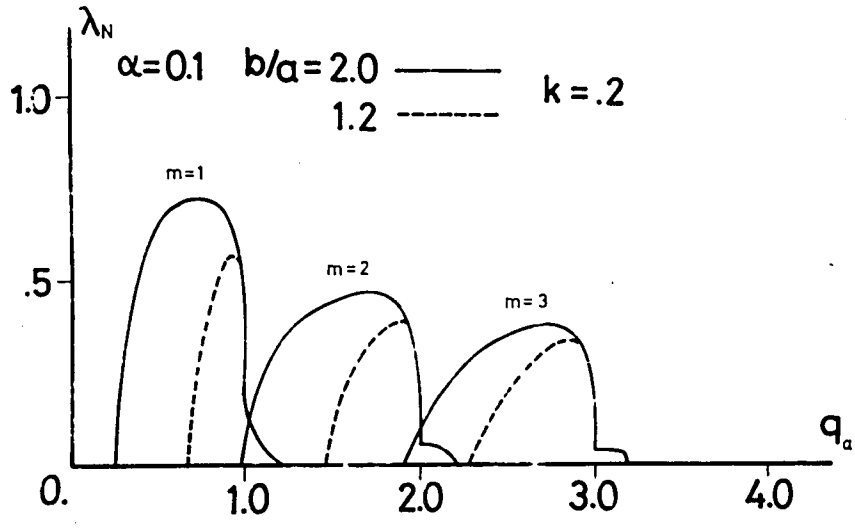

Fig.V-2. Normalized growth rate for toroidal current profile α = 0.1, β = 2%.

Figure V-3 shows the growth rate for α = 1.0-toroidal current profile, or roughly uniform current density over the plasma radius. For m≥2 modes, the stable region against m mode is wide near $q_a \sim$ m-1

in comparison to the α = 0.1 case, while stable region against m = 2 mode is narrow for $q_a \gtrsim 2$. The shell position has the same stabilizing effect as in the α = 0.1 case, but this stabilizing effect is limited to the range q_a < m for the m mode. When q_a> m, or when the singular point is inside the main plasma, the shell loses its stabilizing effect. This is due to the localization of the perturbation to the interior of the singular point (see Fig.V-9). Since the growth rate is small in this case, Shafranov has surmised that this local helical instability can be stabilized by the toroidal effect.

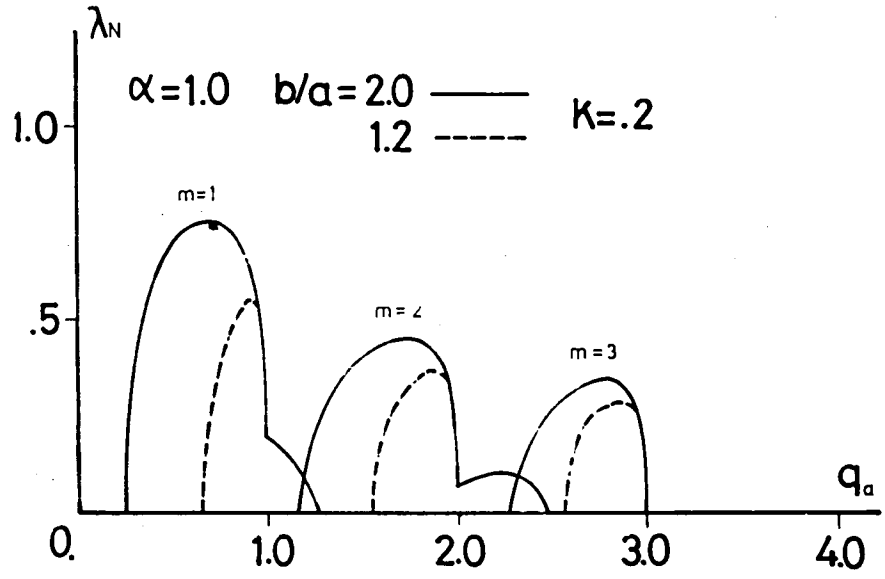

Fig.V-3. Normalized growth rate for toroidal current profile α = 1.0, β = 2%. The region $q_a \sim$ m-1 is relatively stabilized for m mode when the wall is closer to the main plasma. The stability in the region q_a>m, however, is independent of the wall position.

Figure V-4 shows the growth rate for κ = 1.0-toroidal current profile. As the toroidal current density is slightly concentrated toward the center, the stability region is slightly widened. The range $q_a \geq$ m for m $\geq$ 2 modes is stabilized.

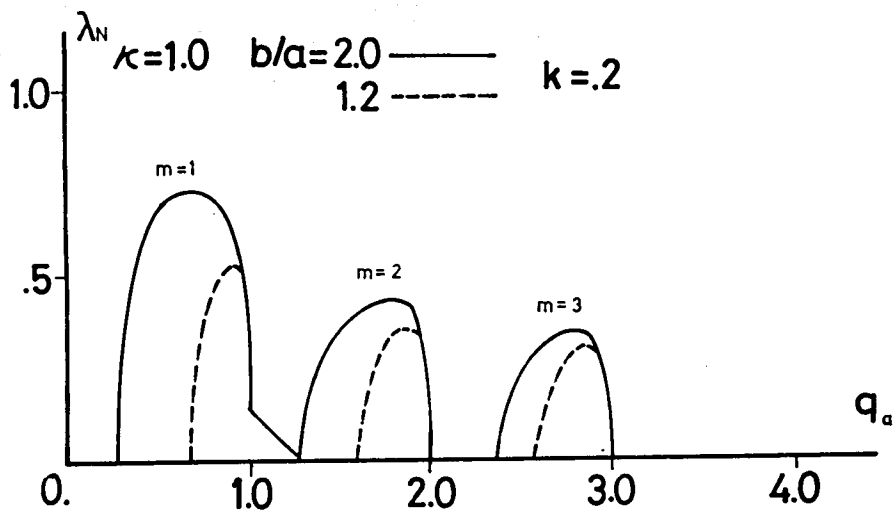

Fig.V-4. Normalized growth rate for toroidal current profile $\kappa = 1.0$, $\beta = 1\%$. The stable region is similar to that of the $\alpha = 1.0$ profile, except that the region $q_a > m$ becomes stable for modes $m \geq 2$. The wall position has the same effect as the $\alpha = 1.0$ profile.

When $\kappa = 1.5$ (not shown in the figure), the stable region for $m \geq 2$ modes is wider than the $\kappa = 1.0$ case. The helical instability of the $m = 1$ mode is independent of the toroidal current profile in the region $q_a \leq 1$, while the concentration of the current density toward the center widens the unstable region for $q_a \geq 1$ or $0 < r_s < a$.

Figure V-5 shows the growth rate for $\kappa = 1.73$-toroidal current profile for $m \geq 2$ modes. (The $m = 1$ mode assumes almost the same growth rate as in other current profiles, and has been omitted from the figure). The shell position is such that $b/a = 1.2$, and the unstable region is highly restricted to the vicinity of $q_a = m$ for the m mode respectively.

Figure V-6 shows the growth rate for $\kappa = 2.0$-toroidal current profile. While the $m = 2$ mode is unstable in the vicinity of $q_a = 2$, $m \geq 3$ modes are stabilized for all range of q_a.

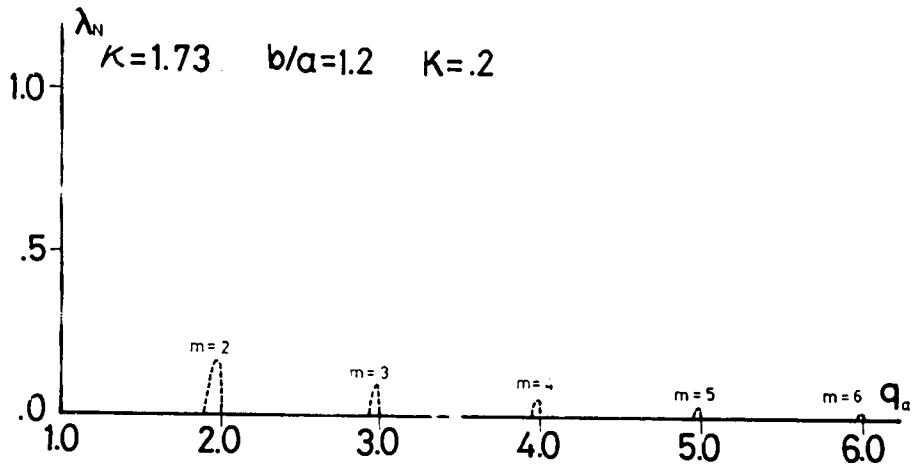

Fig.V-5. Normalized growth rate for toroidal current profile $\kappa = 1.73$, $\beta_p = 1$. In this case, poloidal β_p is fixed. The unstable region for modes $m \geq 2$ is highly restricted to the vicinity of $q_a = m$. (The m=1 mode has been omitted from the figure.)

The unstable region of the m = 1 mode for $q_a > 1$ reaches as far as $q_a \sim 3.4$. This is due to the larger value of the poloidal magnetic field near the center of the plasma column. This leads to a larger negative value of potential energy W_f inside the plasma.

When $\kappa = 2.5$ (not shown in the figure), modes $m \geq 2$ are stabilized for all values of q_a. The m = 1 mode is unstable in the same region for $q_a \leq 1$. On the other hand, unstable region to the m = 1 mode widens for $q_a > 1$ in comparison with $\kappa = 2.0$ case.

Figure V-7 shows the growth rate for higher k values in the case of $\kappa = 1.0$. In this calculation, k has been given by 0.2n. This figure shows that the m = 1 mode becomes unstable in $0 < q_a < 1$, when the singular point lies outside the plasma column.

In Fig.V-8 are shown typical eigenfunction $\xi_r (=\xi)$ for the modes m = 1 and m = 2 when the singular point r_s is outside the main plasma. When the singular point is inside the main plasma, ξ_r falls to zero beyond r_s as shown in Fig.V-9.

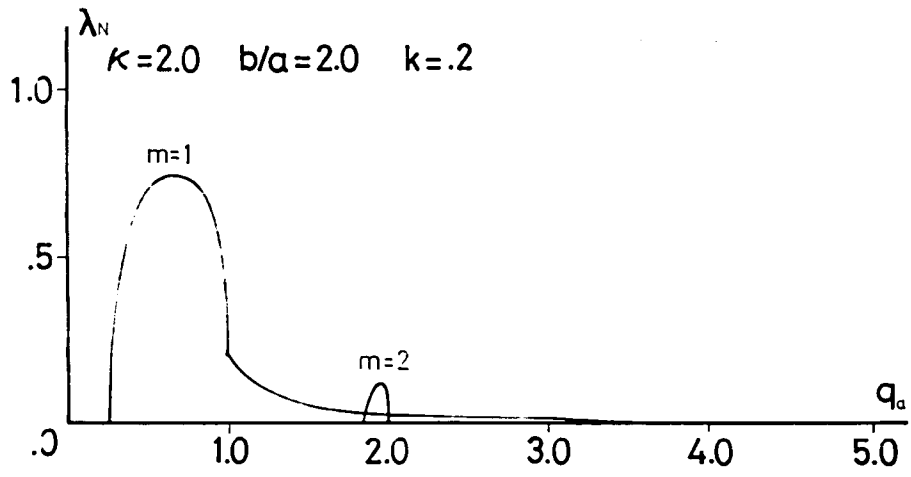

Fig.V-6. Normalized growth rate for toroidal current profile $\kappa=2.0$, $\beta=1\%$. Modes $m\geq 3$ are stabilized. The m=2 mode is unstable only in the vicinity of $q_a=2.0$. The m=1 mode becomes more unstable in the range $q_a>1.0$.

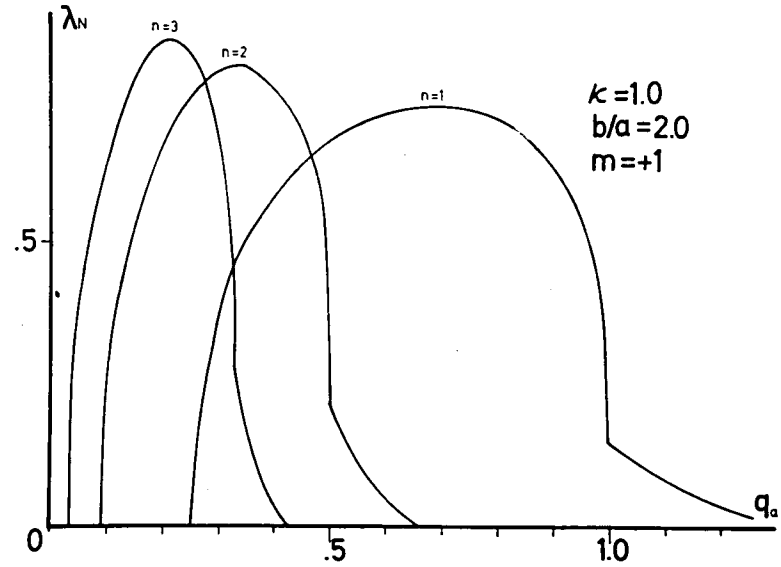

Fig.V-7. Normalized growth rate for toroidal current $\kappa=1.0$, $\beta=1\%$. In this case m=1 is fixed and k=0.2n is varied for n=1,2,3.

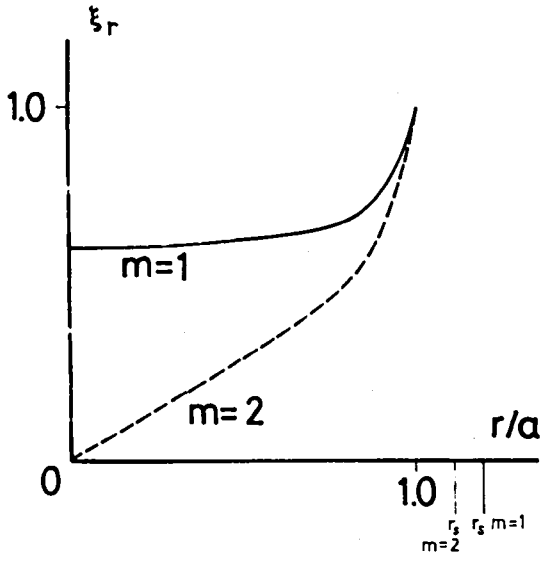

Fig.V-8. Typical eigenfunctions $\xi_r(=\xi)$ for m=1 and m=2 modes when the singular point r_s is outside the main plasma.

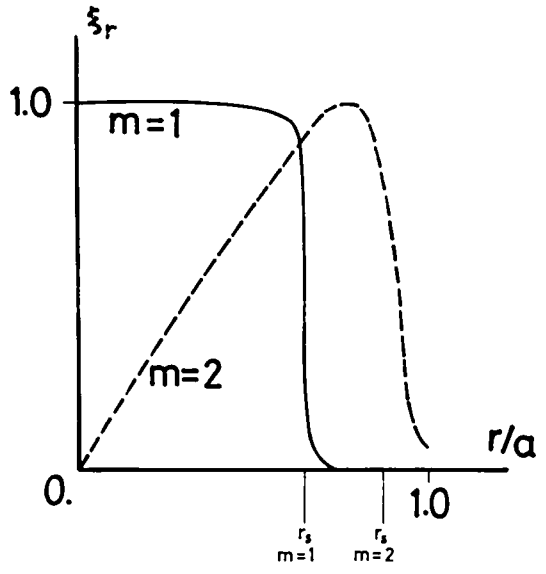

Fig.V-9. Typical eigenfunctions $\xi_r(=\xi)$ for m=1 and m=2 modes when the singular point r_s is inside the main plasma.

§ 4 Resistive Tearing Instability

Dissipative effects remove certain restrictions on the MHD instability associated with 'frozen in' field lines in the plasma.[35),36),38)] In the presence of dissipation, a nonlocal helical instability can also arise in the plasma. This is the so-called tearing mode. Here we consider resistivity as a dissipative effect. Resistivity influences the stability of the plasma column particularly in the vicinity of the singular point. Hence, we must modify the MHD equations to include resistivity η within a resistive layer near the resonant surface, where the quantity $\vec{B}\cdot\nabla\vec{\xi}$ vanishes, as eqs.(1.54) and (1.55). In the region outside the resistive layer we use the ideal MHD equations with $\eta = 0$ (see eq.(1.58)).

As we have noted in § 4 of Chapter I, Coppi, Green and Johnson[38)] have investigated the resistive instabilities in a diffuse linear pinch with a cylindrical configuration. For the treatment of the resistive tearing instability, CGJ have considered the configuration with very small pressure gradient in the resistive layer, since the energy source of the tearing mode does not come from the pressure gradient near the resonant surface but comes from the over-all configuration. In the analysis of the resistive tearing instability it is more convinient to use the variable ψ defined by eq.(5.12).

When the pressure gradient vanishes near the resonant surface, the stability criterion against the tearing mode is given by CGJ as

$$\Delta \equiv \frac{C_1^{(+)}}{C_2^{(+)}} - \frac{C_1^{(-)}}{C_2^{(-)}} < 0. \qquad (5.14)$$

Here $C_1^{(+)}$, $C_2^{(+)}$ are coefficients of ψ in $r > r_s$ and $C_1^{(-)}$, $C_2^{(-)}$ are coefficients in $r < r_s$. The ratio of $C_1^{(\pm)}$ and $C_2^{(\pm)}$ is determined from the boundary condition for ψ (ψ is finite at $r = 0$ and $\psi = 0$ at $r = b$) and the asymtotic form of ψ near r_s (see eq.(1.59)). The tearing mode with positive ω is possible for $\Delta > 0$, as the solution ψ in the resistive layer can be connected with the outer solution.

When β is small and the pressure gradient vanishes near the resonant surface, the growth rate of the tearing mode can be calculated from the relation

$$\Delta = \frac{\pi}{2} Q^{5/4} \frac{\Gamma(\frac{3}{4})}{\Gamma(\frac{5}{4})} , \qquad (5.15)$$

which is derived from eq.(1.69) by substitution of $D = 0$.
Here

$$Q = \omega / \ell^4 Q_R, \qquad \ell = (L_R/r_s)^{1/5},$$

$$L_R = \left(\frac{B^2 r_s^2 a^2}{m^2 B_z^2 l'^2}\right)^{1/6} S^{-1/3}, \qquad Q_R = \left(\frac{m^2 l'^2 B_z^2 r_s^4}{B^2 a^2}\right)^{1/3} S^{-1/3} \tau_H^{-1}$$

and Γ is the Gamma function. S is the ratio of a resistive time $\tau_R = a^2/\eta$ to a hydromagnetic time $\tau_H = \rho^{1/2}/B$, where ρ denotes density of the plasma at the resistive layer.

The numerical analysis of the stability against tearing modes was performed with the CGJ theory for Tokamak systems which have the decreasing current density in the form $J = J_0 \exp(-\kappa^2 r^2/a^2)$ for $r \leq a$. Numerically calculated values of Δ are shown in Fig.V-10 ~ Fig.V-12. The corresponding growth rates of $m = 2$ tearing mode are shown in Fig.V-13 and Fig.V-14. Figure V-10 shows the dependence of Δ on the current profile at fixed value of $q_a = 3.0$.
Also Fig.V-11 shows the dependence of Δ on the current profile at fixed value of $q_a = 2.0$. Figure V-12 shows the dependence of Δ on the safty factor q_a for $\kappa = \sqrt{2}$.

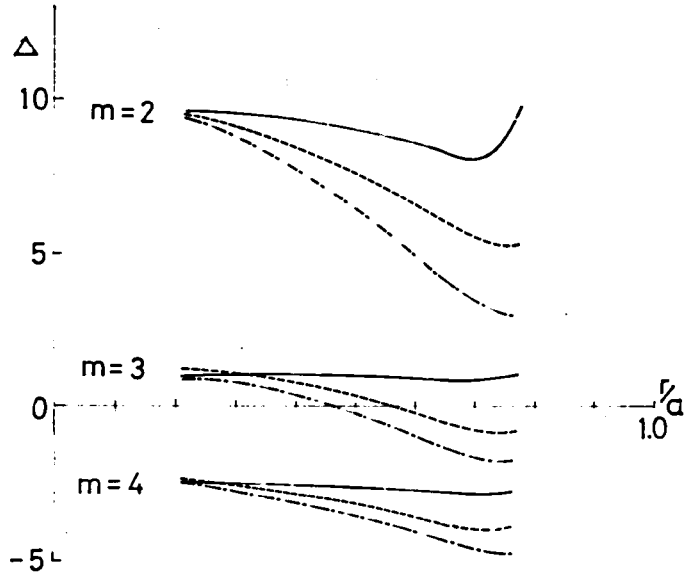

Fig.V-10. Variation of Δ for the current profile $J=J_0\exp(-\kappa^2 r^2/a^2)$ in a plasma column surrounded by a vacuum; $\beta=1.5\%$, $q_a=3.0$ and the conducting shell is located at 1.5a. The solid line shows for $\kappa=1$, the dotted line for $\kappa=\sqrt{2}$ and the dashed line for $\kappa=\sqrt{3}$.

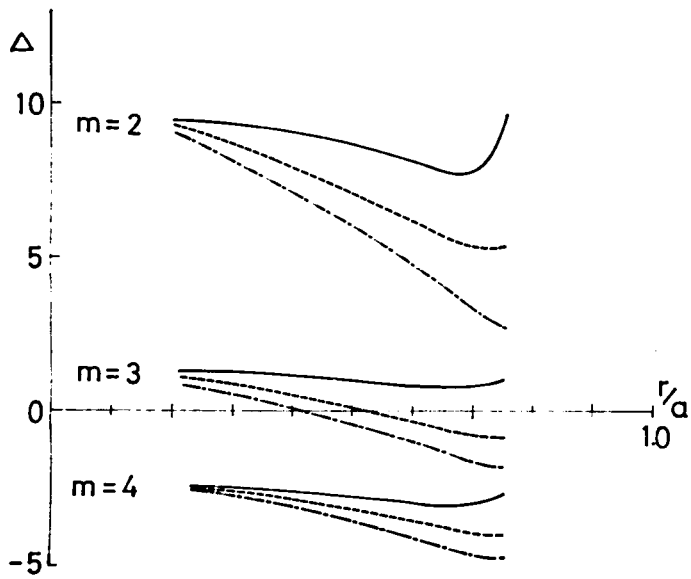

Fig.V-11. Variation of Δ for the current profile $J=J_0\exp(-\kappa^2 r^2/a^2)$ in a plasma column surrounded by a vacuum; $\beta=1.5\%$, $q_a=2.0$ and the conducting shell is located at 1.5a. The solid line shows for $\kappa=1$, the dotted line shows for $\kappa=\sqrt{2}$ and the dashed line for $\kappa=\sqrt{3}$.

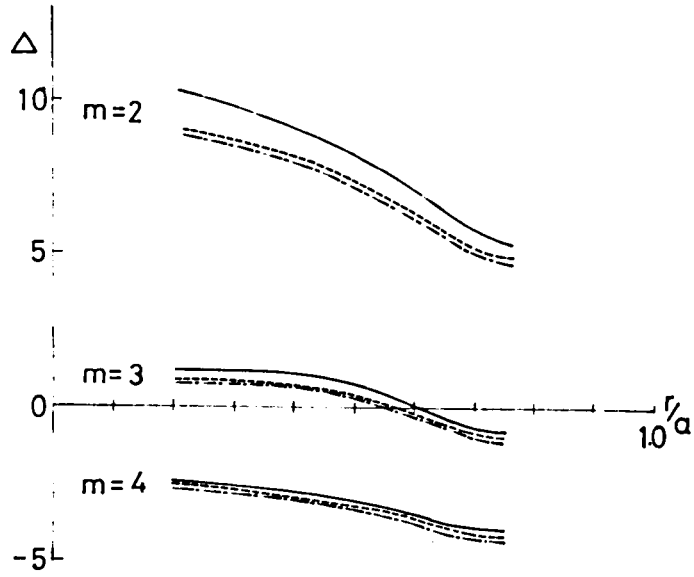

Fig.V-12. Variation of Δ for the safety factor in a plasma column surrounded by a vacuum for the toroidal current profile $\kappa=\sqrt{2}$, $\beta=1.5\%$ and the conducting shell is located at 1.5a. The solid line shows for $q_a=1.5$, the dotted line for $q_a=2.5$ and the dashed line for $q_a=3.5$.

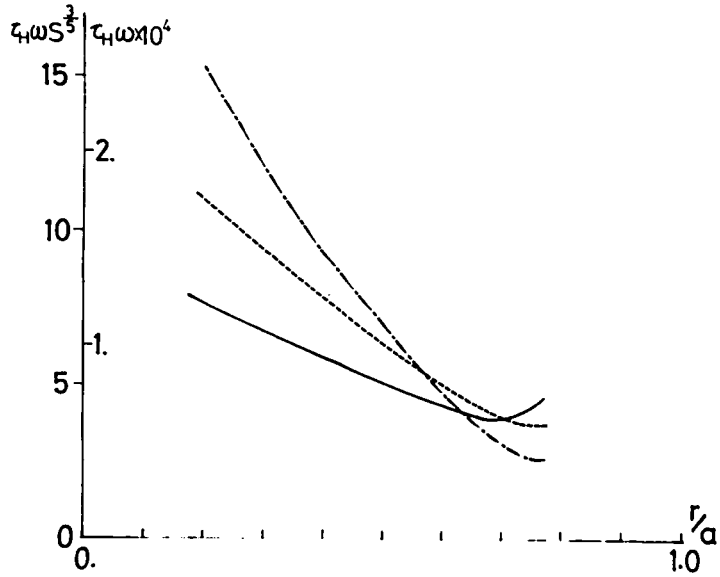

Fig.V-13. The growth rate of the tearing mode with m=2 in the case of Fig.V-10. The solid line shows for $\kappa=1$, the dotted line for $\kappa=\sqrt{2}$ and the dashed line for $\kappa=\sqrt{3}$.

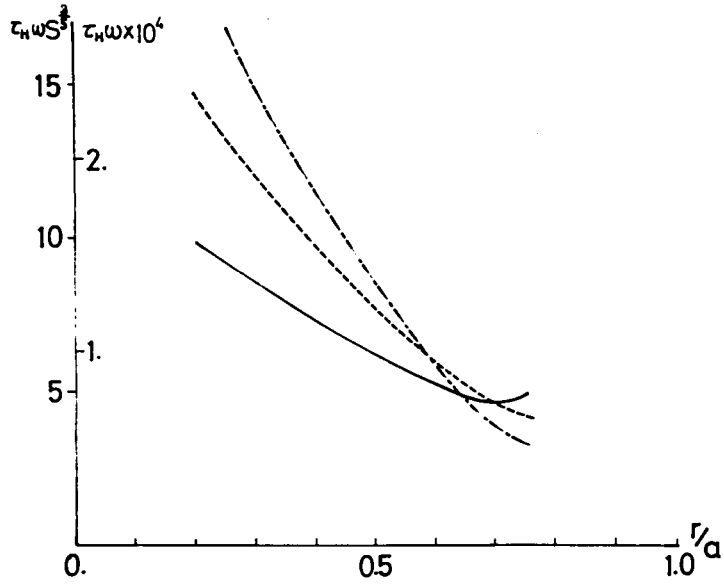

Fig.V-14. The growth rate of the tearing mode with m=2 in the case of Fig.V-11. The solid line shows for $\kappa=1$, the dotted line for $\kappa=\sqrt{2}$ and the dashed line for $\kappa=\sqrt{3}$.

We find from these figures that tearing modes with m = 2 and m = 3 are unstable, while higher m modes are stable. This result is the same as that of Shafranov. Furthermore we find that the concentration of the current density in the center of the plasma column can not stabilize tearing modes. From Fig.V-12 we find that when the total current increases, i.e. q_a decreases, tearing modes become more unstable. From Fig.V-13 and Fig.V-14 we see that growth rate of m = 2 tearing mode is about $10^{-4}\tau_H^{-1}$ for $S = 10^8$ (this parameter corresponds to $T_e \simeq 1$keV, $n \simeq 10^{14}cm^{-3}$, $B_T = 50$KG and a = 20cm). By use of the above plasma parameters we obtain $\tau_H \simeq 2 \times 10^{-8}$sec and $\omega \simeq 5 \times 10^3 sec^{-1}$. As is well known, ω depends on S as $S^{-3/5}$.

Up to here, we considered that a vacuum surrounds the main plasma column. The division of the plasma into an infinitely conductive plasma and a vacuum provides a somewhat unrealistic model of the actual Tokamak discharges. Thus we have treated the configuration

where a tenuous plasma with finite resistivity fills between the infinitely conductive plasma and the conducting shell. We have also applied CGJ theory of the resistive tearing instability in this configuration. Numerically calculated values of Δ vs q_a is shown in Fig.V-15, where we used k = 0.2 and b = 1.5a. The dotted line shows the current profile with κ = 1 and the continuous line shows one with κ = 1.73. This figure shows that unstable region vs q_a appears discretely and becomes narrow by the concentration of current density in the main plasma. Hence the behavior of this tearing mode is similar to that of nonlocal helical instabilities shown in § 3. That the right side of each curve is not clearly ended is due to that, as the singular point becomes nearer to the main plasma, $\vec{\nabla}p$ is not negligible. Thus the assumption about the tearing mode is invalid. Figure V-16 shows the growth rates of tearing modes. The typical growth rate of this tearing mode with m = 3 is about $\omega \approx 10^{-4} \tau_H^{-1}$ for S = 10^8, which may be also smaller than that of nonlocal helical instability for typical plasma parameters in Tokamak devices.

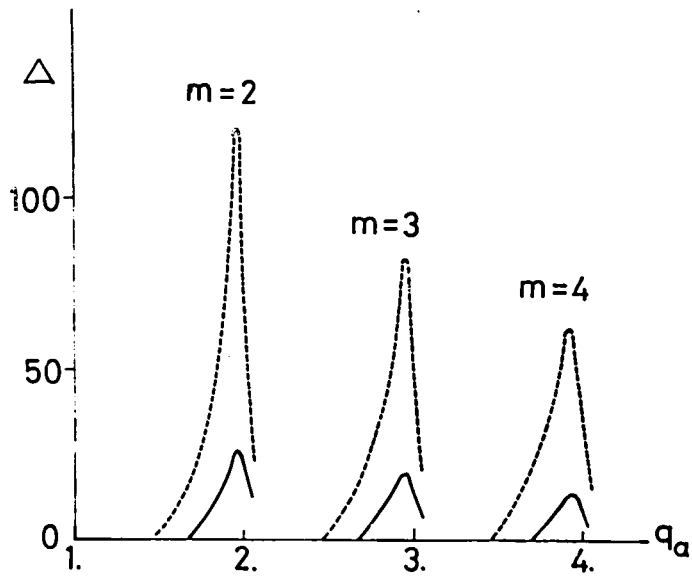

Fig.V-15. The dependence of Δ on the safety factor in a plasma column with a pressureless resistive plasma for b=1.5a and β=1.5%. The solid line shows for $\kappa=\sqrt{3}$ and the dotted line for κ=1.

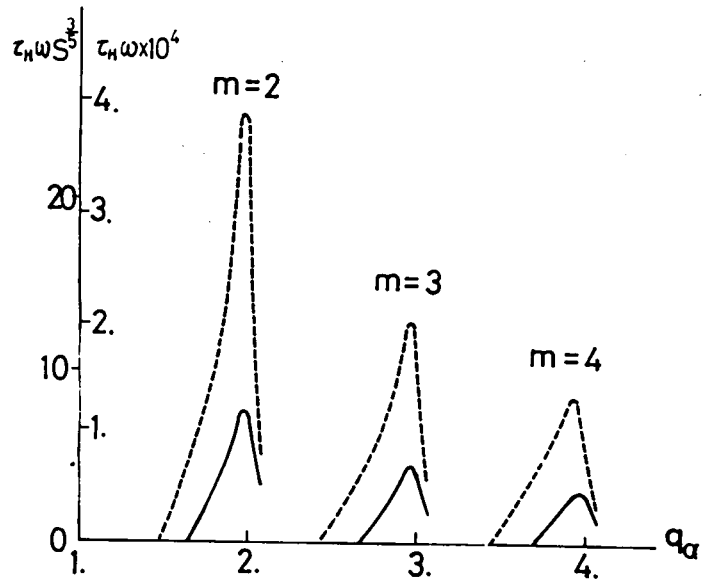

Fig.V-16. The growth rates of tearing modes occured in the pressureless resistive plasma surrounding a plasma column for b=1.5a and β=1.5%. The solid line shows for $\kappa=\sqrt{3}$ and the dotted line for κ=1.

§ 5 Conclusion and Discussion

The stability of a current carrying plasma in a strong longitudinal magnetic field, such as Tokamak type devices, against MHD and resistive tearing instabilities has been investigated in the cylinrical geometry. This may be a good approximation to a torus as long as non-local modes is studied. The growth rates of MHD instabilities has been calculated numerically as eigen-values of linealized MHD equations for several current distributions. This procedure has an advantage of studying the stability against high m helical modes. In Tokamaks, it is important to examine the stability against high m helical modes. Thus the stability diagram showing normalized growth rate λ_N versus q_a has been calculated. Numerically obtained results generally confirm Shafranov's.[28] It is shown that the position of the conducting shell has a rather remarkable influence on the stability of non-local helical modes, but not so on the local helical modes. For the case of $J = J_0 \exp(-\kappa^2 r^2/a^2)$ distributions, the non-local helical instability with $m \geq 2$ is completely stabilized if $\kappa \gtrsim 2.5$. The stability criterion of the $m = 1$ helical mode is almost independent of the current profile for $q_a \lesssim 1$.

For tearing modes, we have calculated two cases according to the position of the singular point: the one is $0 \leqslant r_s < a$ and the other is $a < r_s \leqslant b$. In the former case, we have found that tearing modes with $m = 2$ and $m = 3$ are unstable, while higher m modes are stable. Also we have found that tearing modes of this type can not be completely stabilized by the concentration of the current density in the center of the plasma column. In the latter case, we have obtained the stability diagram showing that unstable regions of q_a appear discretely and become narrow as the current density concentrates near the axis of the plasma column. In this case, the growth rates of tearing modes become small when κ becomes large.

Generally, growth rates of tearing modes are smaller than those of non-local helical modes. It is noted that the growth rate of tearing mode depends on electron temperature as $T_e^{-2/5}$. This suggests that the resistive tearing instability can be avoided by heating a plasma to a sufficiently high temperature.

Recently, experiments to lower q_a smaller than 3 have been carried out[60] and it has been shown that the unstable regions of q_a appear discretely. Although the stability diagrams obtained in § 3 are confirmed experimentally, the experiments are not completely explained from the viewpoint of their growth rates. The growth rates of helical modes calculated with parameters in experiments seem to be larger than the experimental data. Since the tearing modes having a singular point in $a < r_s < b$ have smaller growth rates than helical modes, the experiments may be explained by this type of instability.

CONCLUDING REMARKS

In the present thesis, equilibrium and stability of toroidal pinches and Tokamak systems have been studied, mainly by means of numerical techniques.

In Chapter II, firstly the MHD stability has been studied for a variety of diffuse pinch configurations, which are obtained by the methods devised by the author, by means of Newcomb's criterion. The stability diagrams obtained for reverse field diffuse pinches show: (i) R_W versus the J_z current profile, (ii) R_W versus average beta, (iii) R_W versus the degree of field reversal. It is found that reverse field diffuse pinchs with sufficiently high values of β and compression ratio $R_W \gtrsim 2$ are available in experiments.

Secondly, the growth rates of MHD instabilities for some unstable reverse field configurations have been numerically calculated. It is shown that the kink instability is most dangerous for confining high β plasmas in toroidal pinches because of its large growth rate.

Thirdly, the stability against the resistive instability has been examined with the method given in CGJ.[38] It is shown that the reverse field configuration is vulnerable to the resistive tearing instability. The tearing mode has the growth rate smaller than the kink mode. It is, however, dangerous for a current carrying plasma, since it gives a non-local disturbance.

In Chapter III, collisional diffusion in diffused toroidal pinches has been studied according to the scheme of GS[46] in the banana regime and the plateau regime. For MHD regime, we have adopted MHD equations. The configuration of the toroidal pinch is characterized by the large poloidal magnetic field comparable to the toroidal magnetic field. In considering this fact, the diffusion coefficients given in GS must be modified so as to include that particles can be trapped in the local magnetic mirror formed by the inhomogeneity

of a poloidal magnetic field and of a toroidal magnetic field. It is shown that the diffusion coefficients in toroidal pinches are smaller than those of low β toroidal plasmas and that the toroidal pinches are of great advantage to confining high tempertaure plasmas or high β plasmas.

In Chapter IV, the general formulation to calculate Tokamak equilibrium with large poloidal beta, $\beta_p >> 1$, has been developed. This formulation includes the equilibrium of the toroidal plasma in the weakly non-circular conducting shell. It is confirmed that, if $\beta_p >> 1$, $\beta_p a/R$ should be taken as the expansion parameter to solve the equilibrium equation. This is proved through the analysis of the high β_p equilibrium with a uniform toroidal current. The high β_p equilibria with non-uniform currents have been obtained numerically.

In Chapter V, firstly the MHD stability of Tokamak type devices has been studied in the cylindrical geometry by solving numerically the linealized MHD equations. This procedure has advantages to obtain growth rates of MHD instabilities and eigen functions corresponding to the profiles of displacements. The stability diagrams, showing normalized growth rates versus $q_a(=q(a))$,are obtained by changing the toroidal current profile from the skin like one to the current concentrated in the central region of the plasma column.

Secondly, the stability against resistive tearing instabilities in Tokamaks has been examined. The tearing modes with $m = 2$ and $m = 3$, which occur when the singular point falls into the conducting plasma, are unstable. This means that, if $q(r) > 3$, the Tokamak configuration is stabilized against tearing modes,since the singular point disappears for $m = 2$ and $m = 3$. We have also studied another type of tearing modes, which occur when the singular point falls into the pressureless plasma surrounding the main plasma column. They have the same features of stability as that of helical instabilities, while their growth rates are smaller than those of the helical modes.

We notice here that the following problems are left.

(i) The stability analysis has been carried out in the cylindrical geometry. This may be a good approximation to a toroidal geometry for non-localized helical (or kink) modes. It is, however, unclear for localized helical modes. Also the stability criterion in the toroidal plasma corresponding Newcomb's criterion is not yet formulated.

(ii) Although the formulation to solve the equilibrium equation for Tokamaks with large poloidal beta is developed, it is not discussed that whether there is a limitation of β_p to assure the existence of the equilibrium or not.

(iii) It will be necessary to analyze the effects of electric field driving a plasma current and rotation of plasma column on the collisional diffusion in toroidal pinches.

(iv) In Tokamaks, a high temperature plasma enough to reduce the growth rates of the resistive tearing instability may be obtained in the future. Then, it is necessary to examine the stability against collisionless tearing modes.

Now let us consider the application of the results above mentioned. They are useful to the analysis of the present experiments in toroidal pinches and Tokamaks, and also apply to develop control techniques to avoid dangerous instabilities in CTR (controlled thermonuclear reactors).

(i) The method to obtain equilibrium configuration developed in Chapter II is available to reproduce the configuration in experiments of toroidal pinches or Tokamaks. Thus the stability diagrams obtained in Chapter II or Chapter V give the useful means to compare the theoretical predictions with the experimental data in toroidal pinches or Tokamaks.

In the case of unstable configurations, the growth rates of MHD instabilities also can be calculated by the method in Chapter II or Chapter V.

(ii) A programming of magnetic fields attracts attention to maintain a stable configuration in toroidal pinches for a sufficiently long time. The stability diagrams given in Chapter II may be used for introduction of control techniques such as a programming of magnetic fields.

(iii) It is preferable to maintain stable configurations from the ignition of discharge to the stationary state in toroidal pinches or Tokamaks. Although the computer simulation is powerful to study the equilibrium, it is not developed enough to treat MHD instabilities. Thus the stability diagrams may be used to check the results obtained in computer simulations.

(iv) In the reverse field pinch with a nearly uniform current, it will be difficult to avoid the resistive tearing instability for a sufficiently long time. This is due to the appearance of $\vec{\nabla}p \simeq 0$ region by the resistive diffusion of magnetic fields. Thus, it may be necessary to heat a plasma to reduce the growth rate of the tearing instability. From the viewpoint of the collisional diffusion, experiments of the toroidal pinch may be encouraged.

(v) In Tokamaks, theoretical values of growth rates of MHD instabilities seem to be larger than those estimated from the experiments which aim to lower a safty factor.[60] The results about tearing modes obtained in Chapter V give another possibility to explain the experiments about the stability.

(vi) In Tokamaks, the experiments to realize $q_a \sim 1$ with high values

of β will be carried out in the future. The theoretical results shown in Chapter IV assures the equilibrium with high β_p. The stability diagrams against MHD instabilities show that the unstable region of q_a to the high m mode appears. Therefore the plasma column is vulnerable to the m = 2 mode and/or the m = 3 mode, when $q_a \to 1$. The high m modes can be stabilized by concentrating the current density in the central region of the plasma column. To avoid MHD instabilities with m = 2 and m = 3, the experimental technique to control the current profile needs to develop.

(vii) It is possible to improve the stability against MHD instabilities by distorting the conducting shell of Tokamaks.[17),18)] The formulation to obtain high β_p equilibrium contained in non-circular shell in Chapter IV may be used to investigate this problem.

From the viewpoint of analysis, we shall insist that the methods to examine the stability against MHD and resistive instabilities in Chapters II and V and the method to obtain the high β_p equilibrium in Chapter IV are generally applicable to axisymmetric toroidal plasmas aiming CTR.

REFERENCES

1) H.A.B.Bodin et al.: Fourth Conference on Plasma Physics and Controlled Nuclear Fusion Research (Madison, Wisc., USA), 1971. CN-28/B-5.

2) K.Hirano, M.Ohi, S.Kitagawa and Y.Hamada: Second Topical Conference on Pulsed High Beta Plasmas (Munchen, Germany), 1972. F-6.

3) C.Bobeldlik, L.H.Th.Rietjens, P.C.T. van der Laan and F.Th.de Bats: Plasma Phys. 9 (1967) 13.

4) H.Zwicker, R.Wilhelm and H.Krause: Fourth Conference on Plasma Physics and Controlled Nuclear Fusion Research (Madison, Wisc., USA), 1971. CN-28/B-6.

5) L.A.Artsimovich et al. : Nucl.Fusion Special Suppl. (1969) 17.

6) D.Dimock et.al. : Fourth Conference on Plasma Physics and Controlled Nuclear Fusion Research (Madison, Wisc., USA), 1971. CN-28/C-9.

7) C.F.Barnett et.al. : Fourth Conference on Plasma Physics and Controlled Nuclear Fusion Research (Madison, Wisc,, USA), 1971. CN-28/C-1.

8) S.Ito et al. : JAERI memo 4084 (1970).

9) V.D.Shafranov: Soviet-Physics JETP 6 (1958) 545.

10) V.D.Shafranov: Nucl. Fusion 3 (1963) 183.

11) C.Mercier: Nucl. Fusion 3 (1963) 89.

12) A.A.Ware and F.A.Haas: Phys. Fluids 9 (1966) 956.

13) V.D.Shafranov and E.I.Yurchenko: Fourth Conference on Plasma Physics and Controlled Nuclear Fusion Research (Madison, Wisc., USA), 1971. CN-28/F-13.

14) G.Laval, E.K.Maschke, R.Pellet and M.N.Rosenbluth: International Center for Theoretical Physics, Report IC/70/35 (1970).

15) H.R.Strauss: Phys.Rev.Letters 26 (1971) 616.

16) J.D.Callen and R.A.Dory: Phys. Fluids 15 (1972) 1523.

17) G.Laval, H.Luc, E.K.Maschke, C.Mercier and R.Pellet: Fourth Conference on Plasma Physics and Controlled Nuclear Fusion Research (Madison, Wisc., USA), 1971. CN-28/F-12.

18) L.A.Artsimovich and V.D.Shafranov: JETP Letters 15 (1972) 51.

19) J.M.Green, J.L.Johnson and E.K.Weimer: Phys. Fluids 14 (1971) 671.

20) A.Yoshi, M.Wakatani and T.Amano: Institute of Plasma Physics, Report (to be published), Nagoya University, Nagoya, Japan (1973)

21) M.D.Kruskal and J.L.Tuck: Proc.Roy.Soc. A 245 (1958) 222.

22) V.D.Shafranov: Plasma Physics and the Problem of Controlled Thermonuclear Reactions (Pergamon, Oxford 1959) vol.2, p. 197.

23) W.A.Newcomb: Ann. Phys. 10 (1960) 232.

24) M.N.Rosenbluth: Proceedings of the Second International Conference on the Peaceful Uses of Atomic Energy, Geneva 31 (1958) 85.

25) D.M.Corpley and K.J.Whiteman: Plasma Phys. 4(1962) 103.

26) D.C.Robinson: Plasma Phys. 13 (1971) 439.

27) T.Amano, T.Tamai and M.Wakatani: J. Phys. Soc. Japan 32 (1972) 1385.

28) V.D.Shafranov: Soviet-Physics Technical Physics 15 (1970) 175.

29) I.B.Bernstein, E.A.Frieman, M.D.Kruskal and R.M.Kulsrud: Proc. Roy. Soc. A 244(1958) 17.

30) M.Okabayashi: Princeton University Report, Matt-912 (1972).

31) T.Amano, M.Wakatani and M.Watanabe: J.Phys. Soc. Japan 33 (1972) 782, and Institute of Plasma Physics, Report No. 121, Nagoya University, Nagoya, Japan(1972).

32) K.Hain and R.Lüst: Z. Naturforsh. 13a(1958) 936.

33) J.P.Freidberg: Phys. Fluids 13 (1970) 1812.

34) J.P.Goedbloed and H.J.L.Hagenbeuk: Phys. Fluids 15 (1972) 1090.

35) H.P.Furth, M.N. Rosenbluth and J.Killeen: Phys. Fluids 6 (1963) 459.

36) J.L.Johnson, J.M. Green and B.Coppi: Phys. Fluids 6 (1963) 1169.

37) L.Spitzer, Jr.: Phys. Fluids 1 (1958) 253.

38) B.Coppi, J.M.Green and J.L.Johnson: Nucl. Fusion 6 (1966) 101.

39) B.Coppi: Phys.Fluids 7 (1964) 1501.

40) B.Coppi and M.N.Rosenbluth: Plasma Physics and Controlled Nuclear Fusion Research, International Atomic Energy Agency, Vienna (1966) vol.1, p.617.

41) S.I.Mirnov and I.V.Semenov: Fourth Conference on Plasma Physics and Controlled Nuclear Fusion Research (Madison, Wisc., USA), 1971. CN-28/F-5.

42) J.C.Hosea, C.Bobeldick and D.J.Grove: Fourth Conference on Plasma Physics and Controlled Nuclear Fusion Research (Madison, Wisc., USA), 1971. CN-28/F-7.

43) H.P.Furth, P.H.Rutherford and H.Selberg: Princeton University Report , Matt-897. (1972).

44) P.H.Rutherford, H.P.Furth and M.N.Rssenbluth: Fourth Conference on Plasma Physics and Controlled Nuclear Fusion Research (Madison, Wisc., USA), 1971. CN-28/F-16.

45) D.Pfirsch and A.Schlüter: Max Plank Institute, Report MPI/PA/7/ 62, 1962.

46) A.A.Galeev and R.Z.Sagdeev: Soviet-Physics JETP 26 (1968) 233.

47) L.M.Kovrizhnikh: Soviet-Physics JETP 29 (1969) 475.

48) P.H.Rutherford: Phys. Fluids 13 (1970) 482.

49) M.N.Rosenbluth, R.Hazeltine and F.L.Hinton: Phys. Fluids 15 (1972) 116.

50) A.A.Galeev: Soviet-Physics JETP 32 (1972) 752.

51) T.Stringer: Phys. Fluids 13 (1970) 810.

52) T.Stringer: Phys. Fluids 13 (1970) 1586.

53) A.A.Ware: Phys.Rev.Letters 25 (1970) 916.

54) P.H.Rutherford, L.M.Kovrizhnikh, M.N.Rosenbluth and F.L.Hinton: Phys.Rev.Letters 25 (1970) 1090.

55) A.A.Galeev, R.Z.Sagdeev, H.P.Furth and M.N.Rosenbluth: Phys. Rev.Letters 22 (1969) 511.

56) E.A.Frieman: Phys.Fluids 13 (1970) 490.

57) M.Wakatani and R.Itatani: J.Phys.Soc.Japan 34 (1973) 181.

58) B.R.Suydam: Proceedings of the 2nd International Conference on the Peaceful Uses of Atomic Energy, Geneva, 31 (1958) 157.

59) R.J.Taylor: Proc.Phys.Soc. B 70 (1957) 1049.

60) S.V.Mirnov and I.B.Semenov: Zh.Eksp.teor.Fiz. 60 (1970)2105.

61) V.D.Shafranov: Review of Plasma Physics, vol.2, (Consultants Bureau, New York, 1966) p.103.

62) B.B.Kadomtsev and O.P.Pogutse: Review of Plasma Physics, vol.5, (Consultants Bureau, New York, 1970) p.254.

63) V.D.Shafranov and E.I.Yurchenko: Soviet-Physics JETP 26 (1968) 682.